

COLLECTIVE VIBRATIONS IN LIQUID NUCLEI

by

V. K. KHARARAPPA

Submitted to the Gujarat University
for the Degree
DOCTOR OF PHILOSOPHY

043



B1926

PHYSICAL RESEARCH LABORATORY

ANANDNAGAR

1962

CONTENTS

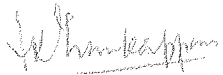
	Page
Preface	iii
Acknowledgement	v
 Chapter I. Introduction	
1. Introductory Remarks	1
2. The Independent-Particle Shell Model	2
3. The Collective Models	6
4. Energy Level Systematics: A = 17 - 40	12
5. Scope of the Thesis	18
References	22
 Chapter II. The Shell Model	
1. Introduction	25
2. One Nucleon (or Hole) Configu- rations: Si^{29} , p^{29} & p^{31}	27
3. Two-Nucleon Configurations: Si^{30} & p^{30}	30
4. Three-Nucleon Configurations: T = 3/2	40
5. Parameters of the Nuclear Interaction	43
6. Conclusion	45
References	46

	Page
Chapter III. The Collective Model	
1. Introduction	48
2. The Formalism	61
3. The Formalism: Electromagnetic Properties	64
4. Applications: One Nucleon outside the Core (81^{83} , p^{23} , p^{31})	76
5. Applications: Two Nucleons outside the Core (81^{30})	98
6. Discussion of the Parameters	113
7. Conclusion	121
References	122
Appendix I	125
Appendix II	134
Chapter IV. Nuclear Interactions in the $F_{1/2} - G_{9/2}$ Configurations	
1. Introduction	137
2. Calculations and Results	138
3. Comparison with other Results	147
4. Conclusion	150
References	152
Chapter V. Summary	154
Appendix. Reprints of published work	156

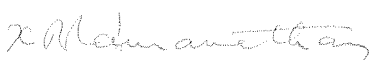
PREFACE

The shell model and the various collective models have had great success in explaining many of the phenomena observed in the study of nuclei in different parts of the periodic table. The collective model was originally applied mostly in the region of heavy nuclei. Recently, however, the strong-coupling collective model has been applied successfully in the mass region 85, which corresponds to nuclei with the largest number of nucleons in unfilled shells 2s - 1d. On the other hand, it is more or less established that the jj -coupling shell model is fairly valid for nuclei around $A \approx 40$, where the shell closes. The nuclei intermediate between these two regions have not been investigated in detail, even though the strong-coupling collective model (Nilsson model) has been tried with some success for Si^{28} and P^{31} . As the subshells $1d_{3/2}$ and $2s_{1/2}$ close for proton or neutron number 14 and 15, we should expect the deformation to be small for $A \approx 25 - 32$; the weak-coupling collective model might be more appropriate for these nuclei. A major part of this thesis is devoted to a discussion of the nuclei following Si^{28} in terms of the collective vibrational model. In chapter IV, the nuclear energy levels of Zr^{90} have been evaluated in terms of the spherical jj -coupling shell model and the nature of the nuclear interaction in this region is discussed.

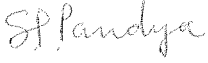
The work described in this dissertation has been carried out by the author at the Physical Research Laboratory, Ahmedabad, under the guidance and supervision of Dr.S.P.Paniya and Professor K.R.Ramanathan. The work reported in chapter IV was done in collaboration with Mr.K.R.Waghmare.


V.K.Thankappan

Certified that this dissertation by Mr.V.K.Thankappan is an account of the research work carried out by him at the Physical Research Laboratory, Ahmedabad.


K.R.Ramanathan
Professor of Atmospheric Physics
and Director,
Physical Research Laboratory,
Ahmedabad.

Dated 22/3/1962


S.P.Paniya
Head, Department of Theoretical Physics,
Physical Research Laboratory,
Ahmedabad.

Dated 22/3/1962

ACKNOWLEDGEMENT

The author would like to express his gratitude to Professor K.R.Ramanathan and Professor V.A.Sarabhai for having extended to him the hospitality of the Physical Research Laboratory.

He is indebted to Dr.S.P.Pandya for introducing him to the subject, for his valuable guidance and helpful discussions, and to Professor K.R.Ramanathan for his keen interest and encouragement during the progress of the work. He wishes to record his indebtedness to his colleagues Mr.Y.R.Waghmare and Mr.S.K.Shah for the help and co-operation they extended to him.

Some of the calculations reported in chapter III have been carried out on the Digital Computer at the Tata Institute of Fundamental Research, Bombay. The author is thankful to Dr.D.V.Phadke for allowing him the facilities of the computer and to the members of the Computer Section, especially to Dr.H.Harasimhan and Mr.K.S.Kene, for their sincere help and co-operation. He is also thankful to Mr.S.R.Thakore of the University of Rochester for computational assistance.

Finally, it is a pleasure to acknowledge the award of a scholarship by the University Grants Commission and the Ministry of Education, Government of India, during the work for the thesis.

CHAPTER I

INTRODUCTION

1. Introductory Remarks

The study of the structure of the nucleus has developed through the introduction of various models which replace the nucleus - a system of many particles interacting through complex short-range strong forces - with greatly simplified systems that can be handled mathematically with ease and accuracy. The two main classes of the models developed are the strong-interaction models and the independent particle models. Whereas in the former the nucleus is treated as an assembly of strongly coupled particles as in a liquid drop, in the latter models the nucleons are assumed to move rather independently of each other in an average central nuclear potential. The liquid drop model and the alpha-particle model are examples of the strong-interaction models, and the optical model and the shell model are typical of the independent particle models. In recent years it has been found necessary to develop a unified model which contains the essential features of both the classes of models.

The success of each of these models has been confined to certain groups of nuclear properties and to certain regions of the periodic table. The liquid drop model was developed to account for the resonances in nuclear reactions and found its most successful application in the phenomenon of nuclear fission.

The optical model is useful for understanding the experimental data on nuclear scattering of nucleons, deuterons, alpha-particles etc. The shell model and the collective model give an insight into the properties of the bound states of nuclei in different mass regions. One of the major problems in the theory of nuclei is to determine and understand the relationship of the various models and the regions of their validity. This may require a derivation of these models from a more fundamental and rigorous theoretical basis, as has been attempted by Brueckner (see EdinSS) in the particular case of the independent particle shell model.

Each nuclear model contains a number of arbitrary parameters. The values of these parameters are generally adjusted during specific calculations to give the best fit with the given experimental data. The second problem then is to study at least phenomenologically the variation of these parameters from nucleus to nucleus, their systematics, and then to understand these regularities or derive them from more fundamental considerations. This is, of course, a part of the larger problem outlined above of providing the models with a unified theoretical basis.

2. The Independent-Particle Shell Model

One of the most successful models for studying the properties of the bound states of nuclei is the independent-particle shell model. The concept of a shell structure for the nucleons in nuclei, somewhat akin to the configuration of

electrons in atoms, was introduced in the early 1930's, was discarded after the success of the liquid drop model proposed by H. Bohr in explaining the resonance phenomena in nuclear reactions, and was again revived with great success by Mayer, and Haxel, Jensen and Suess in the form of the jj -coupling shell model. This version of the shell model provided a most understanding of various nuclear properties and regularities, such as the ground state spins and parities, magnetic moments, beta-decay systematics, occurrence of isomers in certain regions of the periodic table etc.

The main assumption underlying the nuclear shell model is that the nucleons move (to a very good approximation) independently of each other within the nucleus in a spherically symmetric central potential which may be thought of as an average of the interactions of a nucleon with all the others. As long as this potential is a non-singular smoothly varying function of distance r , its details are unimportant. It provides a suitable basic complete set of energy eigenvalues and eigenfunctions. For practical considerations the eigenfunctions are taken to be those of an isotropic harmonic oscillator potential. The energy eigenvalues are generally taken from suitable experimental data. In the jj -coupling version the central potential contains a strong spin-orbit coupling term, so that each eigenfunction is characterised by the quantum numbers n (the principal quantum number), l (the orbital angular momentum), j (the total angular momentum = $l \pm 1/2$) and m (the magnetic quantum number j_z).

All the states differing only in the value of ' m ' are degenerate in energy and form a subshell $2j+1$. The neutrons and the protons in the nucleus fill up successively the energy levels of the harmonic oscillator potential. When all the $2j+1$ states corresponding to different m values with same j are filled up by the nucleons, they form a closed subshell. A configuration of the nucleons is defined as a set of quantum numbers describing all the states occupied by the nucleons. When the configuration contains more than one nucleons outside the closed subshells, it has in general, a number of states with different values of total angular momentum J and total isotopic spin T , but with the same energy, i.e., the sum of the energies of all the occupied single particle states. Conversely, different configurations of N nucleons may have states of the same values of J and T . The states of a single configuration will be called pure states. In this case the wave-function of the nuclear state will be a properly anti-symmetrized product of all the occupied single particle wavefunctions. In general, however, the nuclear interactions mix states of different configurations, i.e., the wave function of a given nuclear state of total angular momentum J and total isotopic spin T may be constructed by superposition (linear combination) of the wavefunctions of suitable states of several different configurations. One of the essential features of the shell model calculations, now well justified by the theoretical work of Brueckner and colleagues (Bd59), is that one considers the mixing of only

those configurations which have the same or almost the same energy. We shall illustrate all these ideas later by explicit examples.

The degeneracy in energy of different states of a single configuration mentioned above is not observed in actual nuclear spectra. In theory it can be removed by introducing interparticle forces between the nucleons in the open subshells. These forces are assumed to be only perturbations over the central single particle potential, and are generally treated by first order perturbation theory. Through extensive work by Brueckner and others some qualitative understanding of the properties of these forces has been gained. Unlike the explicit two-body interactions between free nucleons, these effective perturbation interactions are analytically well-behaved and weak. They are also non-local and configuration dependent. Although Brueckner's theory enables us in principle to calculate exactly the properties of these effective interparticle forces in nuclei (the so-called t -matrix), in practice this is difficult to do, and has not been done for nuclei of practical interest. We shall therefore adopt the well-established procedure of treating this interaction in an empirical fashion.

The shell model has been very successful in correlating and predicting a large number of nuclear data such as energy levels, spins and parities, magnetic moments, stripping and pick-up reactions, beta-decay etc., in several regions of the periodic table--near the doubly closed shell nucleus Pb^{208} , near $A = 90$, in the region of the $f_{7/2}$ shell ($A \approx 40$), and in a

somewhat modified form (intermediate coupling version) for light nuclei ($A < 20$). It should be noted that generally speaking the detailed quantitative success of this shell model has been confined to nuclei with a few ($\leq 3-4$) nucleons in open subshells. For other cases the calculations assume prohibitive complexity.

The major failure of the nuclear shell model is to explain the existence of very large quadrupole moments and very fast electric quadrupole (E2) gamma-ray transitions observed in a large class of nuclei. This suggests that the effect of the interparticle forces in these nuclei must be such as to mix several different configurations which interfere constructively to enhance the E2 transition amplitude. Since in practice it is very difficult to carry out a calculation involving mixing of several configurations for several nucleons, an alternative description is provided by the collective models which try to describe the excited energy levels of nuclei in terms of simple rotations or vibrations of the nucleus as a whole. Various types of collective motions with increasing refinements and complexities are formulated by now. In the next section we give a brief simple resume of the basic features of these collective models.

3. The Collective Models

In the spherical shell model considered above, one assumes that all the nucleons occupying the closed shells form an inert rigid spherical core with zero spin, zero magnetic moment etc.,

so that all the nuclear properties are now attributed only to the nucleons in the open subshells, and only these need be considered in any explicit calculations. The core only serves to provide a central spherically symmetric single particle potential. This is however not strictly true even within the framework of the independent particle shell model. The motion of the nucleons outside the core tends to polarise it and deform it from the spherical shape. It can be shown that this is a consequence of the long-range part of the effective nucleon-nucleon interactions in the nuclei. Because of the long range nature, this deforming or polarising force and its effect increase as $\sim n(n-1)$, where n is the number of nucleons in the open subshell. However, it is known that there are also present strong pairing forces or short-range interactions between nucleons, and it is easily shown that as a consequence of such forces nucleons tend to pair up, each pair taking up a spherical configuration with total spin $J = 0$. Clearly then, these forces, the effect of which will be proportional to n (because of their short range), will tend to stabilise the spherical configuration of the core. The competition between these two forces determines the actual shape of the stable configuration for the nucleus (non- 0).

Qualitatively the general features of the collective excitation spectra of nuclei with different numbers of nucleons in the open subshells can be described as follows: For a closed shell nucleus, one expects the equilibrium

configuration to be spherical and stable against deformations at least for low energy excitation. If the configuration consists of a closed shell plus (or minus) only a few nucleons, the pairing forces dominate and the usual shell model description would apply, i.e. the core would retain a spherical shape but would be unable of collective motion in the form of low frequency vibrations about its spherical shape. So long as the frequency of the single particle orbital motion is large compared to the frequency of the vibrations, the adiabatic approximation would apply, and the spectrum would consist of single particle levels (we consider the example of a simple configuration of closed shell + one nucleon) with vibrational band built upon each of these levels. If the adiabatic approximation does not apply, i.e. the single particle excitations and collective excitations have about the same energy, the coupling of these motions must be explicitly taken into account. For several nucleons outside the closed shell, the configuration would no longer have spherical stability, but would be deformed owing to the domination of long range correlations. A graphical representation of this sequence is given in fig. 1 (Alr66) in which V denotes the potential energy and β some deformation parameter. Curves a and b correspond to nuclei in the vicinity of a closed shell where the spherical shape represents a stable equilibrium. The collective motion in this case corresponds to vibrations about this shape. As more nucleons are added, instability of the spherical shape results and a non-spherical equilibrium shape (curves c and d) is realized for the nucleus.

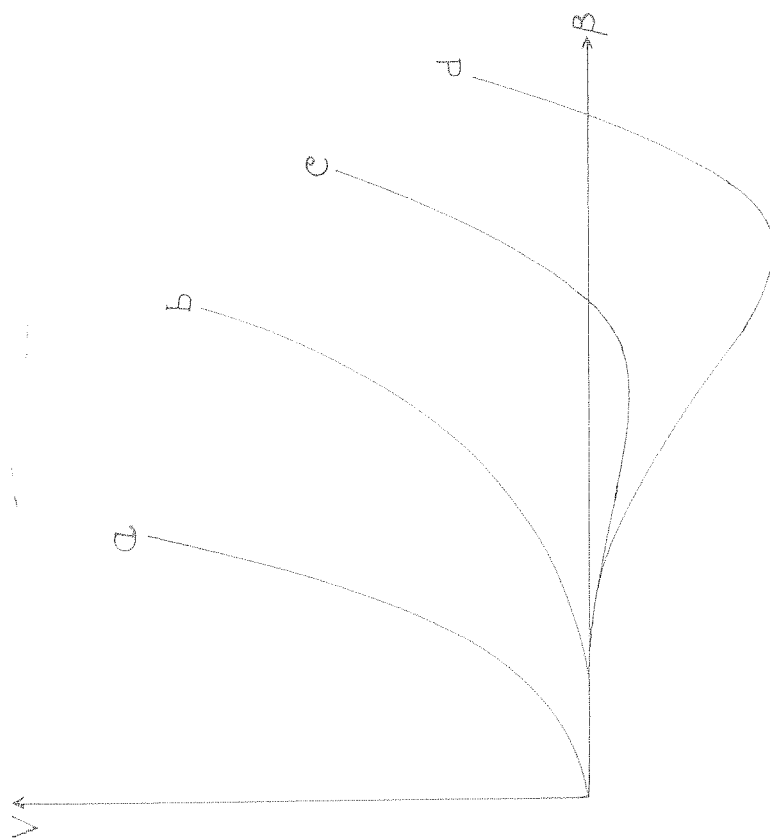


FIG.1. POTENTIAL ENERGY SURFACES FOR EVEN-EVEN NUCLEI. V DENOTES THE POTENTIAL AND β SOME DEFORMATION PARAMETER.

E J
5.06 ——— $d_{3/2}$

0.88 ——— $s_{1/2}$
O ——— $d_{5/2}$

FIG.2. SINGLE-PARTICLE LEVELS OF THE $2s-1d$ SHELL AS OBSERVED IN O^{17} .

Most of the models consider axially symmetric deformations. In case of large deformations, the degeneracy of the single particle states observed in spherical potentials (for example, $2j + 1$ -fold degeneracy described above) is removed, and thus the effect of the pairing forces is also considerably reduced. Now for the non-spherical nuclei the collective motion can be quite complex. We would have the rotational motion of the whole nucleus while preserving the shape, and also the vibrational motion which corresponds to oscillations about the equilibrium shape. Again in the adiabatic approximation, the rotational and the vibrational states may be separated out, the frequency of the rotations (because of the large mass transport involved) being much smaller than the frequency of the vibrational motion. In such a case one would observe rotational states close to the ground states, and at higher energies vibrational states (β -vibrations and γ -vibrations) also with rotational bands built upon them. In actual practice, this simple energy level spectrum would be distorted by rotation-vibration interaction which is well known in molecular spectra, as well as interaction and mixing of states in different rotational and vibrational bands. In general, then, the picture would be quite complicated. It is not surprising therefore that while vibrations of spherical nuclei as well as pure rotational spectra being relatively simple and easily identifiable, are well established and there is a considerable amount of experimental data on such states, the vibrational

levels of deformed nuclei are not yet clearly understood either theoretically or experimentally.

Axially asymmetric deformations of nuclei have also been considered by several authors (Dav58). Rotational states of such nuclei in adiabatic approximation, i.e. assuming rotation only without change in the intrinsic state of the configuration, have been calculated. Also in a later improved version of this model, β -vibrations and vibration-rotation interactions have been taken into account (Dav60, Dav61).

It is now clear that at least theoretically one can visualise several types of collective motions, of varying degrees of complexity. Many nuclei show evidence of simple types of collective motions such as rotational states of a strongly deformed nucleus. In general, however, the experimental data itself is quite complicated and cannot always be interpreted in terms of a unique model. It may be that several different models can explain the same set of data equally well with suitable choice of parameters. For proper understanding of the various types of collective motions it is necessary to investigate theoretically in considerable detail the properties and consequences of these models and then to look for distinctive experimental properties predicted by such models. In a later section we shall study the energy levels of a group of simple nuclei near $A = 30$, in the light of some of these different models.

In the above presentation of the collective models we have followed the conventional description which rests on very simple physical pictures. The collective motions of the nucleus - vibrations or rotations - are treated in these models in a macroscopic fashion. A Hamiltonian with empirical parameters (such as moment of inertia or deformability or frequency of collective vibrations etc.) can easily be written down and nuclear properties can be calculated. In the next chapter we shall show how this is done for a specific model. However, in the last two years a more powerful approach to the problems of collective motion has been developed. This attempts at an understanding of the collective effects in terms of coupling schemes of nucleons moving in independent particle orbits, taking into account explicitly the nucleon-nucleon forces which we mentioned earlier. The methods developed by Bogoliubov for treating the problem of superconductivity are applied (Boya59). Although this technique is powerful and versatile, and leads to a deeper understanding of the collective phenomena than the older picturesque models, one also loses in this procedure the vivid physical picture of the collective motions. We shall not concern ourselves with this new approach in the present dissertation, but shall rather follow the older version which we find more suitable for discussing specific nuclei. Much of the work described in this dissertation was completed before this new understanding of the collective motions gained recognition.

4. Nuclear level systematics: $A = 17 - 40$

In this section we summarise briefly some of the experimental data on nuclei in the mass range $A = 17 - 40$. In terms of the jj -coupling shell model, the single particle orbitals of interest in this region are $d_{5/2}$, $s_{1/2}$ and $d_{3/2}$ in the order of increasing energy (fig.2). In its simplest version the first 8 neutrons and protons would fill up the underlying s - and p -subshells, giving a closed spherical stable core configuration, and subsequent nucleons would go into the $d_{5/2}$, $s_{1/2}$ and $d_{3/2}$ subshells, producing again a closed shell configuration at $N = Z = 20$. A theoretical study of this region is of very considerable interest. One can have simple nuclei with 2 or 3 nucleons outside the $A = 16$ core (for simplicity we shall denote this core by the symbol C in the following discussion) and can treat them in terms of the shell model, including mixed configurations; one may also consider complex nuclei with large number (6 - 10) of nucleons outside C. In the latter case shell model techniques are almost impossible to apply, and study of their properties in terms of collective model has paid rich dividends.

An excellent review of the various properties of the nuclei in the $s - d$ shell is given by Dove (Dove60). We shall only discuss here those features of the data which are of interest to the discussion that is to follow in subsequent chapters. Dove's discussion of the nuclear properties is mostly confined to interpreting them in terms of the rotational spectra of strongly deformed nuclei - the strong coupling

collective model. He does not consider the vibrations or the non-axial deformations. This model has considerable success within certain limitations. In fact most of the nuclei investigated in this region have been discussed by various authors in terms of the rotational model. On the basis of the discussion of the previous section, one may expect a successful description for the nuclear properties of $A = 17, 18, 19$ nuclei in terms of the shell model with proper inclusion of nucleon-nucleon interactions and configuration mixing. The extensive calculations of Elliot and Flowers (Eli55) using the straightforward shell model techniques indeed yield theoretical results which are in very good agreement with the experimental data. However, it was evident that even in these simple nuclei, collective effects do occur. For example, a fast electric quadrupole transition is seen from the first excited state $1/2^+$ to the ground state $5/2^+$ in O^{17} . If there were no collective effects, since the extra core nucleon is a neutron, such a transition would be absolutely forbidden. Raz (Raz57) has shown that the introduction of small collective effects can easily account for this observed electric quadrupole transition. Similar E2 transition observed in F^{19} can also be accounted for by inclusion of small collective effects which would leave the calculated energy levels essentially undisturbed. For nuclei with $A \geq 20$, the application of orthodox shell model methods becomes prohibitively complex, and no such calculations are done. Recently, Levinson, Banerjee, Meshkov and Pal (Bae60) have developed a new and

powerful technique, based on group-theoretic methods, of doing intermediate coupling shell model calculations in this region. Energy levels of several nuclei up to Hg^{84} , and in particular Ne^{20} and Hg^{84} have been studied with these methods, and the results are found to agree very well with the experiments.

Paul (Pal57) was able to interpret the observed energy level spectrum of F^{19} in terms of rotational bands, and also explained other nuclear properties such as magnetic moments, γ -ray branching ratios, $\log ft$ values etc., consistently in terms of this model. The success of this calculation, compared with equally successful calculations of Elliot and Flowers (Elf55), as well as the results of Levinson et al (Lea50) show that the collective rotational model and the intermediate coupling shell model are two equally valid alternate ways of looking at nuclear properties, and should be related in a fundamental way.

The very first suggestion regarding the applicability of the rotational model in the region of the 2s - 1d shell came from Litherland, Paul, Bartholomew and Dove (Lee56). In their study of the energy levels of Al^{25} and Hg^{25} they were able to provide evidence for well-developed rotational bands of levels. Following their success, an attempt has been made to interpret almost all the nuclei from $A = 17$ to $A = 31$ in terms of this model, with varying degrees of success. Let us first discuss the even-even nuclei in this region.

Fig. 3 gives a plot of the low-lying energy levels of the known even-even nuclei in this region. Fig. 4 shows a plot of the energy levels of the first excited states and the ratio of the energies of the second and first excited states and their variation with mass number A . Several interesting regularities appear in these figures.

The first excited state has in all cases the spin 2^+ , except for O^{16} and Ca^{40} (the closed shell nuclei at the two limits of this region) in which case it has spin 0^+ . The second excited state has generally spin values 4^+ or 2^+ . The case of Ne^{22} is not quite clear. In Ne^{22} the second excited state appears to have spin 0^+ . In $A^{32,36}$ this state has odd parity indicating the influence of the $f_{7/2}$ shell into which a particle can now easily be excited. The level scheme becomes complex beyond the second excited state, but it is clear that a 0^+ state often occurs very near the second excited state.

Now consider Fig. 4. At first the energy of the first excited state decreases as the number of particles in the open $s - d$ subshells increases. For $10Ne^{22}$ and $12Mg^{24}$ the energy has the lowest value $E_1 \approx 1.3$ MeV. However, the filling of the $d_{5/2}$ subshell appears to have a definite effect on this energy value. For example, whereas for O^{20} and Ne^{20} E_1 has about the same value of ~ 1.65 MeV, the values for Ne^{24} and Mg^{24} are strikingly different. E_1 for Ne^{24} has a rather large value of 2.0 MeV, whereas for Mg^{24} it is only 1.3 MeV. This difference may be attributed to the filling up

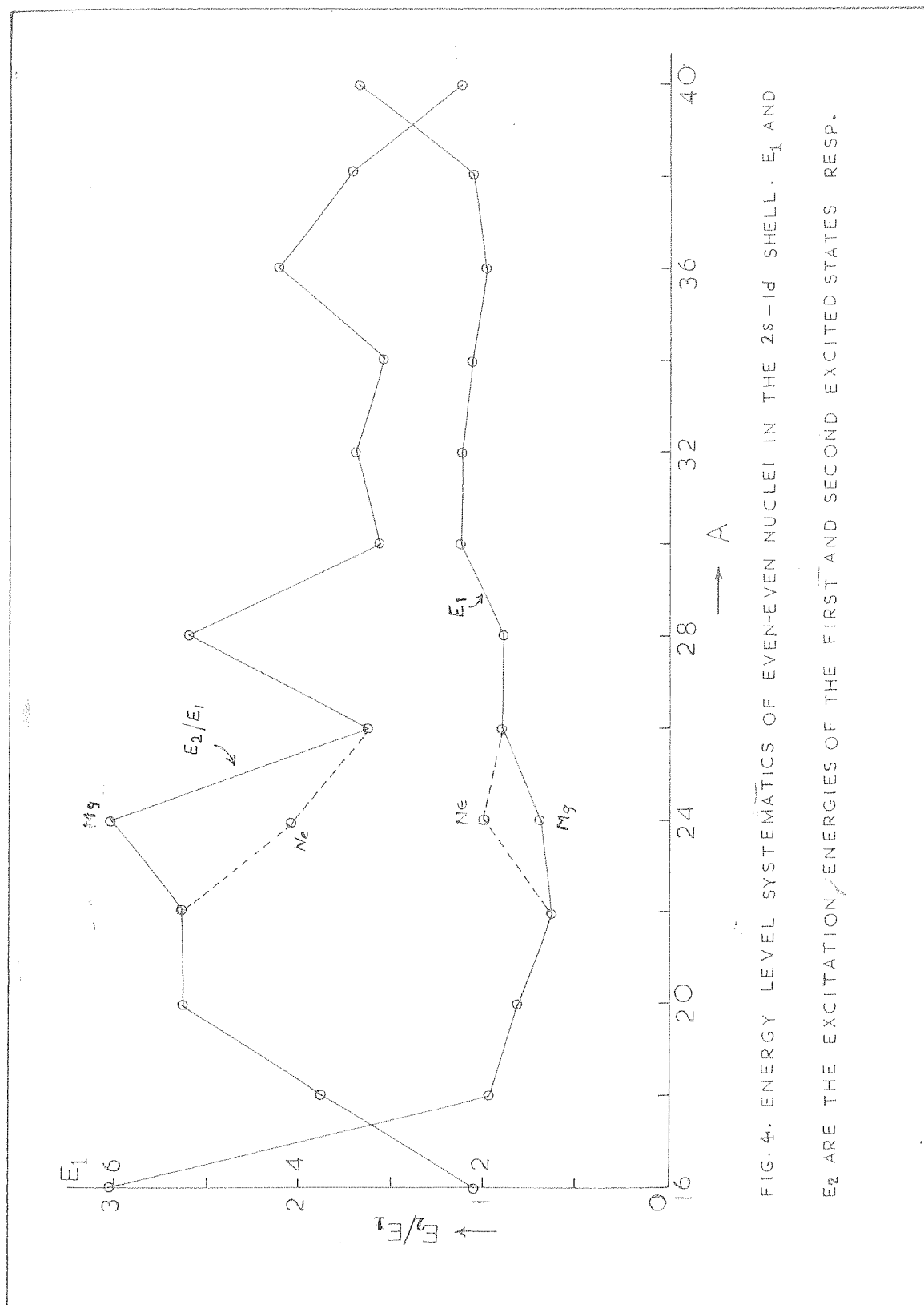


FIG. 4. ENERGY LEVEL SYSTEMATICS OF EVEN-EVEN NUCLEI IN THE 2s-1d SHELL. E_1 AND E_2 ARE THE EXCITATION ENERGIES OF THE FIRST AND SECOND EXCITED STATES RESP.

of neutron subshell $d_{5/2}$ in Ne^{24} . The variation of E_1 in Neon isotopes, as well as the value of E_1 in Mg^{30} and Al^{28} shows that the closure of the $d_{5/2}$ shell increases the value of E_1 to ~ 1.9 MeV. Beyond $A = 28$, the addition of two protons or two neutrons fill up the $d_{5/2}$ subshell, and we note that for Al^{30} , S^{32} and S^{34} , E_1 further increases to 2.2 MeV. This shell structure effect is equally clear in the plot of E_2/E_1 . One sees the well known tendency of E_2/E_1 to increase as E_1 decreases, and vice versa. As the neutron number approaches 14 in the Ne and Mg isotopes, the E_2/E_1 ratio drops sharply to values 1.5 to 2.0. We remark that in the region $A = 30 - 34$, E_1 and E_2/E_1 remain nearly constant at the values ~ 2.2 MeV and 1.7.

Rehavy (Rey57) has discussed the properties of nuclei from $A = 18$ to $A = 28$ in terms of a simple rotational model. He finds that the deformations in this region are large, increasing in magnitude up to $A = 22, 24$ and then diminishing as A further increases. Table 1 of his paper shows that the deformation parameter ϵ changes from 0.48 and 0.47 for Ne^{20} and Ne^{22} to 0.33 for Ne^{24} , from 0.47 for Mg^{24} to 0.34 for Mg^{26} , and 0.23 for Al^{28} . Gove (Goe60) also remarks that whereas the level spectrum for Mg^{24} may be explained on a strong coupling rotational model, Mg^{26} seems to possess some aspects of a vibrational model.

Very little work has been done on the odd-odd nuclei in this region. For Al^{29} Sheline (She57) finds qualitative

agreement of the experimental data with the results of the rotational model, but this model appears to be inadequate to explain the levels of P^{30} (Bat60). On the other hand Cl^{34} and Cl^{36} have been discussed in terms of the jj -coupling shell model by Pandya (Paa56).

Let us now sketch briefly the observed data on odd-even nuclei. Since our interest is only in the region $A \approx 30$, we show the energy levels of only the relevant nuclei in fig. 6. The magnetic moments, the electric quadrupole moments etc., are adequately discussed by Dove and we do not mention them here. In the subsequent chapters, during detailed discussions, we shall refer to these properties whenever necessary. At present we consider only the general trend of energy level systematics.

As we mentioned earlier, it was the experimental data on $A = 25$ nuclei that drew attention to the applicability of the strong coupling rotational model in this region. The excellent agreement of the energy levels of the mirror nuclei Al^{25} and Mg^{25} may be noted. This pair is still the finest example of the occurrence of rotational bands of levels in the $s - d$ shell. We do not discuss this information here. In the rotational model, the energy level spectrum should be determined by the number of odd nucleons. In this sense the nuclei $^{13}Al^{27}$ and $^{14}Si^{27}$ should also exhibit the same level pattern as Al^{25} and Mg^{25} . Fig. 5 shows that this is not so. This change in the character of the level spectrum may again be due to the closure of the $d_{3/2}$ subshell (of neutrons in Al^{27} and protons in Si^{27}), resulting in a drastic reduction

of the deformation of the nucleus. The mirror nuclei P^{29} , Si^{29} and P^{31} , Si^{31} are also shown in the figure. The first three of these have been discussed in terms of the rotational model (Bre58, Bry57) and a good agreement of the theory with experimental data is obtained. It has however been argued (Grin61) that the theoretical calculations in these cases neglect certain important factors, such as proper antisymmetrisation of the wavefunctions etc., and the previous results may be substantially modified by inclusion of these effects. For heavier nuclei, unfortunately the experimental information is rather inadequate, and measurement of many more spins and parities should be made.

We note now that except for $A = 18, 19$ (and later unpublished calculations of Levinson et al for nuclei up to $A = 24$) not very many shell model calculations have been done in this region. Some nuclei such as Cl^{34} , Cl^{36} , A^{37} and Cl^{35} in the $d_{3/2}$ shell have been briefly discussed in terms of simple jj -coupling shell model by Pandya (Pan56). The only other nuclear model discussed in this region is the collective vibrational model which was applied to P^{19} by Abraham and Warko (Abm58). The axially asymmetric deformations or vibrations of spheroidal nuclei do not appear to have been considered in this region.

5. Scope of the Thesis

In the previous section we have pointed out that there is considerable evidence for the validity of the collective

rotational model as applied to nuclei in the region $A = 18 - 31$. It is also clear that the magnitude of the deformation of the nucleus diminishes in magnitude beyond $A = 35$, and the nuclear shape changes rather abruptly at $A \approx 28$ from prolate to oblate. It has been further established that around $A = 40$, where the $s - d$ shell closes, the jj -coupling shell model seems to be quite successful. It would be very interesting to study in detail the transition region beyond $A = 33$ and upto $A = 40$. We have also shown that as the neutron or proton number reaches the value 14, there is a small but marked change in the energy level systematics of nuclei. If the jj -coupling shell model were applicable, one would ascribe this to the closure of the $d_{5/2}$ subshell. However, although such a simple model is certainly invalid in a quantitative sense, in a crude sense one may expect the nuclear structure to change its character as the neutron or proton number passes the value 14. Although the deforming forces cause large deformations of nuclei as the number of nucleons increase beyond $A = 18 = 2$, one would expect the pairing force to play some role as each of the subshells $d_{5/2}$ and $s_{1/2}$ closes. It may be therefore that in the region $A = 30 - 33$, the deforming forces and the pairing forces are equally important, so that on the one hand large deformations would not be expected, on the other hand spherical stable equilibrium shape also may not be expected. In fact, one may expect the collective vibrational model to apply in this transition

region. It is clear that beyond $A = 32$, the pairing forces are dominant so that these nuclei may be validly described in terms of a jj -coupling shell model with a suitable degree of configuration mixing ($s_{1/2}$ and $d_{3/2}$ configuration). To be more precise, the question we ask is the following: Is the nuclear structure in the $s - d$ shell such that we go from strongly deformed nuclei at $A \approx 25$ through slowly decreasing deformations (with a change of sign rather abruptly at $A = 28$) to a spherical shape described by jj -coupling shell model near $A = 40$, or does there occur an intermediate region near $A = 30 - 32$ where collective vibrations of spherical nuclei would occur comprising the transition from large deformations to spherically stable shapes?

The major part of this thesis is devoted to a discussion of several nuclei Si^{28} , P^{30} , P^{31} and Cl^{30} (S^{32}) in terms of a unified approach, i.e. a weak-coupling collective vibrational model. Such a model has been applied by Raa to O^{17} (Raa57), by Abraham and Warko to P^{10} (Abm58), by Ford and Levinson to Calcium isotopes (Fol55), by True to Pb isotopes (Tre55, 58, 61) etc. For our purpose the model takes the following form: We consider nuclei with $A = 28 + n$ to consist of a Si^{28} core + n nucleons in the $s_{1/2}$ and $d_{3/2}$ subshells. For these outer nucleons we consider all the configurations $(s_{1/2})^{n-n} (d_{3/2})^n$ and their mixing produced by nucleon-nucleon interactions. If the Si^{28} core

were spherical and stable against vibrations or deformations, we can neglect it, and describe all the properties of the nuclear levels in terms of the μ outer nucleons by straightforward shell model configuration mixing calculations. Chapter II describes some such simple calculations, which provide an orientation to understand later departures from shell model results produced by introduction of the collective excitation of the core.

The excitations of the $A = 20$ core, which as we have already seen, is by no means inert, are taken into account by attributing to it collective oscillations of the quadrupole type. The interaction of the outer μ nucleons with these vibrations is then also taken into account. This is the approach of the weak-coupling unified model. Chapter III describes in detail the calculations and the results of this approach, and compares them with the experimental data. Finally, in chapter IV, we describe a shell-model calculation for the energy levels of Kr^{90} , which indicates the validity of the spherical shell model for this nucleus and also provides information on the nature of the inter-nucleon forces in this region.

REFERENCES

1. General: (i) P. Aulenberg-Gelove and T. Lauritzen: Nuclear Physics, 11, 1 (1959).
(ii) D. M. Brink: Prog. Nucl. Phys. 8, 97 (1960).
(iii) J. P. Elliot and A. M. Lane: Handbuch der Physik, XXXIX, 241 (1957).
(iv) P. H. Radv and C. M. Braams: Rev. Mod. Phys. 22, 683 (1957).
(v) (Ed) K. H. Hellwege: "Energy Levels of Nuclei, A = 5 to A = 237", Springer-Verlag (1961).
(vi) S. A. Moszkowski: Handbuch der Physik, XXXIX, 411 (1957).
2. Abn53 G. Abraham and C. S. Marks: Nuclear Physics, 8, 69 (1958).
3. Alr56 K. Alder, A. Bohr, T. Huus, B. Mottelson and A. Winther: Rev. Mod. Phys. 28, 443 (1956).
4. Bae60 M. E. Baurjee: Proc. Int. Conf. Nuclear Structure, Kingston (1960), p.461.
5. Bat60 E. E. Beart, L. L. Green and J. C. Willmott: Proc. Int. Conf. Nuclear Structure, Kingston (1960), p.483.

6. Bav59 B.I.Belyaev: Mat.Fys.Medl.Dan.Vid.Selsk.
21, no.11 (1959).

7. Bro58 C.Broude, L.L.Green and J.C.Willmott: Proc.
Phys.Soc. (London), 72, 1132 (1958).

8. Bry57 D.A.Bronley, H.E.Gove and A.E.Litherland:
Can.J.Phys. 35, 1057 (1957).

9. Dav58 A.S.Davydov and G.P.Filippov: Nuclear Physics,
9, 237 (1958).

10. Dav60 A.S.Davydov and A.A.Chaban: Nuclear Physics,
21, 499 (1960).

11. Dav61 A.S.Davydov: Nuclear Physics, 24, 682 (1961).

12. Edn59 H.J.Eden: "Nuclear Reactions", Vol.I, p.1,
North Holland Publishing Company (1959).

13. Ell55 J.P.Elliott and B.H.Flowers: Proc.Roy.Soc.
A282, 536 (1955).

14. For55 R.W.Ford and C.Levinson: Phys.Rev. 100, 1
(1955).

15. Goe58 H.E.Gove, G.A.Bartholomew, H.S.Paul and
A.E.Litherland: Nuclear Physics, 9, 132 (1958).

16. Goe60 H.E.Gove: Proc.Int.Conf.Nuclear Structure,
Kingston (1960), p.432.

17. Gr51 L.L.Green, J.C.Willmott and G.Kaye: Nuclear Physics, 25, 278 (1951).
18. Mon59 B.R.Mottelson: "The Many Body Problem", University de Grenoble (1959), p.283.
19. Pan56 S.P.Paniya: Phys.Rev. 100, 956 (1956).
20. Pa57 H.S.Paul: Phil.Mag. 2, 311 (1957).
21. Ray57 G.Rakavy: Nuclear Physics, 4, 375 (1957).
22. Ras57 B.J.Ras: Phys.Rev. 107, 1201 (1957).
23. Sho57 H.K.Sheline: Nuclear Physics, 2, 322 (1956/57).
24. Tre56 W.W.True: Phys.Rev. 101, 1342 (1956).
25. Tre56 W.W.True and E.W.Ford: Phys.Rev. 102, 1375 (1956).
26. Tre61 W.W.True: Nuclear Physics, 22, 155 (1961).

CHAPTER II

THE SHELL MODEL

1. Introduction

In this chapter we present the results of calculations on the energy levels of some simple nuclei with $A > 28$, on the basis of the nuclear shell model. These will enable us to understand the extent to which the nuclear properties in this region depart from pure shell model results. These calculations will also form the framework in which one may subsequently incorporate the collective vibrations and study the modifications in the nuclear properties brought about.

Apart from the unpublished results of Levinson et al to which we referred in the earlier chapter (Sec 50), we have only the calculations of Elliot and Flowers (1955) on the properties of nuclei with $A = 18, 19$ in terms of the intermediate coupling shell model which was found to be so successful in the p -shell. The results of these calculations agree well with the experiments. We would only mention here that although in general the wavefunctions show that the situation in these nuclei is far from pure jj -coupling, the levels with the highest isotopic spin values $T = 1$ and $T = 3/2$, can be, with a fair amount of approximation, represented by a jj -coupling scheme, and a useful estimate of the energies of the various levels can

be obtained by such a simple calculation. For example, an analysis of the $^{17}\text{O}(d,p)^{18}\text{O}$ reaction data by MacFarlane and French (Mac60) shows that the 2^+ level in ^{18}O at 1.95 MeV is 80 - 85% $(d_{5/2})^2$ and only 15 - 20% $(d_{5/2})(s_{1/2})$, whereas the intermediate coupling shell model predicts a larger mixing, i.e., about 40% for the latter configuration.

Since the calculations of Elliot and Flowers were done, more data have accumulated on the energy levels of ^{18}O and ^{19}F . The known levels of these isotopes (Lid61, Sinf1) are given in fig. 1a and fig. 1b. The lowest five levels of ^{18}O can easily be interpreted in terms of 0, 1 and 2 phonon vibrations. However, with a suitable choice of internucleon forces, the levels can also be interpreted in terms of simple shell model configurations $(d_{5/2})^2$, $(s_{1/2})^2$ and $(d_{5/2})(s_{1/2})$. The study of electromagnetic transitions in these states may enable us to decide between these two alternatives. We do not consider these nuclei in any detail now, except one small point. There exists in case of pure jj -coupling a simple relationship between the energy levels of the $(j)^3$ and the $(j)^2$ configurations. If we consider the first three levels of ^{18}O as due to the configuration $(d_{5/2})^2$ ($^{17}\text{O}(d,p)$ experiments show this to be a good approximation), we can easily calculate the levels in ^{19}O due to the configuration $(d_{5/2})^3$. The result is shown in fig. 1c. The calculation also shows that owing to a cancellation of two large numbers, the separation of the $5/2^+$ and $3/2^+$ states is very sensitive to the positions of

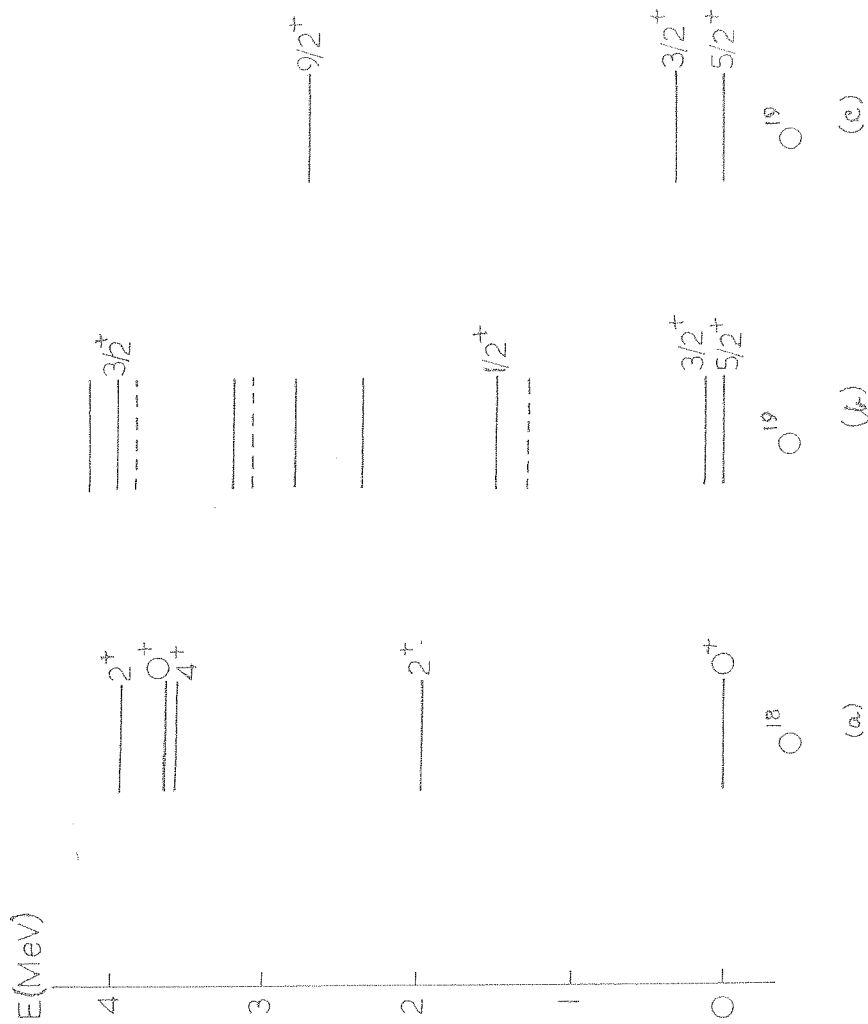


FIG. 1. ENERGY LEVELS OF O^{19} : (b) EXPERIMENTAL. (c) CALCULATED FROM THE LEVELS OF O^{18} (a)

the 2^+ and 4^+ levels of the $(d_{5/2})^2$ configuration. However, it provides a strong indication that the excited state at 0.1 MeV in O^{19} should have spin $3/2^+$. One can similarly argue that the $J = 1/2^+$ level of the configuration $(d_{5/2})^2(s_{1/2})$ should be at or above 1 MeV. Thus a simple calculation enables us to understand the low levels of O^{19} ; we are further able to predict that one of the observed levels at 2.35 and 2.70 MeV should have spin $9/2^+$.

The point here is that within certain limitations, simple calculations in terms of the jj -coupling shell model do give an orientation to the understanding of correct results and provide a framework on which more complicated calculations may be based. Such considerations were also applied by Pandya to nuclei near the end of the $2s - 1d$ shell.

2. One Nucleon (or Hole) Configurations:

Si^{29} , P^{29} and P^{31}

In terms of the simplest form of the jj -coupling shell model we may consider the nuclei Si^{29} , P^{29} and P^{31} as consisting of a nucleon outside an even-even spherical core of closed subshells. For Si^{29} and P^{29} the core consists of 14 protons and 14 neutrons filling all the subshells up to $d_{5/2}$, and for P^{31} there would be two more neutrons in the core filling up the $s_{1/2}$ subshell as well. The extra-core nucleon may occupy the $s_{1/2}$ or $d_{5/2}$ states,

if we confine our attention to positive parity states only. Correspondingly we observe in these nuclei the ground state $1/2^+$ and the first excited state $3/2^+$. There is however considerable evidence that the picture is not so simple and these observed states are not pure single particle states.

Firstly, on the basis of such a model, one would not obtain any more positive parity states, unless core-excitation and break up of the closed shell configurations is considered. The presence of other low-lying positive parity states indicate that the core is easily excited. In fact, one would expect this from the fact that the first excited state in Si^{28} occurs already at 1.78 MeV. Thus it is not surprising to observe a second excited state in Si^{28} and P^{29} at ~ 2 MeV, which one can attribute to the excitation of a $d_{3/2}$ particle from the core. Analysis of stripping experiments by MacFarlane and French (Mac60) also establishes that the Si^{28} ground state configuration contains hardly 50% closed shell configuration.

Secondly, the observed ground state magnetic moments for these nuclei, viz., $-0.55n.m.$ for Si^{28} and $1.13n.m.$ for P^{31} are also in disagreement with the Schmidt values based on a single particle shell model ($-1.91n.m.$ for Si^{28} and $2.80n.m.$ for P^{29} and P^{31}). Similarly, the selection rules for electromagnetic transitions forbid an M1 transition

for $g_{1/2} \leftrightarrow d_{3/2}$ states, whereas experimentally the transition from the first excited state to the ground state is found to have a considerable M1 component.

Unfortunately, the single particle shell model has also been damned on incorrect grounds. On this model, one may interpret the second excited state of Si^{29} or P^{29} as a hole in the closed subshell $d_{5/2}$. It is then clear that an electromagnetic transition from this state to the first excited state would involve a two-nucleon transition $((d_{5/2})^{-1}(g_{1/2})^2 \rightarrow (d_{5/2})^6(d_{3/2})^1)$, and would thus be forbidden. This second excited state can then only decay by an E2 transition to the ground state. This is really in agreement with the experimental data. However, Bromley et al (Bry57) interpret the second excited state as simply a $d_{5/2}$ particle state, and expect a mainly M1 transition to the first excited state; absence of this is then argued against the validity of the single particle shell model.

It is clear now that a simple single particle jj -coupling shell model cannot account for the observed properties of nuclei such as P^{29} , Si^{29} and P^{31} . Configuration mixing involving break up of the underlying closed shells has to be invoked. The contributions of the core to the nuclear properties are most easily taken into account by introducing collective motions - rotations or vibrations. In the next chapter we discuss these topics in more detail.

3. Two-Nucleon Configurations: si^{30} and p^{30} .

We now consider the nuclei si^{30} and p^{30} in terms of a two-nucleon model. The last two nucleons can have the configurations $(s_{1/2})^2$, $(s_{1/2})(d_{3/2})$ and $(d_{3/2})^2$ according to the jj -coupling scheme. We consider harmonic oscillator wavefunctions for single nucleons:

$$\Psi_{nl}(r, \theta, \phi) = R_{nl}(r) \Phi_{jm}(\theta, \phi) \quad (1)$$

with

$$R_{2s}(r) = \left(\frac{2}{\pi}\right)^{1/4} \frac{2\sqrt{3}}{r_s^{3/2}} \left(1 - \frac{4}{3} \cdot \frac{r^2}{r_s^2}\right) e^{-r^2/r_s^2} \quad (1a)$$

and

$$R_{1d}(r) = \left(\frac{2}{\pi}\right)^{1/4} \frac{8\sqrt{2}}{\sqrt{15} r_d^{3/2}} \left(\frac{r}{r_d}\right)^2 e^{-r^2/r_d^2} \quad (1b)$$

r, θ, ϕ denote the polar coordinates of the nucleons with respect to the centre of the nucleus and r_s and r_d the extension of the wavefunctions. We assume $r_s = r_d = r$. Φ is the spin-angular part of the wavefunction.

The Hamiltonian whose matrix we need to construct in this configuration space is taken as

$$H_S = E(n_1 l_1 j_1) + E(n_2 l_2 j_2) + H_{12} \quad (2)$$

where, $E(nlj)$ is the energy of a single nucleon in the oscillator subshell nlj , and H_{12} is a central interaction:

$$H_{12} = (a_{\pm} + b_{\pm} \vec{\sigma}_1 \cdot \vec{\sigma}_2) \exp[-(r/r_0)^2] \quad (3)$$

The + and - suffix distinguish interactions in states of isotopic spin 1 and 0 respectively. For simplicity, we choose Gaussian shape for the radial part of the interaction. The range parameter enters the calculations only in the combination $\lambda = r_0/r_d = r_0/r_d$. It was found by French and Raz (FrR53) on calculations of calcium isotopes, and also by us in the course of calculations on Kr^{90} (Thudl), that $\lambda \approx 1.0$. We are following the conventional shell model methods and assumptions, and do not describe the calculations in any detail. The matrix elements of H_{12} are given by the wellknown equation:

$$\begin{aligned} & \langle l_1' j_1' l_2' j_2' | H_{12} | l_1 j_1 l_2 j_2 \rangle_{J,T} \\ &= 2 a_{j_1 j_2} a_{j_1' j_2'} \sum_k \left[a f_{0k}(l_1 j_1 : l_2 j_2) \right. \\ & \quad \left. + k f_{1k}(l_1 j_1 : l_2 j_2) \right] F^k(l_1' l_2' : l_1 l_2) \\ & \quad + (-1)^{j_1 + j_2 + T - J} \text{ (same with } l_1 \rightleftharpoons l_2 ; j_1 \leftrightarrow j_2 \text{)} \end{aligned} \quad (4)$$

where,

$$f_{nk}(l_1 j_1 : l_2 j_2) = (-1)^{j_1' + j_2 - J + l_1 + l_2 + n + k} \frac{1}{2(2n+1)} \left([j_1] [j_2] [j_1'] [j_2'] \right)^{1/2}$$

$$D_{l_1' l_1 k} D_{l_2' l_2 k} \sum_r (-1)^r [r] W(j_1' j_2' j_1 j_2 : J r) \times$$

$$\left\{ \begin{matrix} 1/2 & l_1' & j_1' \\ 1/2 & l_1 & j_1 \\ n & k & r \end{matrix} \right\} \left\{ \begin{matrix} 1/2 & l_2' & j_2' \\ 1/2 & l_2 & j_2 \\ n & k & r \end{matrix} \right\} \quad (4a)$$

with

$$[j] \equiv (2j+1)$$

$$\begin{aligned} a_{j j'} &= 1/2 \quad \text{if } j = j' \\ &= 1/\sqrt{2} \quad \text{if } j \neq j' \end{aligned}$$

$$D_{l_1 l_2 k} = \sqrt{\frac{(2l_1+1)(2l_2+1)}{2k+1}} C \begin{matrix} l_1 & l_2 & k \\ 0 & 0 & 0 \end{matrix}$$

where, the Clebsch-Gordan coefficient $C \begin{matrix} j_1 & j_2 & j \\ m_1 & m_2 & m \end{matrix} \equiv (j_1 j_2 m_1 m_2 | j_1 j_2 j m)$ in the notation of Condon and Shortley (Con53).

$W(\)$ denote Racah coefficients (Rah42) and the quantities in the curly brackets are X-coefficients or 9j-symbols. $P^{k,s}$ are the Slater integrals (Sl152), and table I lists the integrals relevant for the $s-d$ shell, for the range parameter $\lambda = 0.8$ and 1.0 . We also list in tables II and III the matrix elements of H_{12} for the various states of the configurations considered.

(a) $^{20}_{81}Li$ $1.1 = 1.1$ states:

In this case the energy levels are those of two neutrons outside the stable spherical core of 14 neutrons and 14 protons. We find it more convenient to write the interaction as

$$H_{12} = (1 + \kappa \vec{\sigma}_1 \cdot \vec{\sigma}_2) V_0 e^{-(r/r_0)^2} \quad (4')$$

with $a_+ = V_0$ and $\kappa = b_+/a_+$

Now the parameters of the model are λ , κ , V_0 and the separation of the single particle states $\Delta = \epsilon(1d_{3/2}) - \epsilon(2s_{1/2})$. Since the energy of the first excited state $3/2^+$ in $^{20}_{81}Li$ and $^{20}_{81}P$ is about 1.3 MeV, we take $\Delta = 1.5$ MeV for our

TABLE I

Slater Integrals for the $3s = 14$ Shell.

$F^k(1s_1 1s_2 1s_1 1s_2)$	$\lambda = 0.8$	$\lambda = 1.0$
$F^0(ss:ss)$	0.10435	0.12514
$F^0(dd:dd)$	0.08714	0.14575
$F^2(dd:dd)$	0.12853	0.20946
$F^4(dd:dd)$	0.07371	0.05215
$F^0(sd:sd)$	0.08603	0.14833
$F^2(sd:sd)$	0.08023	0.10931
$F^2(ss:dd)$	-0.12392	-0.14776

TABLE IX

Matrix Elements of U_{12} for $t = 1$.

$\langle U_{12} \rangle$	J	$\lambda = 0.9$		$\lambda = 1.0$	
		coef. of a_1	coef. of b_1	coef. of a_1	coef. of b_1
$\langle (\rho_{1/2})^2 (\rho_{1/2})^2 \rangle$	0	0.1049	-0.3132	0.1551	-0.4094
$\langle (d_{3/2})^2 (d_{3/2})^2 \rangle$	0	0.1249	-0.1365	0.1577	-0.1644
"	2	0.0545	-0.0273	0.1207	-0.0323
$\langle \rho_{1/2} d_{3/2} \rho_{1/2} d_{3/2} \rangle$	1	0.0320	0.0330	0.1271	0.1271
"	2	0.0025	-0.0342	0.1445	-0.1227
$\langle (\rho_{1/2})^2 (d_{3/2})^2 \rangle$	0	0.0235	-0.0766	0.0309	-0.0327
$\langle \rho_{1/2} d_{3/2} (d_{3/2})^2 \rangle$	2	-0.0140	0.0326	-0.0167	0.0527

TABLE III

Matrix Elements of H_{12} for $t = 0$.

$\langle H_{12} \rangle$	j	$\lambda = 0.5$		$\lambda = 1.0$	
		coef. of a_+	coef. of b_+	coef. of a_+	coef. of b_+
$\langle (\beta_{1/2})^2 (\beta_{1/2})^2 \rangle$	1	0.1049	0.1040	0.1051	0.1051
$\langle (d_{3/2})^2 (d_{3/2})^2 \rangle$	1	0.0947	-0.0478	0.1042	-0.0045
"	3	0.0947	0.0507	0.1042	0.0034
$\langle \beta_{1/2} d_{3/2} \beta_{1/2} d_{3/2} \rangle$	1	0.1041	0.1041	0.1008	0.1008
"	2	0.0806	-0.0101	0.1003	-0.0000
$\langle (\beta_{1/2})^2 (d_{3/2})^2 \rangle$	1	-0.0114	-0.0114	-0.0138	-0.0138
$\langle \beta_{1/2} d_{3/2} (d_{3/2})^2 \rangle$	1	-0.0314	-0.0314	-0.0374	-0.0374

calculations. We know that actually this $3/2^+$ state is not pure and configuration mixing would have depressed it from the pure $d_{3/2}$ state; thus Δ should be larger than 1.3 MeV. We have also carried out calculations for $\Delta = 2.0$ MeV, and the results are qualitatively not different.

It has been noted that near the close of the $2s - 1d$ shell, jj -coupling is a good approximation for the calculation of the energies of nuclear states. We can therefore safely interpret the ground and first excited states of A^{38} as 0^+ and 2^+ states of the $(d_{3/2})^2$ configuration. Excitation energy of this 2^+ state is 2.15 MeV. We assume that the nuclear interaction does not change drastically in neighbouring nuclei. Then we use this datum to fix one more parameter. For a given value of λ and κ , V_0 is so chosen as to give correctly this observed separation of the $0^+ - 2^+$ states in A^{38} . The value of κ is varied from -0.4 to +0.2, and λ is given the values 0.5 and 1.0.

Now the matrices of the Hamiltonian H are constructed for different values of J (spin), and are diagonalized. The resulting energy level schemes for various values of the parameters are shown in fig. 3; the energy levels are normalized to the ground state 0^+ . Also shown are the observed levels of Bi^{30} .

We note that for $\kappa > 0$, there occurs a low lying 1^+ state (below 3 MeV), for which there is no observational evidence. For $\kappa \geq 0.2$, we find the ground state to have a

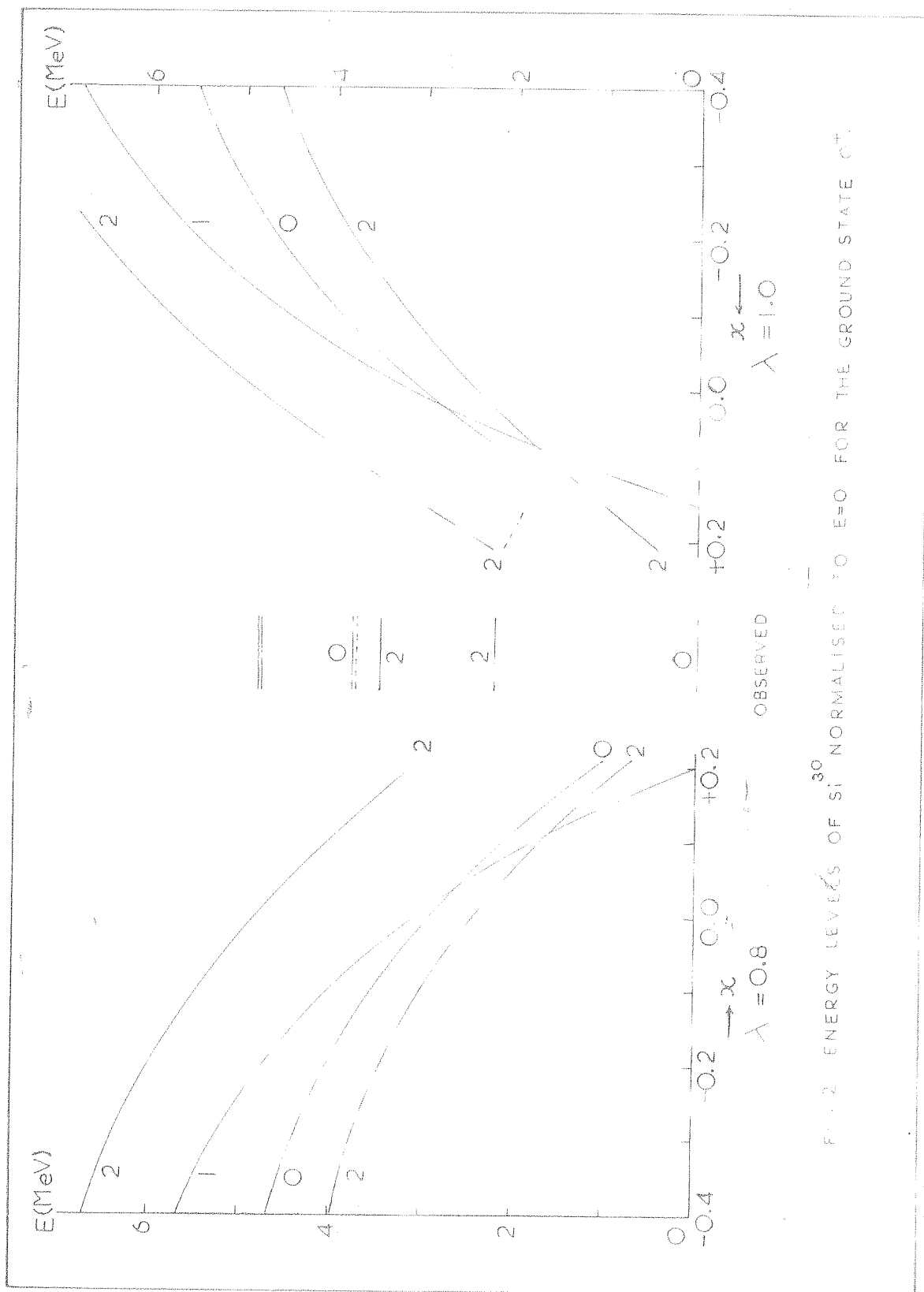


FIG. 2. ENERGY LEVELS OF ^{30}Si NORMALISED TO $E=0$ FOR THE GROUND STATE 0^+ .

dominant component $(1_{3/2})^2$ rather than $(1_{1/2})^2$. On the other hand, for large negative values of χ , the energy of the first excited state increases very rapidly. Thus only the region $\chi \leq 0$ is of some interest for comparison with the observed level scheme. Even in this region, we do not get a 2^+ as the second excited state. It is clear that there are more states than jj -coupling shell model can give, and even qualitatively the calculations do not agree with the observed data, except perhaps for providing an excited 0^+ state at about the right energy.

We shall see in the next chapter that inclusion of collective vibrations of the core improves considerably the agreement between calculations and observations.

(b) $^{30}\text{P}, I = 0$ states.

We first of all remark that $I = 1$ levels have been identified in ^{30}P (Nat50) at 0.583 MeV (0^+), 3.94 MeV (2^+) and at 4.2^(2±) and 4.5 MeV, the last one of unknown spin value. These correspond very well with the $I = 1$ levels of ^{30}Si , and we can safely predict the spin of the 4.5 MeV state to be 0^+ . We should also expect at 4.5 MeV a close doublet.

Now consider the $I = 0$ levels of ^{30}P . Again we take $\Delta = 1.5$ MeV and $\lambda = 0.8$ and 1.0. Earlier calculations of Paniya and Shah (Pan61) on the $I = 0$ levels of the $(1_{3/2})^2$ configuration, give $b_- = -2.6$ MeV and -4.0 MeV respectively for $\lambda = 1.0$ and 0.8. These estimates seem to be quite

TABLE IV

Eigenvalues of H_2 for $T = 1$.

a) $\Delta = 1.5 \text{ MeV}; \lambda = 0.8$

x	$-V_0$ (MeV)	$J = 0$		$J = 2$		$J = 1$
		E_1	E_2	E_1	E_2	
-0.4	20.5	-5.039	-0.376	-1.085	1.655	0.664
-0.3	22.9	-4.671	-0.495	-1.135	1.530	0.410
-0.2	25.9	-4.553	-0.641	-1.239	1.351	0.091
-0.1	29.9	-4.383	-0.839	-1.359	1.129	-0.330
0.0	35.3	-4.014	-1.098	-1.521	0.829	-0.900
+0.1	43.1	-3.508	-1.450	-1.761	0.399	-1.724
+0.2	55.3	-2.919	-1.790	-2.151	-0.248	-3.013

b) $\Delta = 1.5 \text{ MeV}; \lambda = 1.0$

x	$-V_0$ (MeV)	$J = 0$		$J = 2$		$J = 1$
		E_1	E_2	E_1	E_2	
-0.4	17.8	-5.755	-1.233	-2.126	0.815	0.164
-0.3	20.0	-5.569	-1.455	-2.347	0.573	-0.278
-0.2	22.8	-5.326	-1.734	-2.549	0.265	-0.817
-0.1	26.6	-5.032	-2.114	-2.833	-0.151	-1.540
0.0	31.8	-4.618	-2.604	-3.214	-0.720	-2.539
+0.1	39.5	-4.107	-3.221	-3.779	-1.559	-4.018
+0.2	53.3	-3.319	-3.823	-4.733	-2.942	-6.471

TABLE V

Eigenvalues of H_0 for $t = 0$.

a) $\Delta = 1.5$ MeV; $\lambda = 0.8$; $b_+ = -4.0$ MeV

$-a-$ (MeV)	$J = 1$			$J = 2$	$J = 3$
	E_1	E_2	E_3		
30	-3.613	-2.434	0.788	-1.114	-0.020
35	-4.155	-3.046	0.423	-1.533	-0.553
40	-4.702	-3.650	0.063	-2.011	-1.027
45	-5.254	-4.271	-0.292	-2.450	-1.500
50	-5.811	-4.882	-0.644	-2.908	-1.974
55	-6.377	-5.485	-0.992	-3.387	-2.447

b) $\Delta = 1.5$ MeV; $\lambda = 1.0$; $b_+ = -2.0$ MeV

$-a-$ (MeV)	$J = 1$			$J = 2$	$J = 3$
	E_1	E_2	E_3		
30	-5.450	-4.514	-0.893	-3.969	-1.943
35	-6.310	-5.466	-1.537	-3.736	-2.514
40	-7.173	-6.410	-2.173	-4.503	-3.385
45	-8.062	-7.345	-2.805	-5.260	-4.155
50	-8.967	-8.262	-3.435	-6.035	-4.927
55	-9.896	-9.181	-4.061	-6.802	-5.698

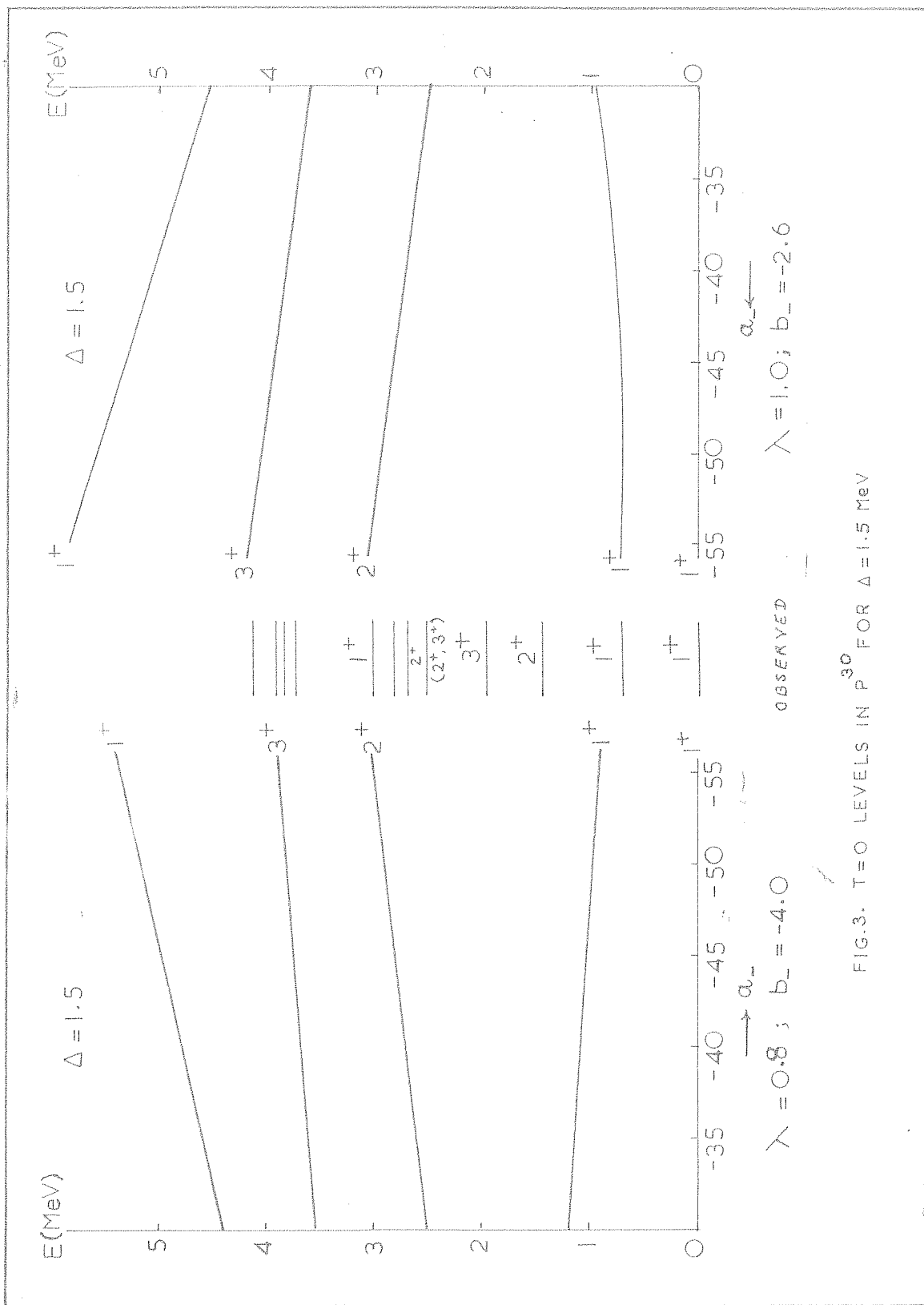


FIG.3. T=0 LEVELS IN ^{30}P FOR $\Delta = 1.5$ MeV

reasonable in this region, and we adopt these values in our calculations. The value of a_{π} is now varied from -30 MeV to -50 MeV. The Hamiltonian matrices for $J = 1^+, 2^+$ and 3^+ are diagonalized, and the resulting level scheme is shown in fig. 3; the levels are normalised to ground state 1^+ as observed in P^{30} . The experimental data on $T = 0$ levels of P^{30} are also shown.

It is obvious that to a considerable extent the level scheme is independent of the value of a_{π} . We find again that the energy levels are predicted at much higher excitation energies than those observed. It may be possible to improve the agreement between calculated levels and experimental data by changing the parameters b_{π} and Δ to some extent. However, we do not attempt to produce a good fit here since arguments have already been presented for expecting collective vibrations in these nuclei.

4. Three-Nucleon Configuration: $T = 3/2$

We only give here results for the simple case of three identical nucleons outside the even-even core of 14 protons and 14 neutrons. In view of the results already described in previous sections, we should not expect a good agreement with the experimental data. The configurations to be considered in this case are

$$(a) (s_{1/2})^2 d_{3/2}, \quad (b) (s_{1/2})(d_{3/2})^2 \quad \text{and} \quad (c) (d_{3/2})^3$$

The wavefunction corresponding to the configuration (c) is just

the one-hole wavefunction. For the configurations (a) and (b), the antisymmetrized wavefunction is given by

$$\Psi_T \{ (j^2)_{J_0}, j' \} = \frac{1}{\sqrt{3}} \left[\Psi_{J_0}(j^2) \times \phi_{j'} \right. \\ \left. - (-1)^{\frac{j+J}{2}} \sum_{J_1} (-1)^{J_1} U(jj j' : J_0 J_1) \Psi_{J_1}(jj') \times \phi_j \right] \quad (5)$$

where, $U(abcd: ef) = \{ (2a+1)(2b+1) \}^{1/2} U(abcd: ef)$ and 'x' denotes vector-coupling. The matrix elements of the two-body Hamiltonian H_{12} are given by

$$\langle (j^2)_{J_0}, j' | H_{12} | (j^2)_{J_0'}, j' \rangle_{J,T} \\ = \frac{1}{3} \left[\delta_{J_0 J_0'} \delta_{j' j'} \langle j^2 | H_{12} | j^2 \rangle_{J_0} \right. \\ - \delta_{j' j} (-1)^{\frac{j+J}{2}} \frac{1}{\sqrt{2}} U(jj j j' : J_0' J_0) \langle j^2 | H_{12} | jj' \rangle_{J_0} \\ - \delta_{j' j'} (-1)^{\frac{j+J}{2}} \frac{1}{\sqrt{2}} U(jj j j' : J_0 J_0') \langle jj' | H_{12} | j^2 \rangle_{J_0'} \\ \left. + \delta_{jj'} 2 \sum_{J_1} U(jj j j' : J_0 J_1) U(jj j j' : J_0' J_1) \langle jj' | H_{12} | jj' \rangle_{J_1} \right] \quad (6)$$

The two-particle matrix elements are the same as evaluated for $d1^{30}$ (eq.4), and we use the same parameters and the same values. The matrix elements of the Hamiltonian for three nucleons given by $\langle H \rangle = 3 \langle H_{12} \rangle$ are tabulated in

TABLE VI

Matrix Elements of the Hamiltonian for Three Nucleons: $\lambda = 0.8$

$\langle H \rangle$	$\begin{array}{c} \chi \\ \psi \end{array}$	τ						
		-0.4	-0.3	-0.2	-0.1	0.0	+0.1	+0.2
$\langle (d_{3/2})_0^2 \delta_{1/2} (d_{3/2})_0^2 \delta_{1/2} \rangle$	1/2	-7.234	-7.700	-8.214	-8.913	-9.849	-11.203	-12.319
$\langle (d_{3/2})_2^2 \delta_{1/2} (d_{3/2})_2^2 \delta_{1/2} \rangle$	3/2	-3.936	-4.537	-5.216	-5.919	-7.339	-9.101	-11.557
"	5/2	-5.923	-6.230	-6.670	-7.229	-7.973	-9.061	-10.754
$\langle (\delta_{1/2})_0^2 d_{3/2} (\delta_{1/2})_0^2 d_{3/2} \rangle$	3/2	-3.340	-3.470	-3.623	-3.843	-4.143	-4.570	-5.023
$\langle (d_{3/2})_0^2 d_{3/2} (d_{3/2})_0^2 d_{3/2} \rangle$	3/2	-5.711	-6.057	-6.509	-7.105	-7.907	-9.055	-10.578
$\langle (\delta_{1/2})_0^2 d_{3/2} (d_{3/2})_2^2 \delta_{1/2} \rangle$	3/2	-0.806	-0.784	-0.711	-0.645	-0.551	-0.423	-0.215
$\langle (\delta_{1/2})_0^2 d_{3/2} (d_{3/2})_0^2 d_{3/2} \rangle$	3/2	-0.813	-0.735	-0.747	-0.700	-0.635	-0.542	-0.326
$\langle (d_{3/2})_2^2 \delta_{1/2} (d_{3/2})_0^2 d_{3/2} \rangle$	3/2	0.804	0.784	0.711	0.645	0.551	0.423	0.215

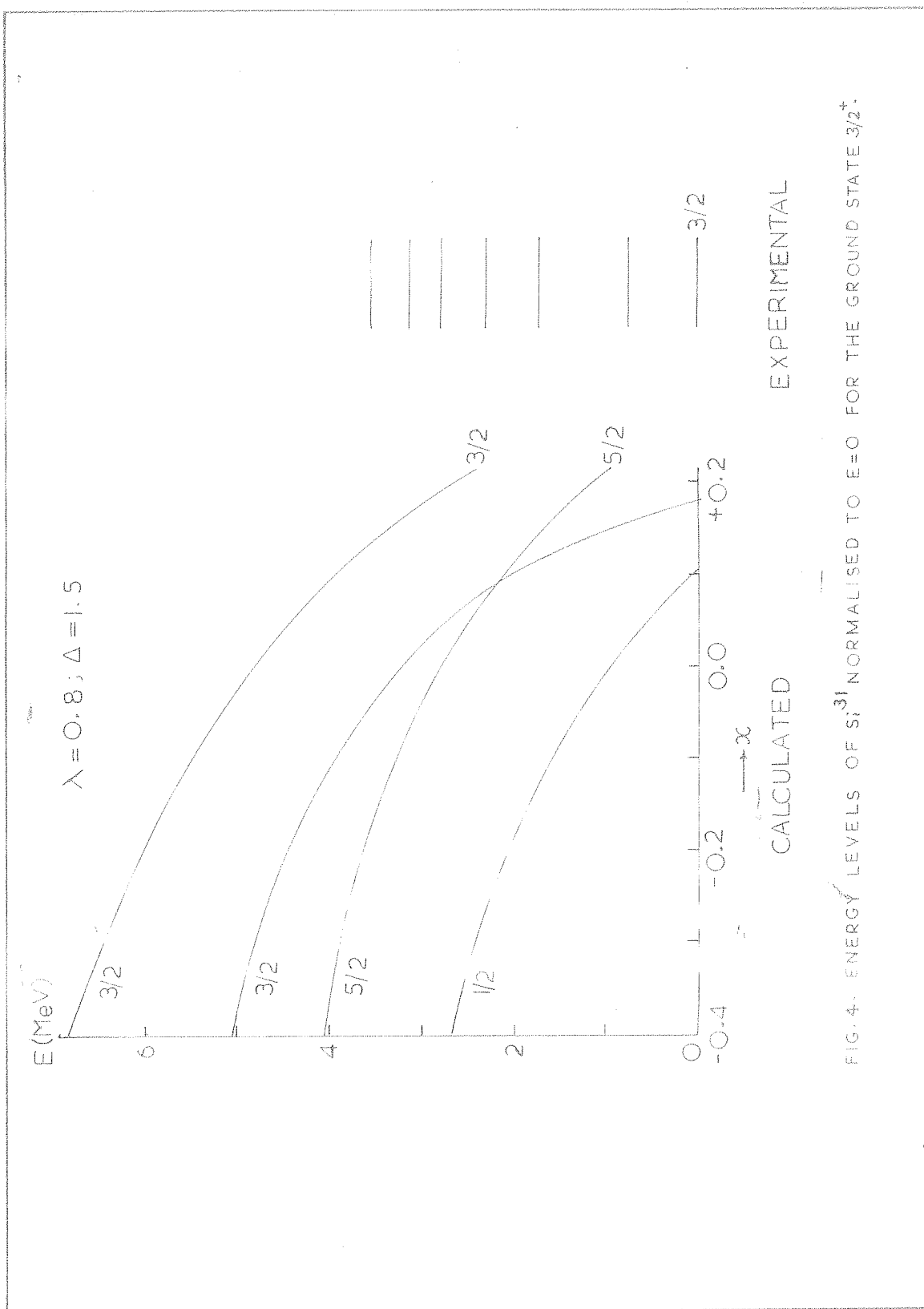


FIG. 4. ENERGY LEVELS OF ^{31}Si NORMALISED TO $E=0$ FOR THE GROUND STATE $3/2^+$.

table VI for $\lambda = 0.8$. The energy levels obtained with $\Delta = 1.5$ MeV and $\lambda = 0.8$ are shown in fig. 4. Detailed comparison with experimental data is not attempted.

5. Parameters of the Nuclear Interaction

We shall make some comments on the nature of the two-body interaction H_{12} that we have chosen for the above calculations. The shape and the range of the potential need no comment, since the Gaussian shape is adopted for convenience and the range is typical of usual shell model calculations. The parameters a_1 and b_1 of the interaction in $T = 1$ states have been varied and from the results of this chapter, as well as the results to be described in the subsequent chapter, we find that the best values are

$$a_1 = -25 \text{ MeV}; \quad b_1 = +5 \text{ MeV}; \quad \lambda = 0.8$$

The value of b_1 is chosen to give the separation of the $I = 3^+$ and 1^+ levels of the $(d_1/2)^{-2}$ configuration as observed in K^{38} . Here the assumption is that the 0.44 MeV state observed by Hashimoto and Alford (1960) is indeed a $T = 0, I = 1$ state. With this value of b_1 , the splitting of the $(d_1/2)(d_3/2)$ neutron-proton $T = 0$ doublet has been calculated, giving 0.25 and 0.32 MeV respectively for $\lambda = 0.8$ and 1.0. Such a doublet should be seen among the excited $T = 0$ states of p^{30} . In fact, it is tempting to assume the 0.7 MeV(1^+) and 1.4 MeV(3^+) states to belong to this doublet.

These levels may also be seen in Cl^{36} excited states, and the observed 1^+ and 2^+ states at 1.6 and 1.9 MeV may be identified with this doublet. The energy levels of p^{30} calculated in this chapter are relatively independent of a_- . However, following Pandya and Shah (Paa61) one can calculate a_- to fit the separation of the $J = 2^+$ and 3^+ states of the $(d_{3/2})^2$ configuration, combining the data of K^{38} and A^{38} . This gives

$$a_- = -40.0 \text{ MeV}; \quad b_- = -4.0 \text{ MeV for } \lambda = 0.8$$

A characteristic of these interactions is that the spin-dependence is very weak, i.e., $|b/a| \approx 0.1 - 0.2$. This qualitative result is already confirmed by many authors.

In terms of A_{JJ} , the strength of the potential in a state of isotopic spin T and spin J of the two nucleons, we find

$$A_{01} = -44 \text{ MeV}; \quad A_{00} = -28 \text{ MeV}; \quad A_{10} = -40 \text{ MeV};$$

$$A_{11} = -20 \text{ MeV}$$

Our knowledge of the effective inter-nucleon forces in nuclei is very meagre and many different types of interactions have been proposed by various authors. Hence in the absence of a more fundamental derivation, it does not seem worth while to discuss this problem further.

We, however, note that there is considerable evidence to assume a good validity of the jj -coupling scheme in the $d_{3/2}$ subshell. If the energy levels of the pure $(d_{3/2})^2$

configuration were known, we could easily determine the precise nature of the nuclear interaction. Unfortunately, all the experimental data to-date are insufficient. Energy levels have been seen in Cl^{34} , K^{38} , Cl^{35} , Cl^{36} and A^{37} which partially support the validity of jj -coupling in this region, but additional identification of spins and parities of many levels is needed. When more data are available, it will be very fruitful to discuss the nuclei $A \geq 34$ in terms of a jj -coupling scheme.

6. Conclusion

We may now summarize the results reported in this chapter. We have considered the core configuration of the first 14 protons and neutrons to be spherical, stable and the nuclear properties independent of this core. We have calculated the energy levels of nuclei which correspond to one, two or three nucleons outside this core. It is generally found that experimentally one obtains many more levels than predicted by this simple model. The shell model levels have a wide spread in energy, and some other mechanism like core excitation must be invoked to obtain the additional low-lying energy levels. The electro-magnetic properties of the nuclear levels are also in disagreement with the shell model predictions.

REFERENCES

1. Bat60 E.B.Daart, L.L.Green and J.C.Willmott:
Proc.Int.Conf.Nuclear Structure,
Kingston (1960), p.466.
2. Con53 E.U.Condon and G.H.Shortley: "The Theory
of Atomic Spectra", Cambridge University
Press (1953).
3. Eli55 J.P.Elliott and B.H.Flowers: Proc.Roy.Soc.
A222, 536 (1955).
4. Fra53 J.B.French and B.J.Raz: Phys.Rev. 104,
1411 (1953).
5. Hae59 Y.Hashimoto and Y.H.Alford: Phys.Rev. 115,
981 (1959).
6. Lit61 A.B.Lithariani, R.Bachelor, A.J.Ferguson
and H.E.Gove: Can.J.Phys. 39, 276 (1961).
7. Mac60 H.H.MacFarlane and J.B.French: Rev.Mod.Phys.
32, 557 (1960).
8. Pan61 S.P.Paniya and S.K.Shah: Nuclear Physics,
21, 326 (1961).
9. Raz62 G.Razeh: Phys.Rev. 122, 466 (1962).
10. Sjo61 B.Sjogren, G.Nickelberg and N.Johansson:
Arkiv Fysik, 20, 117 (1961).

11. Tsi32 I. Faind: *Helv. Phys. Acta*, **25**, 185 (1952).
12. Tsi51 V. K. Thadkappan, L. C. Waghmare and A. P. Panikar:
Prog. Theo. Phys. **25**, 22 (1961).

ooo o ooo

CHAPTER III

THE COLLECTIVE MODEL

1. Introduction

We have shown in the previous chapter that the treatment of the properties of the nuclei with mass number $A \sim 30$ (P^{30} , Si^{30} , Si^{30} , P^{31} and Si^{31}) in terms of a pure jj -coupling shell model (including mixing of the $s_{1/2}$ and $d_{3/2}$ configurations by two-body nuclear forces) is inadequate to explain the experimental data. Some of these nuclei have been discussed in the literature in terms of a strong-coupling collective model (Bre53b, Ary57b), which presumes a considerable permanent deformation of the nuclei. This model has been very successful in explaining all the observed properties of nuclei in the region $A \sim 25$ (Lid58). However, as pointed out in the first chapter, there is some semi-theoretical reason to believe that as A increases and approaches $28 \sim 30$, the coupling of the individual nucleons with the nuclear surface may become weaker. Although 2 (or 2) $= 14$, 16 are not true 'magic' numbers, closing of the $d_{3/2}$ and $s_{1/2}$ subshells in quick succession may have the effect of enhancing to some extent the pairing forces giving rise to a spherical equilibrium shape. We have discussed in chapter I some experimental evidence relating to this. The attempt in this chapter is, therefore, to apply a weak-coupling collective model to the nuclei under consideration.

The difference from the jj -coupling model of the previous chapter is quite simple. We now consider the core of 14 protons and 14 neutrons (15 neutrons in the case of ^{31}P) to be not rigid, but deformable to some extent. If this deformation in shape is quite small and not permanent, i.e., has large fluctuations in time, one may analyse it in terms of oscillations of the surface of various multipole types. If we assume that the collective potential seen by an individual nucleon outside the core has the same shape as the nuclear surface, we are led directly to a coupling of the independent particle motion to the surface oscillations of the nucleus. The weak-coupling model assumes small deformations, i.e., the amplitude of the oscillations are small and correspondingly the term in the Hamiltonian coupling the particle motion and the surface oscillations is also small. In an extreme weak-coupling formalism, one may consider only one quantum of surface oscillations and the coupling term as a small perturbation. In an intermediate coupling formalism, one would consider two or three quanta of oscillations (to be referred to as 'phonons' in subsequent discussion) and would solve the Hamiltonian matrix including the coupling term exactly. This is the procedure that we shall follow.

This weak-coupling collective model was first discussed by Rainwater and Bohr (Bar50, Bor52) and was applied to considerations of electric quadrupole moments of nuclei by Rainwater (Bar50) and to magnetic moments by Foldy and

Milford (Foy50, Mil54). Kerman (Kem53) applied this model in one-phonon approximation to one- and two-nucleon configurations. Choudhury (Chy54) has worked out in detail an intermediate coupling calculation (including three phonons) for a single nucleon in a state $j = 5/2$. This calculation does not consider mixing of single particle states produced by coupling with surface oscillations. Feenberg (Feg55) has worked out the case of a single nucleon including mixing of single particle orbitals, in a weak-coupling perturbation approximation. He has in particular discussed some nuclei of interest to us, and we shall refer to his results in later discussion. Ford and Levinson (Fol55) and Scherff-Goldhaber and Weneser (Scr55) have considered the energy levels of the configurations $(f_{7/2})^2$, $(f_{7/2})^3$ and $(f_{7/2})^4$ using the intermediate coupling version of the collective model, but proper account of the direct two-body nuclear interactions is not included in these calculations, and the results are of qualitative interest. Calculations with realistic parameters and of practical interest were carried out by Raz (Raz57) for O^{17} and by Abraham and Warko (Abr58) for F^{19} . It was at this time that the calculations reported in this thesis were undertaken. While this work was in progress, a number of other calculations on similar lines for nuclei in other regions of the periodic table have been reported. Raz (Raz59) has investigated the properties of the $(f_{7/2})^2$ configuration, taking into account the interparticle forces as well as coupling with surface oscillations quite rigorously. However, the possibility of mixing

other single particle states is again neglected. In a series of papers, True (Tre55, 58, 61) has discussed the energy levels of Pb isotopes in terms of the weak-coupling collective model. Similar and equally extensive calculations have been performed by Sliv and others (Gus61, Slv61) on Pb^{206} , Pb^{208} and Bi^{210} during the last year.

In the next section, we describe the formalism for the weak-coupling collective model.

2. The Formalism

In the independent particle shell model calculations, core configuration plays no role and is not included in the Hamiltonian of the system. In this case the Hamiltonian for a number of particles outside the core is given by

$$H_p = \sum_i \left(\frac{1}{2M} p_i^2 + V_i \right) + \sum_{i < j} H_{ij} \quad (1)$$

$V(r)$ being the single particle spherically symmetrical potential experienced by each nucleon and H_{ij} the two-body nuclear interactions. We must add to this, the Hamiltonian corresponding to the collective motion of the core, H_c . Thus, the total Hamiltonian is given by

$$H = H_p + H_c \quad (2)$$

If the core deformation has small amplitude and fluctuates in time, the radius vector describing the nuclear surface

can be expanded in terms of spherical harmonics:

$$R(\theta, \phi; t) = R_0 \left[1 + \sum_{k\mu} \alpha_{k\mu}(t) Y_{k\mu}^{\mu}(\theta, \phi) \right] \quad (3)$$

We assume that the single particle potential seen by an extra-core nucleon is of the same shape as the nuclear surface; hence it now takes the form

$$V(r) = V(R) = V(R_0) + R_0 \left(\frac{\partial V}{\partial r} \right)_{r=R_0} \sum_{k\mu} \alpha_{k\mu} Y_{k\mu}^{\mu}(\theta, \phi) \quad (4)$$

where, only linear terms in $\alpha_{k\mu}$ are retained. The Hamiltonian for the particles is then

$$H_p = \sum_i \left(\frac{1}{2M} p_i^2 + V_i(R_0) \right) + \sum_{i < j} H_{ij} - \sum_i k(r_i) \sum_{k\mu} \alpha_{k\mu} Y_{k\mu}^{\mu}(\theta_i, \phi_i) \quad (5)$$

where,

$$-k(r) = R_0 \left(\frac{\partial V}{\partial r} \right)_{r=R_0}$$

The first two terms in eq.(5) are identical to the conventional shell model Hamiltonian, and the last term on the R.H.S. denotes now interaction of the extra-core nucleons with the core oscillations; we denote this term by H_{int} and the first two terms by H_0 .

$$H = H_0 + H_c + H_{int} \quad (6)$$

For a given nuclear configuration, we must evaluate the Hamiltonian matrix and diagonalize it to obtain its eigenvalues and eigenfunctions. We note that H_0 itself consists of two parts, the first term being the sum of single

particle Hamiltonians (including the usual spin-orbit coupling term $\vec{l} \cdot \vec{s}$), and the second term being the nuclear interactions. The eigenfunctions of the single particle potentials are well-known harmonic oscillator wavefunctions and were explicitly written down in the last chapter for $2s_{1/2}$ and $1d_{3/2}$ states. For a nuclear configuration of n particles in these states, we can construct a total anti-symmetrised eigenfunction of total angular momentum J and $J_z = M$. We shall denote this eigenfunction by $|\alpha JM\rangle$, α denoting the nuclear configuration. It is obvious that the eigenvalue of the single particle Hamiltonian for this eigenfunction will be sum of the single particle energies, $\sum_i^n \epsilon(n_i l_i j_i)$. The Matrix of H_{12} for such states can be evaluated by standard methods using coefficients of fractional parentage and Racah's tensor algebra.

We next consider the Hamiltonian of the core configuration. In eq.(3) of the nuclear surface, the first term in the series expansion ($k = 0$) corresponds only to a constant dilatation of the sphere R_0 , whereas the second term ($k = 1$) corresponds to a translation of the centre of mass of the core, so that it is of no importance in the study of excited states. For small deformations we are then justified in keeping only the lowest important term, viz., that corresponding to $k = 2$, and neglect all other terms. The particular term $k = 3$ would represent octupole vibrations the quantization of which would lead to a phonon of spin parity, 3^- . These vibrations have been investigated

for some nuclei but do not seem to be of any interest in the region under consideration here.

With the approximation of only quadrupole deformations, we have

$$R(\theta, \phi; t) = R_0 \left[1 + \sum_{\mu} \alpha_{\mu}(t) Y_2^{\mu}(\theta, \phi) \right] \quad (3a)$$

Here, α_{μ} may be treated as dynamical variables, and for small harmonic oscillations of the surface, one may obtain, in analogy with the one-dimensional harmonic oscillator, the expression for the Hamiltonian (assuming 6-dimensional isotropy),

$$H_c = T + V$$

$$T = \frac{1}{2} B \sum_{\mu} |\dot{\alpha}_{\mu}|^2 ; \quad V = \frac{1}{2} C \sum_{\mu} |\alpha_{\mu}|^2 \quad (3')$$

where, $\dot{\alpha}_{\mu}$ denotes time-derivative of α_{μ} , and B and C are parameters corresponding to mass and elastic constant or deformability. Initially, the nuclear core was assumed to be akin to a liquid drop and hydrodynamical values for B and C were generally calculated. However, it was soon discovered that these values would give wrong results and that it is better to treat B and C as free parameters pending their calculation from a more fundamental theory of the nucleus.

Introducing the conjugate momentum $\pi_{\mu} = \frac{\partial T}{\partial \dot{\alpha}_{\mu}} = B \dot{\alpha}_{\mu}^*$, we can write the Hamiltonian of the quadrupole oscillations

as

$$H_c = \frac{1}{2B} \sum_{\mu} |\pi_{\mu}|^2 + \frac{1}{2} C \sum_{\mu} |\mathcal{L}_{\mu}|^2 \quad (7')$$

and the frequency of oscillation as $\omega = \sqrt{C/B}$. The oscillations can be quantized using the formalism of the quantum field theory (Weiss); we introduce creation and destruction operators b_{μ}^* and b_{μ} :

$$\begin{aligned} \mathcal{L}_{\mu} &= \sqrt{\frac{\hbar \omega}{2C}} \left[b_{\mu} + (-1)^{\mu} b_{-\mu}^* \right] ; \quad \mathcal{L}_{\mu}^* = (-1)^{\mu} \mathcal{L}_{-\mu} \\ \pi_{\mu} &= i \sqrt{\frac{\hbar \omega B}{2}} \left[b_{\mu}^* - (-1)^{\mu} b_{-\mu} \right] ; \quad \pi_{\mu}^* = (-1)^{\mu} \pi_{-\mu} \end{aligned} \quad (8)$$

and the commutation relations

$$[b_{\mu}, b_{\mu'}] = [b_{\mu}^*, b_{\mu'}^*] = 0 ; \quad [b_{\mu}, b_{\mu'}^*] = \delta_{\mu\mu'} \quad (9)$$

The Hamiltonian H_0 now takes the form

$$H_c = \hbar \omega \left[S/2 + \sum_{\mu} b_{\mu}^* b_{\mu} \right] \quad (7)$$

with $b_{\mu}^* b_{\mu} = n_{\mu}$, n_{μ} being the operator corresponding to the number of quanta with z -component of angular momentum equal to μ .

The eigenfunctions of H_0 can easily be written in terms of occupation-number representation as $[n_{-2}, n_{-1}, n_0, n_{+1}, n_{+2}]$, and we have for the matrix elements of creation and destruction operators,

$$b_{\mu} [n_{-2} \dots n_{\mu} \dots n_{+2}] = \sqrt{n_{\mu}} [n_{-2} \dots (n_{\mu}-1) \dots n_{+2}]$$

$$b_{\mu}^* [n_{-2} \dots n_{\mu} \dots n_{+2}] = \sqrt{n_{\mu}+1} [n_{-2} \dots (n_{\mu}+1) \dots n_{+2}] \quad (10)$$

It is, however, more convenient for nuclear spectroscopy calculations to write the wavefunctions in angular momentum representation. We denote by $|NR M_R\rangle$ the wavefunction corresponding to a state of N phonons of spin 2, coupled to a resultant angular momentum N , M_R being the z -component of N . The wavefunction in this representation has to be explicitly symmetrized with respect to the N phonons. In practice, it will only be necessary to be able to write an N -phonon symmetrized wavefunction as a linear sum over $(N-1)$ -phonon symmetrized wavefunctions coupled to the N^{th} phonon. That is

$$|NR M_R\rangle = \sum_{R', \mu} \langle (N-1, R' | NR \rangle |N-1 R' M_{R'}\rangle |2 \mu\rangle C_{M_R' \mu}^{R' 2 R} \quad (11)$$

Here, $\langle N-1 R' | NR \rangle$ are the coefficients of fractional parentage. They are identical with the coefficients of fractional parentage for the space symmetric orbital wavefunctions of the nuclear configuration $(d)^N$, and are already tabulated for $N \leq 4$ (Jans1).

The eigenvalues of the Hamiltonian are clearly $0, \hbar\omega, 2\hbar\omega$ etc., corresponding to the presence of $0, 1, 2, \dots$ phonons. We do not write explicitly the zero point energy

$3\hbar\omega$ ————— 0,2,3,4,6

$2\hbar\omega$ ————— 0,2,4

$\hbar\omega$ ————— 2

0 ————— 0

FIG.1. ENERGY LEVEL SPECTRUM OF A VIBRATING CORE.
ON THE LEFT OF EACH LINE IS SHOWN THE EXCITATION
ENERGY, WHILE THE NUMBERS ON THE RIGHT DENOTE THE
SPIN VALUES.

(5/2) $\hbar\omega$, since for calculations of excited states it is irrelevant. The wavefunction for $N > 1$ are in general degenerate, since all permissible states with different values of R but the same number of phonons N have the same energy. In particular, for $N = 2$, $R = 0, 2, 4$ (three-fold degeneracy) and for $N = 3$, $R = 0, 2, 3, 4, 6$ (five-fold degeneracy). Thus the energy level spectrum for the nuclear core will appear as shown in fig. 1.

The evaluation of the matrix elements of the creation and destruction operators for the eigenfunctions in the angular momentum representation will be needed in subsequent calculations. The expression for this has been evaluated by various authors; it can be written in the form

$$\langle N'R'M' | b_\mu | NRM \rangle = \frac{1}{\sqrt{2R+1}} \cdot C_{MM}^{R' 2 R'} \langle N'R' || b || NR \rangle \quad (12)$$

$$\langle N'R' || b || NR \rangle = (-1)^{R'-R} \sqrt{N(2R+1)} \langle N'R' | NR \rangle \delta_{N', N-1}$$

The first equation above is the definition of the reduced matrix element (Appendix II, eq.(8)). We shall indicate here briefly how the value of the double-barred or reduced matrix element can be deduced in a very simple way. Consider the operator for the total number of phonons,

$$\sum_{\mu} b_{\mu}^{\dagger} b_{\mu}$$

$$N = \sum_{\mu} n_{\mu} = \langle NRM | \sum_{\mu} b_{\mu}^{\dagger} b_{\mu} | NRM \rangle$$

$$\begin{aligned}
&= \sum_{\mu, R'} \langle NRM | b_{\mu}^{\dagger} | N'R'M' \rangle \langle N'R'M' | b_{\mu} | NRM \rangle \\
&= \sum_{R', \mu} |\langle N'R'M' | b_{\mu} | NRM \rangle|^2 \\
&= \sum_{R', \mu} \frac{1}{2R'+1} \cdot \left(C_{M \mu M'}^{R \ 2R'} \right)^2 |\langle N'R' || b || NR \rangle|^2
\end{aligned}$$

Summation over μ on the right side yields,

$$N(2R+1) = \sum_{R'} |\langle N'R' || b || NR \rangle|^2$$

Now we may use the property of the coefficients of fractional parentage, $\sum_{R'} |\langle N-1, R' | NR \rangle|^2 = 1$, and write,

$$\sum_{R'} |\langle N'R' || b || NR \rangle|^2 = \sum_{R'} N(2R+1) |\langle N-1 R' | NR \rangle|^2$$

so that with a suitable choice of the phase, we obtain,

$$\langle N'R' || b || NR \rangle = (-1)^{R'-R} \frac{1}{\sqrt{N(2R+1)}} \langle N-1 R' | NR \rangle \delta_{N', N-1}$$

For the construction of the total Hamiltonian matrix, we shall need a basic complete set of orthonormal functions. For this we choose the complete set of the product wave-functions,

$$|\alpha J; NR; IM\rangle = \sum_{M_1, M_2} C_{M_1 M_2 M}^{J R I} |\alpha J M_1\rangle |N R M_2\rangle \quad (13)$$

where, I is the total angular momentum of the nuclear system, obtained by coupling the total angular momentum J of the extra-core nucleons and the angular momentum I of the H -phonon state of the core. We construct the Hamiltonian matrix for a state of total spin I ,

$$\langle \mathcal{L}'J': N'R': IM | H | \mathcal{L}J: NR: IM \rangle$$

and diagonalise it to find the eigenfunctions in the form

$$\psi_{IM} = \sum_{\mathcal{L}J, NR} c_I (\mathcal{L}J: NR) | \mathcal{L}J: NR: IM \rangle \quad (14)$$

with

$$\sum_{\mathcal{L}J, NR} | c_I (\mathcal{L}J: NR) |^2 = 1$$

We now proceed to derive an explicit expression for the matrix element of H in eq.(6). We get,

$$\begin{aligned} & \langle \mathcal{L}'J': N'R': IM | H_s + H_c + H_{int} | \mathcal{L}J: NR: IM \rangle \\ &= \delta_{NN'} \delta_{RR'} \langle \mathcal{L}'J' | H_s | \mathcal{L}J \rangle + \delta_{\mathcal{L}\mathcal{L}'} \delta_{JJ'} \langle N'R' | H_c | NR \rangle \\ &+ \langle \mathcal{L}'J': N'R': IM | H_{int} | \mathcal{L}J: NR: IM \rangle \end{aligned} \quad (15)$$

From our previous discussion,

$$\langle N'R' | H_c | NR \rangle = \delta_{NN'} \delta_{RR'} N \hbar \omega \quad (15a)$$

$$\begin{aligned} \langle \mathcal{L}'J' | H_s | \mathcal{L}J \rangle &= \delta_{\mathcal{L}\mathcal{L}'} \delta_{JJ'} \sum_i E(n_i l_i j_i) \\ &+ \delta_{JJ'} \langle \mathcal{L}'J | \sum_{i \leq j} H_{ij} | \mathcal{L}J \rangle \end{aligned} \quad (15b)$$

For one extra-core nucleon, the second term on the right side of eq. (19) is zero, whereas for two extra-core nucleons, it reduces to eq. (4) of chapter II.

To derive the matrix elements of H_{int} , we write it as

$$\begin{aligned} H_{int} &= - \sum_i k(r_i) \sum_{\mu} b_{\mu} Y_2^{\mu}(\theta_i, \phi_i) \\ &= - \sqrt{\frac{\hbar \omega}{2C}} \sum_i k(r_i) \sum_{\mu} (b_{\mu} + (-1)^{\mu} b_{-\mu}^*) Y_2^{\mu}(\theta_i, \phi_i) \quad (16) \\ &= - \sqrt{\frac{\hbar \omega}{2C}} \sum_i k(r_i) [A \cdot Y_2(i) + (A \cdot Y_2(i))^{\dagger}] \end{aligned}$$

where,

$$b_{\mu} = (-1)^{\mu} A_{-\mu}$$

and the scalar product is defined by Racah (1942; also Appendix II, eq. (8)): $(A \cdot B) = \sum_{\mu} (-1)^{\mu} A_{\mu} B_{-\mu}$. We calculate the matrix elements of the first term of H_{int} ; the matrix elements of the second term then follow from these as

$$\begin{aligned} \langle \mathcal{L}' J' : N' R' : IM | (A \cdot Y_2)^{\dagger} | \mathcal{L} J : NR : IM \rangle \\ = \langle \mathcal{L} J : NR : IM | A \cdot Y_2 | \mathcal{L}' J' : N' R' : IM \rangle \quad (17) \end{aligned}$$

Now,

$$\begin{aligned} \langle \mathcal{L}' J' : N' R' : IM | - \sqrt{\frac{\hbar \omega}{2C}} \sum_i k(r_i) (A \cdot Y_2(i)) | \mathcal{L} J : NR : IM \rangle \\ = - \sqrt{\frac{\hbar \omega}{2C}} (-1)^{J'+R-I} W(J' R' J R : I 2) \langle N' R' || A || NR \rangle \times \quad (18) \\ \cdot \langle \mathcal{L}' J' || \sum_i k(r_i) Y_2(i) || \mathcal{L} J \rangle \end{aligned}$$

Here we have used eq. (6) of Appendix II.

TABLE I

Values of the Matrix Element

$\langle n'n' || b || nn \rangle$ for $n \leq 3$.

$n'n'$	nn	$\langle n'n' b nn \rangle$
00	12	$(5)^{\frac{1}{2}}$
12	20	$(2)^{\frac{1}{2}}$
12	22	$(10)^{\frac{1}{2}}$
12	24	$(18)^{\frac{1}{2}}$
20	32	$(7)^{\frac{1}{2}}$
22	30	$(3)^{\frac{1}{2}}$
22	32	$(20/7)^{\frac{1}{2}}$
22	33	$-(15)^{\frac{1}{2}}$
22	34	$(90/7)^{\frac{1}{2}}$
24	32	$6/(7)^{\frac{1}{2}}$
24	33	$(6)^{\frac{1}{2}}$
24	34	$(90/7)^{\frac{1}{2}}$
24	36	$(39)^{\frac{1}{2}}$

It may be noted that since A and b differ only in their dependence on μ , the double-barred matrix elements of these two operators are identical:

$$\langle N'R' \| A \| NR \rangle \equiv \langle N'R' \| b \| NR \rangle$$

For all values of N and $N' \leq 2$, these matrix elements are tabulated in table I.

The matrix element for the nucleon part can be written using the coefficients of fractional parentage. For a single nucleon,

$$\langle n'l'j' \| k(r) Y_2 \| nlj \rangle = k (-1)^{\frac{j_2-j'}{2}} \frac{(2j+1)(2j'+1)}{4\pi} C_{\frac{j_2-j'}{2}}^{jj'2} G_{ll'} \quad (19)$$

where,

$$G_{ll'} = \frac{1}{2} [1 + (-1)^{l+l'}]$$

and for a two-nucleon configuration,

$$\begin{aligned} & \langle j_1' j_2' J' \| \sum_i k(r_i) Y_2(i) \| j_1 j_2 J \rangle \\ &= \delta_{j_2 j_2'} (-1)^{j_2 - j_1 - J'} \left\{ (2J+1)(2J'+1) \right\}^{\frac{1}{2}} W(j_1' J' j_1 J; j_2 2) \times \\ & \quad \cdot \langle j_1' \| k(r_1) Y_2(1) \| j_1 \rangle \quad (20) \\ &+ \delta_{j_1 j_1'} (-1)^{j_1 - j_2' - J} \left\{ (2J+1)(2J'+1) \right\}^{\frac{1}{2}} W(j_2' J' j_2 J; j_1 2) \times \\ & \quad \cdot \langle j_2' \| k(r_2) Y_2(2) \| j_2 \rangle \end{aligned}$$

In deriving the above expression, eqs. (4) and (5) of Appendix II are used. Special cases of this formula are

listed by Ford and Levinson (Fol55). The above expression does not take into account explicit antisymmetrisation of the two-nucleon wavefunction. The antisymmetric wavefunction may be written as

$$|j_1 j_2 JM : TM_T\rangle = a_{j_1 j_2} \left[|j_1 j_2 JM : TM_T\rangle + (-1)^{j_1 + j_2 + T - J} |j_2 j_1 JM : TM_T\rangle \right] \quad (21)$$

where $a_{j_1 j_2}$ is defined in eq. (4) of chapter II. Matrix elements of $\sum_i k(r_i) Y_2(\hat{r}_i)$ for this antisymmetrised wavefunction are given by

$$\begin{aligned} \langle \alpha' j' J' || \sum_i k(r_i) Y_2(\hat{r}_i) || \alpha j J \rangle_T &= a_{j_1 j_2} a_{j'_1 j'_2} \left[\langle j'_1 j'_2 J' || \sum_i k(r_i) Y_2(\hat{r}_i) || j_1 j_2 J \rangle + (-1)^{j'_1 + j'_2 + T - J'} \langle j'_2 j'_1 J' || \sum_i k(r_i) Y_2(\hat{r}_i) || j_1 j_2 J \rangle \right] \\ &\quad + (-1)^{j_1 + j_2 + T - J} \text{ (Same with } j_1 \leftrightarrow j_2 \text{)} \end{aligned} \quad (22)$$

For more than two nucleons in equivalent orbits, the matrix element can easily be written in a simple form, and is given by Ford and Levinson (Fol55). We do not treat the case of more than two nucleons here, and so do not write down these expressions.

The radial matrix element of $k(r)$ is given here as

$$k = \langle n'l' | k(r) | nl \rangle = \int_0^\infty R_{n'l'}(r) R_{nl}(r) k(r) r^2 dr \quad (23)$$

It is found by extensive calculations by Feenberg and Hammack (Feg51) that for various shell model forms of the single-particle potential, k is almost independent of the quantum numbers n, l and the details of the potential shape. It has a rather constant value of ~ 40 MeV. We, therefore, take k as a constant.

We have now all the results needed to evaluate the Hamiltonian matrix in cases of interest to us. For subsequent calculations, we shall consider the case of weak or intermediate coupling in the sense that we shall consider a limited number of core-excited states, i.e., only those involving ≤ 3 phonons. With this approximation, the Hamiltonian matrices will be exactly diagonalized. On the other hand, this approximation implies that the predicted energy levels will be reasonably good only for states with energies $\leq 3 \hbar \omega$. Thus our discussion shall be confined to nuclear states of excitation energy ≤ 5 MeV ($\hbar \omega \leq 2.5$ MeV in our case), and our results will be more reliable for the lowest few states of each spin value.

3. The Formalism: Electromagnetic Properties

Electromagnetic properties, and in particular the electric quadrupole transitions, in nuclei are strongly affected by the collective motion of the core. It is possible in many cases to determine the parameters of the collective motion and the strength of the core-particle coupling by studying the electromagnetic transitions.

We shall now describe the derivation of the transition probabilities, as well as the magnetic dipole and the electric quadrupole moments of nuclei in the weak-coupling collective model.

A. The Matrix Elements

The transition probability $T(x\lambda)$ for a multipole radiation of order λ is given by

$$T(x\lambda) = \frac{8\pi(\lambda+1)}{\lambda[(2\lambda+1)!!]^2} \cdot \frac{1}{\hbar} \cdot \left(\frac{\Delta E}{\hbar c}\right)^{2\lambda+1} B(x\lambda) \quad (24)$$

where, c = the velocity of light in vacuum, and

$\Delta E = \hbar\omega$, is the energy of the emitted quantum of radiation, ω being the angular frequency.

$B(x\lambda)$, the reduced transition probability, is given by[†]

$$\begin{aligned} B(x\lambda) &= \frac{1}{2I'+1} \sum_{M, M'} |\langle I'M' | \mathcal{M}(x\lambda\mu) | IM \rangle|^2 \\ &= \frac{1}{2I'+1} |\langle I' || \mathcal{M}(x\lambda) || I \rangle|^2 \end{aligned} \quad (25)$$

Here, x denotes the electric or magnetic character of the radiation, IM and $I'M'$ are the spin quantum numbers for the initial and the final states respectively of the nucleus, and $\mathcal{M}(x\lambda)$ is the proper multipole operator. Wigner-Eckart Theorem (see Appendix II, eq. (3)), as well as the sum rules

[†] This definition is as given in ref. (Gur51). Some authors use the factor $\frac{1}{2I+1}$ instead of $\frac{1}{2I'+1}$.

for Clebsch-Gordan coefficients, have been used for deriving the last expression in terms of the double-barred matrix element.

The operator for magnetic dipole (M1) transition and the electric quadrupole (E2) transition are

$$M(M1) = (3/4\pi)^{1/2} \bar{\mu}^{(op)} \quad (26)$$

and

$$M(E2) = (5/16\pi)^{1/2} \bar{Q}^{(op)} \quad (27)$$

where, the dipole moment operator $\bar{\mu}^{(op)}$ and the quadrupole moment operator $\bar{Q}^{(op)}$ are given by

$$\bar{\mu}^{(op)} = \mu_0 \left[\sum_i g_i \vec{j}_i + g_R \vec{R} \right] \quad (28)$$

$$\bar{Q}^{(op)} = (16\pi/5)^{1/2} \sum_i e_i r_i^2 Y_2^0(\theta_i, \phi_i) \quad (29)$$

g_i and g_R are the gyromagnetic ratios given by

$$g_{j=l \pm 1/2} = g_l \pm \frac{g_s - g_l}{2l + 1} \quad (3)$$

$$g_l = \begin{cases} 1 & \text{for proton} \\ 0 & \text{for neutron} \end{cases} \quad ; \quad g_s = \begin{cases} 5.586 & \text{for proton} \\ -3.826 & \text{for neutron} \end{cases}$$

$$g_R \approx Z/A$$

The value of g_R is not precisely known and appears to vary to some extent from nucleus to nucleus; in the absence of a

more satisfactory estimate, it is customary to take the value given above.

\vec{s}_i and \vec{R} in eq. (28) are respectively the nucleon spin- and the surface angular momentum- operators, and μ_0 denotes the nuclear magneton ($\mu_0 = eh/2M_p c$). In eq. (29), e_i is the electric charge and r_i, θ_i, ϕ_i the polar coordinates of the i^{th} nucleon. The summation in eq. (28) is only over the extra-core nucleons, whereas in eq. (29), it is over all the nucleons in the nucleus.

The measured values of the magnetic dipole moment and the electric quadrupole moment in a state of spin I are given by

$$\begin{aligned} \mu &= \langle IM | \bar{\mu}_z^{(0p)} | IM \rangle_{M=I} \\ &= \langle II | \mu_o^{(0)} | II \rangle \\ &= \frac{1}{\sqrt{2I+1}} C_{I \ 0 \ I}^{I \ 1 \ I} \langle I || \mu^{(0)} || I \rangle \\ &= \sqrt{I/(I+1)(2I+1)} \langle I || \mu^{(0)} || I \rangle \end{aligned} \quad (31)$$

and

$$\begin{aligned} Q &= \langle IM | \bar{Q}_z^{(0p)} | IM \rangle_{M=I} \\ &= \langle II | Q_o^{(2)} | II \rangle \\ &= \frac{1}{\sqrt{2I+1}} C_{I \ 0 \ I}^{I \ 2 \ I} \langle I || Q^{(2)} || I \rangle \\ &= \{I(2I-1)/(I+1)(2I+1)(2I+3)\}^{1/2} \langle I || Q^{(2)} || I \rangle. \end{aligned} \quad (32)$$

similarly,

$$T(M1) = \frac{4\pi}{3\hbar} \left(\frac{\Delta E}{\hbar c} \right)^3 \cdot \frac{1}{2I+1} |\langle I' \| \mu^{(1)} \| I \rangle|^2$$

and

$$T(E2) = \frac{4\pi}{75} \cdot \frac{1}{\hbar} \left(\frac{\Delta E}{\hbar c} \right)^5 \cdot \frac{5}{16\pi} \cdot \frac{1}{2I+1} |\langle I' \| Q^{(2)} \| I \rangle|^2$$

putting,

$$\hbar = 6.58 \times 10^{-22} \text{ MeV. sec, and}$$

$$e = 3 \times 10^{10} \text{ cm. sec}^{-1},$$

we get,

$$T(M1) = 0.16703 \times 10^{60} (\Delta E)^3 \frac{1}{2I+1} |\langle I' \| \mu^{(1)} \| I \rangle|^2 \quad (33a)$$

and

$$T(E2) = 0.54285 \times 10^{80} (\Delta E)^5 \frac{1}{2I+1} \cdot \frac{5}{16\pi} |\langle I' \| Q^{(2)} \| I \rangle|^2 \quad (33b)$$

where, ΔE is in MeV.

Thus we need calculate only the reduced matrix elements of the dipole and the quadrupole operators.

B. The Reduced Matrix Elements dipole operator

Let us now consider the evaluation of the matrix element,

$$\begin{aligned} \langle I' \| \mu^{(1)} \| I \rangle &= \mu_0 \left[\langle I' \| \sum_i g_{ji} \vec{r}_i^{(1)} \| I \rangle \right. \\ &\quad \left. + g_R \langle I' \| R^{(1)} \| I \rangle \right] \end{aligned} \quad (34)$$

Since

$$|IM\rangle = \Psi_{IM} = \sum_{\mathcal{L}J, NR} c_I(\mathcal{L}J:NR) |\mathcal{L}J:NR:IM\rangle,$$

we find,

$$\langle I' || \sum_i g_{ji} j_i^{(1)} || I \rangle = \sum_{\substack{\mathcal{L}J, NR \\ \mathcal{L}'J'}} c_I(\mathcal{L}J:NR) c_{I'}(\mathcal{L}'J':NR) \times \quad (35)$$

$$(-1)^{\frac{R+1-J-I'}{2}} \{ (2I+1)(2I'+1) \} W(J'I'J I: R1) \langle \mathcal{L}'J' || \sum_i g_{ji} j_i^{(1)} || \mathcal{L}J \rangle \delta_{NN'} \delta_{RR'}$$

The case of practical interest to us is for a single extra-core nucleon; the reduced matrix element for this case is (eq. (8) of appendix II).

$$\langle j' || g_j j^{(1)} || j \rangle = \delta_{jj'} g_j \sqrt{j(j+1)(2j+1)} \quad (35a)$$

For the case of two extra-core nucleons, the matrix elements are given by an equation similar to (22), with,

$$\begin{aligned} & \langle j_1' j_2' J' || g_{j_1} j_1^{(1)} + g_{j_2} j_2^{(1)} || j_1 j_2 J \rangle \\ &= \delta_{j_1 j_1'} \delta_{j_2 j_2'} \sqrt{(2J+1)(2J'+1)} \left[(-1)^{j_2+1-j_1-J'} g_{j_1} W(j_1' J' j_1 J: j_2) \times \right. \\ & \quad \left. \sqrt{j_1(j_1+1)(2j_1+1)} + (-1)^{j_1+1-j_2-J} g_{j_2} W(j_2 J' j_2 J: j_1) \times \right. \\ & \quad \left. \sqrt{j_2(j_2+1)(2j_2+1)} \right] \quad (35b) \end{aligned}$$

Similarly, we obtain,

$$\begin{aligned} \langle I' || g_R R^{(1)} || I \rangle &= g_R \sum_{\substack{\mathcal{L}J, NR \\ N'R'}} c_I(\mathcal{L}J:NR) c_{I'}(\mathcal{L}J:N'R') \times \\ & (-1)^{\frac{J+1-R-I}{2}} \sqrt{(2I+1)(2I'+1)} W(R'I'R I: J1) \langle N'R' || R^{(1)} || NR \rangle \end{aligned}$$

$$= g_R \sum_{\alpha J, NR} C_I(\alpha J: NR) C_I(\alpha J: NR) (-1)^{J+1-R-I} \{(\alpha I+1)(\alpha I+1)\}^{1/2} \times$$

$$W(R I' R I: J I) \sqrt{R(R+1)(\alpha R+1)} \delta_{NN'} \delta_{RR'} \quad (36)$$

We can now write down the complete expression for the magnetic moment. In units of nuclear magnetons, we have,

$$\mu = \mu(\text{particle}) + \mu(\text{core}) \quad (37)$$

$$\mu(\text{particle}) = \sqrt{I(\alpha I+1)/(I+1)} \sum_{\alpha J, NR} C_I(\alpha J: NR) C_I(\alpha J': NR) \times$$

$$(-1)^{R+1-J-I} W(J' I J I: R I) \langle \alpha J' || \sum_i g_i \hat{p}_i^{(1)} || \alpha J \rangle \quad (37a)$$

$$\mu(\text{core}) = \sqrt{I(\alpha I+1)/(I+1)} g_R \sum_{\alpha J, NR} C_I(\alpha J: NR) \times$$

$$(-1)^{J+1-R-I} W(R I R I: J I) \sqrt{R(R+1)(\alpha R+1)} \quad (37b)$$

The matrix element for $T(M)$ can similarly be written down.

C. The Reduced Matrix Element quadrupole operator

We write the quadrupole operator as

$$Q_0^{(2)} = \sqrt{\frac{16\pi}{5}} \sum_i^{\text{core}} e_i r_i^2 Y_2^0(\theta_i, \phi_i) + \sqrt{\frac{16\pi}{5}} \sum_i^n e_i r_i^2 Y_2^0(\theta_i, \phi_i) \quad (38)$$

where, the first term consists of sum over all the nucleons in the core and the second term the sum over the extra-core nucleons. The reduced matrix element for the second term can

easily be evaluated using the methods described in the previous section:

$$\begin{aligned}
 \sqrt{\frac{16\pi}{5}} \langle I' \| \sum_i e_i r_i^2 Y_2(\theta_i, \phi_i) \| I \rangle \\
 = \sqrt{\frac{16\pi}{5}} \sum_{\substack{\alpha J, NR \\ \alpha' J'}} C_I(\alpha J, NR) C_{I'}(\alpha' J', NR) (-1)^{R+J-I'} \times \\
 \cdot \{ (2I+1)(2I'+1) \}^{\frac{1}{2}} W(J' I' J I; R 2) \langle \alpha' J' \| \sum_i e_i r_i^2 Y_2(\theta_i, \phi_i) \| \alpha J \rangle
 \end{aligned} \quad (39)$$

We shall write down the reduced matrix element in the above equation explicitly for the case of one and two extra-core nucleons.

(1) one nucleon:

$$\begin{aligned}
 \langle n'l'j' \| e r^2 Y_2 \| nlg \rangle = e \langle n'l' | r^2 | nl \rangle (-1)^{\frac{1}{2} - j'} \frac{1}{\sqrt{4\pi}} \times \\
 \cdot \sqrt{(2j+1)(2j'+1)} C_{\frac{1}{2} - \frac{1}{2}}^{jj'2} G_{ll'}
 \end{aligned} \quad (39a)$$

where,

$$\langle n'l' | r^2 | nl \rangle = \int_0^\infty R_{n'l'}(r) R_{nl}(r) r^4 dr$$

$R_{nl}(r)$ being the radial part of the harmonic oscillator wavefunction given by eq. (1) of chapter II. The wavefunctions for 1d and 2s orbitals give

$$\begin{aligned}
 \langle 2s | r^2 | 2s \rangle &= \langle 1d | r^2 | 1d \rangle = 1.75 r_d^2 \\
 \langle 2s | r^2 | 1d \rangle &= \langle 1d | r^2 | 2s \rangle = -1.33 r_d^2
 \end{aligned} \quad (40)$$

$$r_d = r_s = r_d$$

(11) two nucleons:

The matrix element is given by an expression similar to (22) with,

$$\begin{aligned}
 & \langle j_1' j_2' J' || \sum_i e_i r_i^2 Y_2(1) || j_1 j_2 J \rangle \\
 &= \delta_{j_2 j_2'} (-1)^{j_2 - j_1 - J'} \{ (2J+1)(2J'+1) \}^{1/2} W(j_1' J' j_1 J; j_2 j_2') \times \\
 & \quad \cdot \langle n_1' l_1' j_1' || e_1 r_1^2 Y_2(1) || n_1 l_1 j_1 \rangle \\
 & \quad + \delta_{j_1 j_1'} (-1)^{j_1 - j_2 - J} \{ (2J+1)(2J'+1) \}^{1/2} W(j_2' J' j_2 J; j_1 j_1') \times \\
 & \quad \cdot \langle n_2' l_2' j_2' || e_2 r_2^2 Y_2(2) || n_2 l_2 j_2 \rangle.
 \end{aligned} \tag{30b}$$

The contribution of the quadrupole moment due to the core arises from the fact that the radius vector R is now a function of θ and ϕ . We begin by assuming that the charge distribution in the core is uniform, so that the sum over the independent nucleons may be replaced by an integral over the volume. That is

$$\sum_i^{\text{core}} e_i r_i^2 Y_2^0(\theta_i, \phi_i) = \int_0^\pi \int_0^{2\pi} \int_0^R \rho(r) r^2 Y_2^0(\theta, \phi) r^2 \sin\theta dr d\theta d\phi \tag{41}$$

Secondly, we assume that the deformation of the core changes only the shape, but not the density, of the nuclear core, so that for $\rho(r)$ we may take the density of a uniform spherical

nucleus,

$$\rho(r) = 3Ze / 4\pi R_0^3$$

Integration over \mathbf{r} is then easily carried out, and we get,

$$Q_0^{(2)} = \sqrt{\frac{16\pi}{5}} \cdot \frac{3Ze}{4\pi R_0^3} \int \frac{1}{5} R^5 Y_2^0(\vartheta, \phi) d\Omega \quad (42)$$

$$d\Omega = \sin\vartheta d\vartheta d\phi$$

It is obvious that if R , the radius vector of the surface, is independent of ϑ and ϕ ($R = R_0$), then $Q_0^{(2)} = 0$. However, we have,

$$R = R_0 \left[1 + \sum_{\mu} \alpha_{\mu} Y_2^{\mu}(\vartheta, \phi) \right] \quad (43)$$

$$R^5 = R_0^5 \left[1 + 5 \sum_{\mu} \alpha_{\mu} Y_2^{\mu}(\vartheta, \phi) \right]$$

where, we retain only terms in first order of α_{μ} . Substituting for R^5 in eq. (42) from eq. (43), we find,

$$\begin{aligned} Q_0^{(2)} &= \left(\frac{16\pi}{5} \right)^{1/2} \left(\frac{3Ze}{4\pi R_0^3} \right) \cdot [R_0^5 \alpha_0] \\ &= \sqrt{16\pi/5} \left(\frac{3Ze}{4\pi} \right) R_0^2 \sqrt{\hbar\omega/2c} (b_0 + b_0^*) \quad (44) \end{aligned}$$

In the second step, we have introduced the definition of α_{μ} in terms of the creation and destruction operators (eq. 8). We note that α_{μ} contains the factor $\sqrt{\hbar\omega/2c}$ and that generally $\hbar\omega \sim 2 - 3$ MeV, whereas $c \sim 100 - 1000$ MeV,

so that we are justified in neglecting the higher powers of $d\mu$ in the expansion of χ^2 (eq. 43).

The evaluation of the matrix element now follows the standard pattern:

$$\begin{aligned} \langle I' || Q^{(2)} || I \rangle &= \sqrt{16\pi/5} (3Ze/4\pi) R_0^2 \sqrt{A W / 2 C} \times \\ &\quad \sum_{\substack{J, NR \\ N'R'}} C_J(2J:NR) C_{I'}(2J:N'R') \times (-1)^{J-R'-J} \times \\ &\quad \cdot \{ (2I+1) (2I'+1) \}^{1/2} W(R'I'RI:J2) \langle N'R' || b || NR \rangle \quad (45) \\ &\quad + (-1)^{I'-I} (\text{hermitian conjugate}) \end{aligned}$$

We have now all the equations required to evaluate the electromagnetic properties of various nuclear states.

We point out that a description of an even-even nucleus exhibiting collective oscillations as a whole, i.e., neglecting entirely the intrinsic structure and the independent-nucleon part of the wavefunctions, shows some very simple properties. Eigenfunctions of the various states would be $|NR\rangle$ and the level spectrum would appear as shown in Fig. 1.

The magnetic moment operator is diagonal in N and R , so that no magnetic dipole transitions are possible between different states. We also see from eq. (37b) by taking $J = 0$ and $I = R$, that the magnetic moment of a state $|NR\rangle$ is

$\mu = g_R R$. This simple result enables us to study experimentally the values of g_R by measuring the magnetic moments of, say, the first excited state ($N = 1, n = 2$).

Similarly for quadrupole transitions, we obtain from eq. (45),

$$\langle I' = R' || Q^{(2)} || I = R \rangle = \sqrt{\frac{16\pi}{5}} \cdot \frac{3Ze}{4\pi} \sqrt{\frac{\hbar W}{2C}} R_0^2 (-1)^{R+R'} \langle N' R' || b || N R \rangle \quad (46)$$

This shows that only those transitions are allowed in which the phonon number changes by unity ($|\Delta N| = 1$). In particular, the cross over transition from the second excited 2^+ state (we denote this level by 2^*) to the ground state 0^+ is forbidden ($\Delta N = 2$). Secondly, the transition probability is proportional to $\hbar W/2C$, and a measure of the transition probability from the first excited state to the ground state ($2 \rightarrow 0$) should give a measure of C . A further simple result emerges by substituting the explicit values of the reduced matrix elements of b for transitions $|22\rangle \rightarrow |12\rangle$ and $|12\rangle \rightarrow |00\rangle$. The ratio of the matrix elements,

$$\frac{\langle 22^* || Q^{(2)} || 12 \rangle}{\langle 12 || Q^{(2)} || 00 \rangle} = \sqrt{2} \quad (47)$$

All these simple results have been used in the analysis of the observed properties of nuclei in terms of the collective vibrational model. We note that these results neglect the internal structure of the nuclei, and therefore to that extent should be unreliable. Analysis of experimental data

does reveal sizable discrepancies. We shall show in subsequent discussion of Si^{30} that taking into account the interaction of the last two nucleons can substantially modify the above results.

The odd-even nuclei can also be discussed in terms of a simple model consisting of an odd nucleon coupled to an even-even vibrating core. Here it is difficult to write down any simple results except perhaps in an extreme weak-coupling approximation. The results in general would depend not only on the parameters B and C of the core motion, but also on the spacing of the single particle levels, strength of the core-particle coupling etc. Raz (Raz60) has discussed the case of one extra-core nucleon in terms of the first order perturbation theory and has shown that for quadrupole moments or quadrupole transitions, the result of collective motion is to introduce an additional effective charge, e_{eff} , for the extra-core nucleon

$$e_{\text{eff}} = (3Ze R_0^2 / 4\pi C) \langle k / \langle r^2 \rangle \rangle \quad (48)$$

4. Applications: One nucleon outside the core (Si^{29} , P^{30} , P^{31}).

We shall now apply the formalism developed in the previous sections to the nuclei Si^{29} , P^{30} and P^{31} . As we have mentioned in chapter II, these nuclei may be described in terms of a single nucleon outside an even-even core. The odd nucleon can occupy either the $2s_{1/2}$ or $1d_{3/2}$ orbit, and

We now assume that the core is not rigid but executes harmonic quadrupole oscillations.

2.1. Eigenvalues and Eigenfunctions

We construct the Hamiltonian matrices for $J = 1/2, 3/2, 5/2$ and $7/2$ states of positive parity. From equations (15) - (19), we have for the matrix elements of the Hamiltonian,

$$\begin{aligned}
 & \langle n'l'j': N'R': IM | H | nlg: NR: IM \rangle \\
 &= \delta_{nn'} \delta_{ll'} \delta_{jj'} \delta_{NN'} \delta_{RR'} \{ N\hbar\omega + E(nlg) \} \\
 &+ \left\{ (-1)^{R+3/2-I} \frac{q \sqrt{(2j+1)(2j'+1)}}{\sqrt{(2j+1)(2j'+1)}} W(j'R'jR: I 2) x \right\} \quad (49) \\
 &\cdot \langle N'R' || b || NR \rangle C_{\frac{1}{2} - \frac{1}{2}}^{jj' 2} \epsilon_{ll'} \\
 &+ \text{the same with } (jNR \leftrightarrow j'N'R') \}
 \end{aligned}$$

where, $q = k(\hbar\omega/8\pi C)^{1/2}$; the non-dimensional parameter $(q/\hbar\omega)^{1/2}$ may be compared with Feenberg's parameter P (Feg55) and the parameter α of Bohr and Mottelson (Boh53; also Raz59), as

$$P = \frac{5}{4} \left(\frac{q}{\hbar\omega} \right)^2 ; \quad \alpha = \frac{5}{2j} \left(\frac{q}{\hbar\omega} \right)^2 \quad (50)$$

The parameters of our model are $\hbar\omega$, q and $\Delta = E(11_2/2) - E(3_2/2)$. In order to determine the best values of these parameters, the following procedure is

adopted: The Hamiltonian matrices are constructed including core excitations of 0, 1 and 2 phonons, and are diagonalised explicitly for various values of q , Δ and $\hbar\omega$. We next plot the eigenvalues of the Hamiltonian, E , in units of $\hbar\omega$, i.e., $E/\hbar\omega$, against $q/\hbar\omega$ and $\Delta/\hbar\omega$. The results are shown in Fig. 2.

We shall first discuss the energy levels of P^{31} . It is at once clear that the ground state and the first and second excited states always have the spins $1/2^+$, $3/2^+$ and $5/2^+$. Further, the energy of the $5/2^+$ state (all the energies are normalised to $E = 0$ for the ground state) appears to a large extent independent of $q/\hbar\omega$ and $\Delta/\hbar\omega$, and $E_{5/2}/\hbar\omega \approx 0.9$. Since the observations (Bro38a) show the excitation energy of this state to be 2.83 MeV, we obtain $\hbar\omega \approx 2.5$ MeV. This value is close to the energy of the first excited state in Si^{30} (2.34 MeV). We further note that the separation of the first and second excited states with $J = 3/2$, as well as the splitting of the triplet $5/2^+$, $1/2^+$ and $3/2^+$ is quite sensitive to variation of $q/\hbar\omega$, but relatively independent of the value of $\Delta/\hbar\omega$. Comparing these data with the experimental results, we find $q/\hbar\omega \approx 0.45$. From the next figure (3b) we see that for this value of $q/\hbar\omega$, we can determine the best value of $\Delta/\hbar\omega$ by comparing the

[†] The notation here is that the lowest state of a given spin J is distinguished from the first and second excited states of the same J by putting one and two asterisks on the latter states, e.g. $3/2^{**}$ denotes second excited state of spin $3/2$.

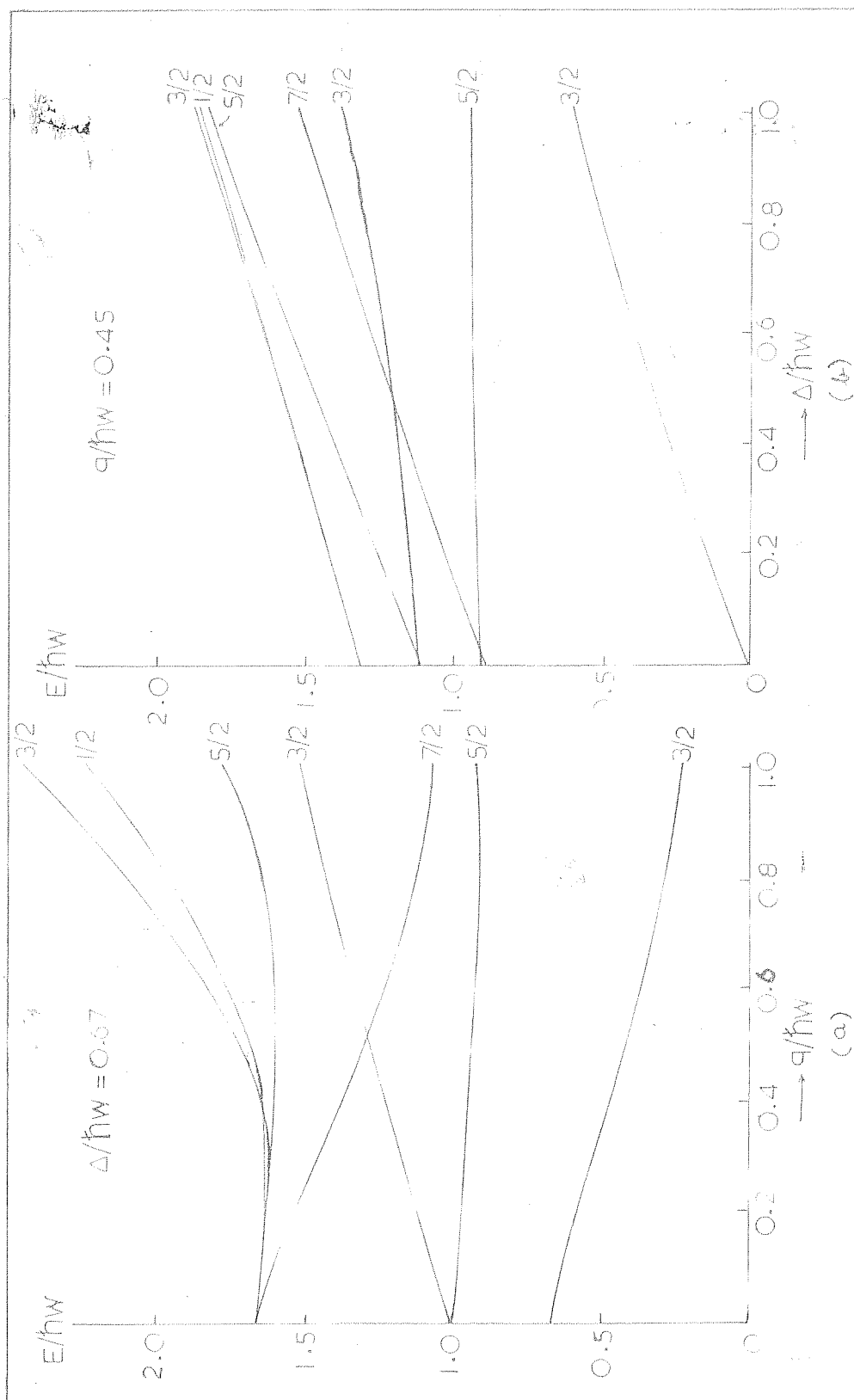


FIG. 2. THE VARIATION OF THE LEVEL SCHEME WITH THE PARAMETERS (a) q AND (b) Δ .
NORMALISED TO $\hbar\omega = 0$ FOR THE GROUND STATE $1/2^+$.

excitation energy of the first excited state $3/2$ with the observed data. This then fixes $\Delta/\hbar\omega \approx 0.8$. Thus we are able to determine easily and to a very good approximation the values of the parameters:

$$\hbar\omega \approx 2.5 \text{ MeV}; \quad \eta \approx 1.0 \text{ MeV}, \quad \Delta \approx 2.0 \text{ MeV}.$$

Now, with these values of the parameters, we refine the calculations including upto 3 phonons of vibration and diagonalize the resulting matrices. The results are shown in fig. 3. Comparison with the observed level spectrum below 4 MeV shows that the agreement between theory and experiment is quite good. We also list in table II the wavefunctions for the ground and first three excited states $3/2$, $5/2$ and $3/2^*$. We remark that the ground state appears to be almost pure $s_{1/2}$ state, whereas the $5/2$ state is almost pure one-phonon state based on the ground state. In the $J = 3/2$ states the $s_{1/2}$ and the $d_{3/2}$ orbitals are mixed up through the core-nucleon interaction, so that the first excited state is no longer a pure $d_{3/2}$ state as may be expected in a pure shell model calculation. These results will have important consequences for the electromagnetic properties of the states of P^{31} . We discuss these in a later section.

It may be noted that for the lowest four states whose wavefunctions are listed in table II, the components in the wavefunctions $|jM\rangle$ with $M \geq 2$ are quite small, and for the description of these states our restriction on

TABLE II

The amplitudes $c_I(j : NR)$ of the wavefunctions for the lowest four states of p^{31} .

J N R	$c_I(j : NR)$			
	I = 1/2	I = 3/2	I = 5/2	I = 3/2 ^a
1/2: 0 0	0.9480	-	-	-
: 1 2	-	-0.6305	0.9280	0.6557
: 2 0	0.0471	-	-	-
: 2 2	-	0.0861	-0.0304	0.3329
: 3 0	-0.0086	-	-	-
: 3 2	-	-0.0364	0.0317	0.0435
: 3 3	-	-	-0.0034	-
3/2: 0 0	-	0.7058	-	0.4353
: 1 2	0.3084	-0.2513	-0.0724	-0.4538
: 2 0	-	0.1096	-	-0.0368
: 2 2	-0.0563	0.1386	0.1219	-0.2241
: 2 4	-	-	0.3315	-
: 3 0	-	-0.0218	-	-0.0135
: 3 2	-0.0257	-0.0231	-0.0143	-0.0267
: 3 3	-	0.0072	0.0332	-0.0975
: 3 4	-	-	-0.0533	-

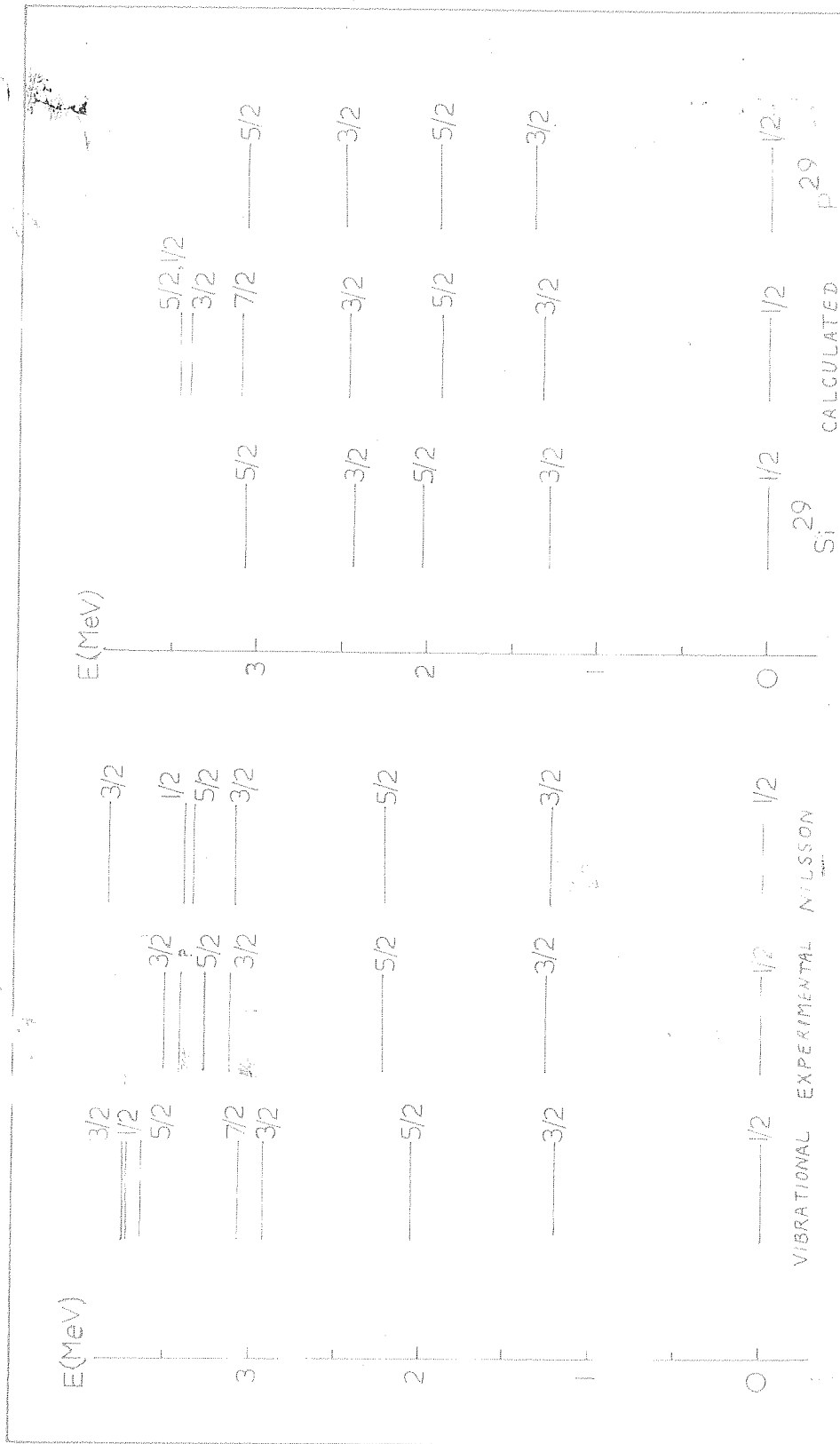


FIG. 3. POSITIVE PARITY LEVELS OF ^{29}Si AND ^{29}P

FIG. 4. POSITIVE PARITY LEVELS OF ^{29}Si AND ^{29}P

the number of phonons included ($N \leq 3$) is, therefore, satisfactory. On the other hand, for states of higher excitations, the components involving $N > 1$ are expected to play a dominant role, and for these states our approximation may not be adequate. It may also be possible at higher excitation energies ($E \gtrsim 4$ MeV) to excite other modes of collective motion or particle excitations. Thus we consider the agreement of the calculated and the observed level schemes shown in figure 3 to be quite satisfactory. The agreement for lower levels could still be improved by small changes in the variables of the problem and in view of the above remarks the fact that the calculated triplet of levels $5/2^+$, $1/2^+$ and $3/2^{++}$ lies a little above the observed levels is also not considered as disturbing.

The calculated level spectrum shows a $7/2^+$ state to occur below the triplet of states at 3.6 MeV (fig.3). As fig.2 shows, this feature cannot be avoided by a change in the values of the parameters. The experimental data do not show any $7/2^+$ state below 4 MeV. This is the most serious discrepancy of the model. It is just possible that in view of the closely spaced levels occurring in the experimental spectrum at 3.13 - 3.51 MeV, the $7/2^+$ state may be degenerate with one of the states in this region. Further study of electromagnetic transitions from these states would be required to resolve this point. It may also be noted that for $q/\hbar\omega > 0.5$, this $J = 7/2$ state occurs even below the $J = 3/2^+$ state; this is a strong argument for restricting $q/\hbar\omega < 0.5$.

We shall now consider the energy levels of Si^{29} and P^{31} . The experiments (Bry57a, Wne60) show that although for the lowest three levels $1/2$, $3/2$ and $5/2$, the excitation energies in these nuclei are approximately equal to the corresponding excitation energies in P^{31} , the structure of the level spectrum for $E > 2$ MeV appears to be quite different. The $3/2^*$ state occurs in these nuclei at energies ~ 0.5 MeV below that in P^{31} nucleus, and in place of the close triplet of levels in P^{31} at $\sim 3.3 - 3.5$ MeV, only one level of spin $5/2$ is seen in P^{31} and Si^{29} . In this connection it is well to remember that the level spectra of Si^{28} and Si^{30} also appear to be quite different beyond the first excited state, and hence such differences in the higher levels of $A = 29$ and $A = 31$ nuclei are to be expected.

If we apply the same process of analysis as described above for P^{31} to these nuclei, we find $\hbar\omega \approx 2.2$ MeV, as compared to 1.8 MeV for the excitation of the first excited state of Si^{28} . The separation of the states $3/2$ and $3/2^*$ gives $q/\hbar\omega \approx 0.25$, i.e., $q \approx 0.6$ MeV, and comparison with the energy of the $3/2$ state gives $\Delta/\hbar\omega \approx 0.8$ or $\Delta \approx 1.8$ MeV. Figure 4 shows the energy levels of Si^{29} and P^{31} calculated in a 3 phonon-approximation for the above values of the parameters and table III lists the corresponding wavefunctions for the lowest four states. For the lowest four levels the agreement is fairly good. The discrepancy with regard to the $7/2$ state persists in this case also. The vibrational model would predict an almost degenerate triplet $5/2^*$, $1/2^*$, $3/2^{**}$

TABLE III

The amplitudes $c_1(j : M)$ of the wavefunctions
for the lowest four states of Si^{29} a p²⁹

	$c_1(j : M)$			
	$I = 1/2$	$I = 3/2$	$I = 5/2$	$I = 3/2^*$
$1/2: 0 0$	0.9756	-	-	-
$: 1 2$	-	-0.6826	0.9679	0.7425
$: 2 0$	0.0382	-	-	-
$: 2 2$	-	0.0493	-0.0052	0.1656
$: 3 0$	-0.0029	-	-	-
$: 3 2$	-	-0.0183	0.0317	0.0127
$: 3 3$	-	-	0.0074	-
$3/2: 0 0$	-	0.7421	-	0.5476
$: 1 2$	0.2162	-0.1908	-0.0234	-0.2989
$: 2 0$	-	0.0729	-	0.0149
$: 2 2$	-0.0271	0.0976	0.1296	-0.1715
$: 2 4$	-	-	0.2131	-
$: 3 0$	-	-0.0103	-	0.0004
$: 3 2$	-0.0023	-0.0104	-0.0041	-0.0134
$: 3 3$	-	0.0048	0.0196	-0.0403
$: 3 4$	-	-	-0.0268	-

at about 3.4 MeV, whereas experiment shows only a $5/2$ state at 3.1 MeV.

The values of the parameters $\hbar\omega$ and Δ for $A = 29$ and $A = 31$ are in reasonable agreement, but surprisingly the coupling constant q appears to have a lower value for Si^{29} and P^{29} . We conclude that the behaviour of the Si^{28} core is quite different from the behaviour of the Si^{30} core for excitations greater than 2 MeV.

4.2. Electromagnetic Properties

In this section we use the eigenfunctions calculated in the previous section to evaluate the magnetic moments of the ground states and the electromagnetic transitions in the Si^{29} , P^{29} and P^{31} nuclei.

For the ground state magnetic moment ($I = 1/2$), we have from equations (35a), (37a) and (37b),

$$\mu = \mu(\text{particle}) + \mu(\text{core})$$

$$\mu(\text{particle}) = \sqrt{2/3} \sum_{jNR} |c_{Y_2}(j:NR)|^2 (-1)^{R+1/2-j} W(j\frac{1}{2} j\frac{1}{2}; R) \times (51a)$$

$$g_j \sqrt{j(j+1)(2j+1)}$$

with

$$g_{Y_2} = g_{\delta Y_2} = g_\delta$$

$$g_{3/2} = g_{d_{3/2}} = 1.2 g_c - 0.2 g_s$$

and

$$\mu(\text{core}) = \sqrt{2/3} \sum_{j \in \text{NR}} g_R |C_{Y_2}(j: \text{NR})|^2 (-1)^{j+1/2-R} W(R \frac{1}{2} R \frac{1}{2}; j) \times \sqrt{R(R+1)(2R+1)} \quad (51b)$$

where,

$$g_R = (Z/A)_{\text{core}} = 0.487 \text{ for } p^{31} \\ = 0.500 \text{ for } si^{29} \text{ and } p^{29}$$

In table IV we tabulate the values of μ (particle) and μ (core) together with the total magnetic moments, Schmidt values and the experimental values.

TABLE IV

Ground state magnetic moments of si^{29} ,
 p^{29} and p^{31} in units of n.m.

Nucleus	μ (part.)	μ (core)	μ	Schmidt value	Experimental
si^{29}	-1.803	0.024	-1.779	-1.910	-0.555
p^{29}	2.658	0.024	2.682	2.730	-
p^{31}	2.512	0.045	2.558	2.730	+1.130

We note that the introduction of the collective motion makes only a slight improvement over the Schmidt values. The

Result is not surprising in view of our earlier remark that the ground state wavefunctions are almost entirely $s_{1/2}$ single particle orbits. Thus the cause of the magnetic moment discrepancy has to be sought elsewhere, perhaps in the modification of the intrinsic single-particle magnetic moment.

Next we consider the electromagnetic transitions. We recall that in the simple single-particle shell model picture, the transition from the first excited state (interpreted as $d_{3/2}$) to the ground state, $s_{1/2}$, would be a pure E2 transition ($d_{3/2} \rightarrow s_{1/2}$). Similarly, the transition from the second excited state, $g_{7/2}$, (interpreted as $(d_{5/2})^{-1}$) to the ground state would again be a pure single-particle E2 transition ($s_{1/2} \rightarrow d_{5/2}$) and the transition to the first excited state would be completely forbidden. It is thus seen that in this picture there are no M1 transitions (because of 1-forbiddenness). It is easy to see even qualitatively that the introduction of the collective motion enhances the E2 transitions.

We shall discuss the electromagnetic transitions in the lowest three or four states only, and since an inspection of tables II and III shows that the components of the wavefunctions with $N \geq 2$ are quite small, we can easily understand at least qualitatively the nature of the transitions by considering the wavefunctions in a one-phonon approximation. We see that the ground state, $I = 1/2$, is 90 - 95% $|s_{1/2} : 00\rangle$

with 5 - 10% $|d_{3/2} : 12\rangle$ mixed in, whereas the first excited state, $I = 3/2$, is 80% $|d_{3/2} : 00\rangle$, 35 - 40% $|s_{1/2} : 12\rangle$ and about 10% $|d_{3/2} : 12\rangle$. It is then obvious that the presence of the $|s_{1/2} : 12\rangle$ component in the $3/2$ state will enhance the E2 transition to the ground state. In addition, the presence of the $|d_{3/2} : 12\rangle$ component in both the states, although small, will introduce an M1 component in the transition, whereas in simple shell model this was absolutely forbidden. Similarly we notice that the second excited state, $5/2$, is now 85 - 90% $|s_{1/2} : 12\rangle$ with an admixture of 10 - 15% $|d_{3/2} : 24\rangle$. Thus the presence of even a small $|s_{1/2} : 12\rangle$ component in the $I = 3/2$ state will give rise to an M1 transition between these states. Further, it is also clear that there will be a strong E2 transition from the $5/2$ state to the ground state.

Exact calculations of the transition probabilities, $T(\lambda)$, for various transitions are carried out using the wavefunctions in tables II and III. For the matrix elements of r^2 that occur in eq. (39a), we assume the value $\gamma_s^2 = \gamma_d^2 = \gamma_l^2 = 6.67 \times 10^{-26} \text{ cm}^2$, following Carlson and Talmi (Can54) (in their notation, $\gamma_l^2 = 2/\nu$; $\nu \approx 0.3 \times 10^{26}$ for $A \approx 30$). Then from eq. (40), we get,

$$\langle 2s | r^2 | 2s \rangle = \langle 1d | r^2 | 1d \rangle = +11.67 \times 10^{-26} \text{ cm}^2$$

$$\langle 2s | r^2 | 1d \rangle = \langle 1d | r^2 | 2s \rangle = -10.54 \times 10^{-26} \text{ cm}^2$$

Also, eq. (44) shows that the quadrupole transitions due to the core oscillations involve the additional parameters R_0 , the nuclear radius, and $\hbar W/C = \hbar [BC]^{-1/2}$. We take the value

$$R_0 = 1.3A^{1/3} \times 10^{-13} \text{ cm}$$

where, A is the mass number of the core. For the other parameter, we can write

$$\sqrt{\frac{\hbar W}{2C}} = \sqrt{4\pi} \cdot \frac{q}{k}$$

where the best value of q is already determined. The quadrupole transition probabilities are now evaluated for several values of k ranging from 10 MeV to 40 MeV. Smaller values of k correspond to smaller values of C , i.e. to higher deformability of the nucleus. M1 transition probabilities are calculated using equations (33a), (34), (35) and (36). The results of all these calculations are listed in tables V, VI and VII. Also listed are some single-particle transition probabilities for comparison.

Unfortunately, the absolute transition probabilities or the life-times of the various transitions in these nuclei are not at all known. However, the available experimental data (Bro58a, Bry57a) can be summarized as follows:

- (1) The transition from the first excited state, $3/2$, to the ground state has a large E2 component.

TABLE I

Transition probabilities for the low-lying levels of ^{31}P .

Initial State	Final State	ΔE (MeV)	$\Gamma(E2) (10^{11} \text{ sec}^{-1})$				$\Gamma(M1)$ $(10^{11} \text{ sec}^{-1})$
			$k = 10$	$k = 20$	$k = 30$	$k = 40$	s.p.
$3/2$	$1/2$	1.21	13.21	2.50	0.81	0.31	0.57
$5/2$	$1/2$	2.05	539.34	128.98	54.73	23.41	4.10
$5/2$	$3/2$	0.85	0.07	0.01	0.004	0.002	-
$3/2^*$	$1/2$	2.93	516.33	161.67	63.05	59.57	-
$3/2^*$	$3/2$	1.71	23.26	6.10	3.96	2.44	-
							145.53
							7.51
							59.30

TABLE VI

Transition probabilities for the low-lying levels of ^{23}P .

Initial state	Final state	ΔE (MeV)	$T(22) (10^{11} \text{ sec}^{-1})$				$T(21)$ $(10^{11} \text{ sec}^{-1})$
			$k = 10$	$k = 20$	$k = 30$	$k = 40$	
$3/2$	$1/2$	1.33	4.155	0.475	0.056	0.0001	0.921
$5/2$	$1/2$	1.93	119.171	87.974	11.650	3.130	2.961
$5/2$	$3/2$	0.60	0.000	0.000	0.000	0.000	-
$3/2^*$	$1/2$	2.47	521.725	74.979	63.313	39.719	-
$3/2^*$	$3/2$	1.14	0.934	0.302	0.153	0.135	-
							53.498
							1.203
							19.588

TABLE VII

Transition probabilities for the low-lying levels of Si^{20} .

Initial State	Final State	ΔE (keV)	$T(E2) (10^{11} \text{ sec}^{-1})$				$T(E1)$ (10^{11} sec^{-1})
			$k = 10$	$k = 20$	$k = 30$	$k = 40$	
3/2	1/2	1.33	7.32	1.83	0.81	0.46	0.47
5/2	1/2	1.93	126.68	31.67	14.08	7.92	-
5/2	3/2	0.80	0.00	0.00	0.00	0.00	40.41
3/2*	1/2	2.47	155.42	38.85	17.27	9.71	0.56
3/2*	3/2	1.14	0.53	0.13	0.06	0.03	12.00

- (ii) The branching ratio of the cross-over to the stop-over transitions from the second excited state, $5/2$, is

$$\frac{5/2 \rightarrow 1/2}{5/2 \rightarrow 3/2 \rightarrow 1/2} \approx 100$$

- (iii) The radiation in the transition $5/2 \rightarrow 3/2$ is purely M1 or purely E2, and very likely M1.
- (iv) The third excited state, $3/2^*$, decays primarily to the ground state. No transitions to the first or second excited states are observed.

Our calculations show that all these results may be derived from the vibrational model for sufficiently small value of k , i.e., $k \leq 10$ MeV. To be more precise,

- (i) For $k < 30$ MeV, the transition $3/2 \rightarrow 1/2$ is predominantly an E2 transition. An exact determination of the multipole mixture in this transition would enable us to determine accurately the value of the parameter k .
- (ii) The branching ratio for the transitions from the second excited state is ~ 1 for $k = 30$ MeV, ~ 4 for $k = 10$ MeV and increases rapidly for smaller values of k .
- (iii) The $5/2 \rightarrow 3/2$ transition is almost purely M1.

- (iv) The branching ratio for the third excited state

$$\frac{I(3/2^* \rightarrow 1/2)}{I(3/2^* \rightarrow 5/2)} \approx 15 - 20$$

In general, one may say that the nature of the electromagnetic transitions in the lowest few states have been fairly satisfactorily explained by this model. We shall show later that the agreement is better than that obtained with the strong-coupling model which involves permanent deformation and rotation of the core. The electromagnetic properties provide a severe test of the nature of the wavefunctions, and apart from the magnetic moment anomaly, the weak-coupling collective model appears to give a satisfactory account of these properties. However, a more stringent test and a much better determination of the parameter k would be available when absolute lifetimes of the various transitions are measured.

We conclude that the weak-coupling collective vibrational model can, with a suitable choice of parameters, give a reasonably good account of the observed level spectra (lowest seven levels of P^{31} and four levels of Si^{28} and P^{29}), and a satisfactory understanding of the electromagnetic transitions in the lowest few states of these nuclei. We shall discuss in a later section whether the values of the parameters thus obtained are reasonable or comparable to those obtained in case of other such nuclei.

4.3. Comparison with other models

The weak-coupling collective model was indeed applied to P^{30} and Si^{29} by Feenberg (Feg55) and to P^{31} by Goldhammer (Gor55). However, the assumed values for the parameters of the model are entirely different from our values. They adopt

$$\Delta = 0, \quad \hbar W \approx 5 \text{ MeV}, \quad k = 40 \text{ MeV}$$

$$\text{and } P = (5/4) (q/\hbar W)^2 = 0.5, \text{ i.e. } q \approx 2.2 \text{ MeV.}$$

Their calculations include not more than 2 phonon excitation of the core.

For Si^{29} and P^{30} , the order of the energy levels is predicted correctly, but the spacing of the levels is too large by a factor of 4. The corrections to the Schmidt values of the ground state magnetic moments are -0.835 n.m. and $+0.536$ n.m. respectively for P^{30} and Si^{29} , whereas in our model these corrections are only ~ -0.1 n.m. and $+0.1$ n.m. Further the transition probabilities for the deexcitation of the $3/2$ state are

$$T(M1) = 5.37 \times 10^{10} \text{ sec}^{-1}$$

$$T(E2) = 10.60 \times 10^{10} \text{ sec}^{-1}$$

which may be compared to the values reported in our tables VI and VII.

For P^{31} , Goldhammer considers three nucleons outside a vibrating core and constructs 3-nucleon antisymmetrised

wavefunctions with definite isotopic spin values. However, the calculations then show that the weak-coupling procedure does not converge, the components in the wavefunctions with $N = 1, 2$ having very large values. This may be partly due to the choice $\Delta = 0$ and partly as a result of the over-estimation of the coupling constant P . We also remark that with our parameters, $P \approx 0.26$.

The strong-coupling collective model has been applied to Si^{29} by Bromley et al (Bry57b) and to P^{31} by Broude et al (Bre58b). The primary motivation in these studies was the extraordinary success of the strong-coupling model for $A = 25$ nuclei and the observation of enhanced E2 transitions in the nuclei under consideration. While the possible role of the collective vibrational model was not excluded by these authors, this approach was not explored due to the unavailability of detailed eigenfunctions and eigenvalues such as are calculated in the previous sections. Both the group of authors have emphasized the need for these calculations, and it is now possible to assess the relative merits of the results of these two models - the rotational model and the vibrational model.

The analysis of the experimental data on Si^{29} and P^{31} by Bromley et al and Broude et al proceeds by first determining the parameters of the model, such as the nuclear deformation δ , moment of inertia, decoupling parameter a , Kerman parameter A_K etc. The values obtained for both the

nuclei are fairly consistent and show an oblate deformation corresponding to $\delta \approx -0.15$ and $\hbar^2/2J \approx 0.4$ MeV. Then using the single-particle wavefunctions obtained by Nilsson (1955), various other properties are calculated. We shall describe and compare the results on the energy level schemes and the electromagnetic transitions.

The energy levels for Si^{29} are not reported in any detail but those for P^{31} are calculated with some precision and are reproduced in figure 3. The agreement between the calculated and the observed values is indeed quite good[†], and comparable to the results of the weak-coupling model. It may be noted that the strong-coupling model does not predict a $7/2^+$ state below 4 MeV. However, it is clear from fig. 7 of Broude et al, that the position of this level is depressed very strongly by Kerman mixing of the bands 8 and 11; the Kerman parameter in this case is quite large as estimated from the Nilsson wavefunctions and a small change in it may depress the $7/2$ level below 4 MeV. In other words, the position of the $7/2^+$ level does not necessarily indicate a better agreement with experiment for the strong-coupling

[†] In a recent paper by Baart, Green and Willmott (Bat62) it is reported that the agreement between the experimental results and the calculations based on the Nilsson wavefunctions is not as good as was indicated in the paper by Broude et al and that the agreement is only for six of the low-lying levels instead of seven.

model. On the other hand, the rotational model does not predict any additional levels between 4 and 8 MeV.

The electromagnetic transitions calculated on this model do not give equally satisfactory results. We summarize the results of these authors:

- (i) For P^{31} it is reported that the theoretical $B2/M1$ amplitude mixing ratio in the $3/2 \rightarrow 1/2$ transition is -0.07 compared to the experimental value of -1.2 .
- (ii) The branching ratio for the transitions from the second excited state is calculated to be ~ 1 for Si^{30} and $2/3$ for P^{31} compared to the experimental value ~ 100 .
- (iii) For Si^{30} , the calculations show that the state $3/2^+$ decays predominantly to the $3/2$ state at 1.25 MeV, whereas the observations show the decay of the $3/2^+$ state to take place only to the ground state.

It is therefore obvious that the collective vibrational model accounts for the electromagnetic transitions in a much more satisfactory fashion than the rotational model.

It should be remarked that there seems to be no possibility of removing the magnetic moment discrepancy within the weak-coupling model as we have previously mentioned, whereas

the strong-coupling model gives values for the magnetic moments which are in good agreement with the observed values.

Applications: Two nucleons outside the core (Si^{30})

We shall now consider the case of two identical nucleons (neutrons in this case) outside the $A = 28$ core, and apply the results to understand the observed properties of Si^{30} (also $T = 1$ levels of P^{30}).

3.1. Eigenvalues and Eigenfunctions

We consider the following two-nucleon states: $(s_{1/2})^2, J = 0; (s_{1/2}d_{3/2}), J = 1, 2; (d_{3/2})^2, J = 0, 2$. These intrinsic states are coupled to upto 3 phonon-states of the collective motion of the core. The Hamiltonian matrices are constructed for $I = 0, 2, 4$ and 1 . The matrix elements are given by equations (15) - (22) of this chapter and eq.(4) of chapter II. The eigenvalues and the eigenfunctions corresponding to the lowest three states for $I = 0, 2, 4$ and the lowest state for $I = 1$ are calculated. For $I = 2$, only upto two-phonon states are included owing to computational difficulties.

The parameters in the calculations are now in addition to $\hbar\omega$, q and Δ , the parameters of the two-body interaction V_0 , \propto specifying the strength and spin-dependence, and λ specifying the range of the potential. On the basis of our previous discussion for $A = 28, 31$ nuclei we choose

$\hbar\omega = 2.5$ MeV and $\Delta = 2.0$ MeV. Further, we take $\lambda = 0.8$ as seems to be a reasonable value for the range adopted in most shell model calculations. For $\gamma_{\lambda}^2 = 6.67 \times 10^{-26}$ cm² as chosen in the previous section, this choice of λ gives the range of the Gaussian nuclear interaction to be $r_0 = 2.0 \times 10^{-13}$ cm. Finally, the choice of V_0 for each value of κ is so adjusted as to give the correct splitting of the $(d_{3/2})^2$, $J = 0, 2$ levels as observed in, say, 38 . Thus the only free parameters in our calculations are κ and q , and their determination will give us the information on the nuclear interaction as well as the strength of the core-particle coupling.

The eigenvalues of the lowest few energy levels are shown in figure 5. The energies of the levels are normalised to $E = 0$ for the ground state 0^+ . Figure (5a) shows the variation of the energy levels with the parameter κ for $q = 0.6$ MeV. Comparison with fig. 2 of chapter II shows that we have now for $\kappa < 0$, a low-lying state 2^+ which is essentially collective in nature. For $\kappa > 0$, the nature of the level spectrum for the lowest few levels (below 2 MeV) is essentially the same in both cases. This is natural since the first phonon-state occurs only at 2.5 MeV.

($\hbar\omega = 2.5$ MeV by our choice of parameters). A study of the energy and the eigenfunction of the first excited 2^+ state reveals an interesting relationship between the collective and particle aspects. For $\kappa > 0$, where the low-lying levels, and particularly the 2^+ level, occur

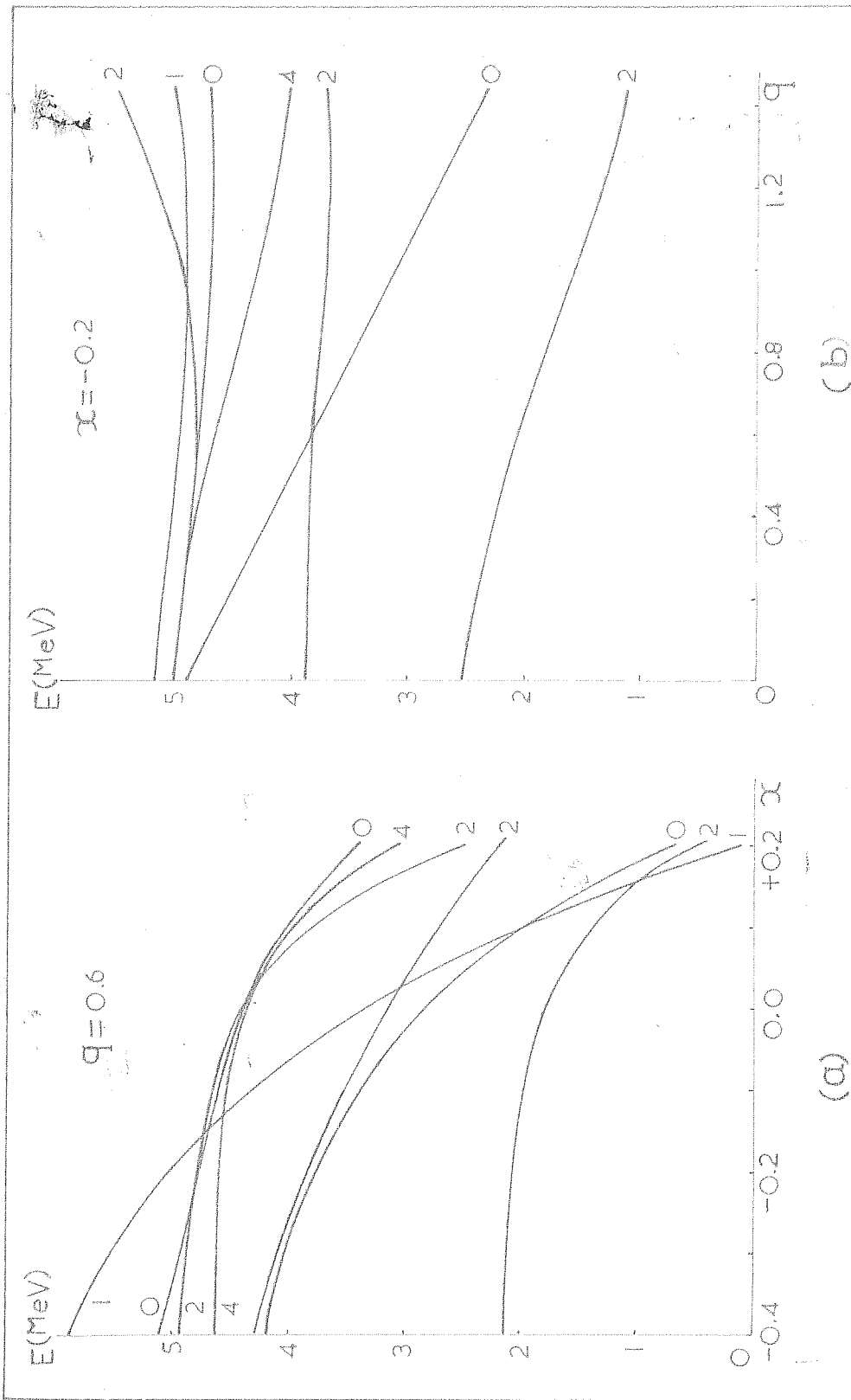


FIG. 5. ENERGY LEVELS OF ^{30}Si AS A FUNCTION OF (a) α AND (b) q , NORMALISED TO $E=0$ FOR THE GROUND STATE 0^+

below $\hbar\omega = 2.5$ MeV, the major component of the eigenfunction of the 2^+ state is $|(s_{1/2}^2 3/2), 2 : 00\rangle$. For example, for $\chi = 0.2$ ($q = 0.6$) this component has the value 0.85 (see table IX). However, for $\chi < 0$, where the particle states shown in Fig. 2 of chapter II are well above 2.5 MeV, the lowest 2^+ state is predominantly collective in nature, the major component being

$|(s_{1/2}^2 1/2), 0 : 12\rangle$. Thus the character of this state changes completely as the value of the parameter changes. This must affect the electromagnetic transition probabilities of the state as well, and a measure of the transition probability would provide a valuable piece of information on the relative roles of the collective and interparticle forces. Note that as χ varies from +0.2 to -0.4, the strength of the potential V_0 changes from 55 MeV to 30 MeV.

Fig. (5a) shows that the position of the lowest 1^+ level is quite sensitive to variation of χ . The experimental data show no 1^+ level below 4.8 MeV; it is also clear from Fig. (5b) that variation of q does not change the excitation energy of this level to any large extent. Hence, we conclude that the values of $\chi > -0.1$ are not permissible. We further note from Fig. (5b) that the energy of the second excited spin 2 state, 2^+ , is also relatively unaffected by change in the parameter q . Comparing the calculated and the observed energies of the state, we get $\chi \approx -0.2$. For this value of χ , one can then determine the best value of q by comparing the calculated

TABLE VIII

The amplitudes $a_1(j_1 j_2 J; \chi)$ of the wavefunctions for the ground state 0^+ of ^{61}Co .

$j_1 j_2 J; \chi$	$\chi = -0.2$				$q = 0.6$	
	$q = 0.4$	$q = 0.6$	$q = 0.8$	$q = 1.0$	$\chi = 0.0$	$\chi = +0.2$
$1/2 \ 1/2 \ 0; \ 00$	0.9723	0.9689	0.9623	0.9442	0.9623	0.9300
" " 20	-0.0103	-0.0256	-0.0378	-0.0820	-0.0258	-0.0451
" " 30	0.0005	0.0017	0.0042	0.0098	0.0022	0.0041
$1/2 \ 3/2 \ 2; \ 12$	-0.1014	-0.1534	-0.2138	-0.2843	-0.1525	-0.2788
" " 22	0.0051	0.0125	0.0233	0.0432	0.0151	0.0313
" " 32	-0.0015	-0.0052	0.0022	-0.0282	-0.0069	-0.0157
$3/2 \ 3/2 \ 0; \ 00$	0.2073	0.1832	0.1536	0.1137	0.1553	0.2257
" " 20	-0.0045	-0.0112	-0.0197	-0.0417	-0.0143	-0.0275
" " 30	0.0005	0.0019	0.0045	0.0102	0.0026	0.0052
$3/2 \ 3/2 \ 2; \ 12$	-0.0103	-0.0112	-0.0081	0.0073	-0.0142	-0.0274
" " 22	-0.0081	-0.0142	-0.0253	-0.0444	-0.0182	-0.0351
" " 32	0.0005	0.0013	0.0024	0.0106	0.0024	0.0053

TABLE IX

The amplitudes $c_1(j_1 j_2^j; M)$ of the wavefunctions
for the first excited spin 2 state in ^{61}Co

$j_1 j_2^j; M$	$\chi = -0.2$					$q = 0.6$				
	$q = 0.4$	$q = 0.6$	$q = 0.8$	$q = 1.0$	$\chi = 0.0$	$\chi = +0.2$	$\chi = 0.0$	$\chi = +0.2$	$\chi = 0.0$	$\chi = +0.2$
$1/2 \ 1/2 \ 0; \ 12$	0.9321	0.9735	0.9330	0.7734	0.7495	0.3321	0.7495	0.3321	0.7495	0.3321
$\quad \quad \quad ; \ 22$	-0.0080	-0.0211	-0.0379	-0.0543	-0.0336	-0.0379	-0.0336	-0.0379	-0.0336	-0.0379
$1/2 \ 3/2 \ 2; \ 00$	0.2339	0.3331	0.3819	0.4098	0.5213	0.8453	0.5213	0.8453	0.5213	0.8453
$\quad \quad \quad ; \ 12$	-0.0373	-0.0745	-0.1143	-0.1513	-0.1300	-0.2172	-0.1300	-0.2172	-0.1300	-0.2172
$\quad \quad \quad ; \ 20$	0.0366	0.0639	0.0770	0.0932	0.0937	0.0571	0.0937	0.0571	0.0937	0.0571
$\quad \quad \quad ; \ 22$	0.0821	0.1127	0.1354	0.1513	0.1108	0.0582	0.1108	0.0582	0.1108	0.0582
$\quad \quad \quad ; \ 24$	0.1150	0.1323	0.1390	0.2231	0.1623	0.0227	0.1623	0.0227	0.1623	0.0227
$3/2 \ 3/2 \ 0; \ 12$	0.3305	0.2579	0.2782	0.2982	0.3737	0.2300	0.3737	0.2300	0.3737	0.2300
$\quad \quad \quad ; \ 22$	-0.0047	-0.0136	-0.0263	-0.0366	-0.0235	-0.0407	-0.0235	-0.0407	-0.0235	-0.0407
$3/2 \ 3/2 \ 2; \ 00$	-0.0539	-0.0949	-0.1076	-0.1276	-0.1300	-0.1702	-0.1300	-0.1702	-0.1300	-0.1702
$\quad \quad \quad ; \ 12$	0.0250	0.0455	0.0750	0.0934	0.0804	0.1234	0.0804	0.1234	0.0804	0.1234
$\quad \quad \quad ; \ 20$	-0.0097	-0.0166	-0.0247	-0.0333	-0.0220	-0.0257	-0.0220	-0.0257	-0.0220	-0.0257
$\quad \quad \quad ; \ 22$	-0.0178	-0.0251	-0.0332	-0.0422	-0.0279	-0.0231	-0.0279	-0.0231	-0.0279	-0.0231
$\quad \quad \quad ; \ 24$	-0.0251	-0.0355	-0.0527	-0.0666	-0.0429	-0.0301	-0.0429	-0.0301	-0.0429	-0.0301
$1/2 \ 3/2 \ 1; \ 12$	-0.0106	-0.0191	-0.0273	-0.0337	-0.0439	-0.1514	-0.0439	-0.1514	-0.0439	-0.1514
$\quad \quad \quad ; \ 22$	0.0011	0.0032	0.0064	0.0100	0.0030	0.0085	0.0030	0.0085	0.0030	0.0085

TABLE X

The amplitudes $a_l(j_1 j_2 j : M)$ of the wavefunctions
for the second excited 2^+ state in ^{24}Mg .

$j_1 j_2 j : M$	$\chi = -0.2$						$q = 0.6$	
	$q = 0.4$	$q = 0.6$	$q = 0.8$	$q = 1.0$	$\chi = 0.0$	$\chi = +0.2$		
$1/2 \ 1/2 \ 0 : 12$	-0.2591	-0.3530	-0.4043	-0.4327	-0.5403	-0.6504		
	-0.1012	-0.2113	-0.3105	-0.3590	-0.1137	-0.0197		
$1/2 \ 3/2 \ 2 : 00$	0.8954	0.7901	0.6347	0.5314	0.7200	0.2593		
	-0.2019	-0.3147	-0.4094	-0.4891	-0.2958	-0.0723		
	0.0053	0.0150	0.0335	0.0359	-0.0053	-0.0457		
	-0.0314	-0.0522	-0.0942	-0.1230	-0.0398	-0.1534		
$3/2 \ 3/2 \ 0 : 12$	-0.0284	-0.0475	-0.0643	-0.0827	-0.1072	-0.2357		
	0.0003	0.0003	-0.0045	-0.0141	-0.0336	-0.3582		
	-0.0392	-0.0847	-0.1294	-0.1522	-0.0613	-0.0156		
	-0.2312	-0.2489	-0.2517	-0.2575	-0.2038	-0.0353		
$3/2 \ 3/2 \ 2 : 00$	0.1030	0.1487	0.1767	0.1910	0.1293	0.0237		
	-0.0093	-0.0221	-0.0393	-0.0489	-0.0159	-0.0043		
	0.0042	0.0094	0.0152	0.0236	0.0172	0.0293		
	-0.0010	-0.0044	-0.0095	-0.0135	0.0134	0.1103		
$1/2 \ 3/2 \ 1 : 12$	-0.0760	-0.0950	-0.1071	-0.1106	-0.1156	-0.4717		
	0.0059	0.0126	0.0229	0.0315	0.0114	-0.0462		

energies of the 2^+ and 0^+ states shown in fig. (6b) with the observed values. In this way, we find $q \approx 0.6$ as the best value. Figure 6 shows for $q = 0.6$ MeV, $\alpha = -0.2$ the energy levels of 81^{30} calculated for $\hbar\omega = 2.0, 2.5$ and 3.0 MeV. It appears that the choice

$$q = 0.6 \text{ MeV}, \quad \alpha = -0.2 \text{ and } \hbar\omega = 2.5 \text{ MeV}$$

gives a reasonable account of the observed spectrum. It should, however, be borne in mind that inclusion of 3-phonons in the Hamiltonian matrix of $I = 2$ states may depress these states to some extent, and to obtain a better fit, we may have to vary these parameters to some extent. In particular, it may be necessary to take a larger negative value of α . We do not think that these changes would drastically affect our conclusions, as the wavefunctions in tables IX and X indicate that the convergence with increasing N is quite good.

Comparison of the observed (Mue60, Roy61) and calculated level spectra shown in fig. 6 shows that the lowest four energy levels are successfully predicted by the model. A further group of states with spins 1, 0, 4 and 3 are predicted near $4.6 - 5.0$ MeV, and it will be of interest to measure the spins of the observed levels at $4.8 - 5.3$ MeV. Some experiments report the occurrence of a close doublet at 3.79 MeV, one of the two levels being 0^+ . Our calculations do not show any such doublet, but only a single level 0^+ . Further experimental evidence for this doublet seems to

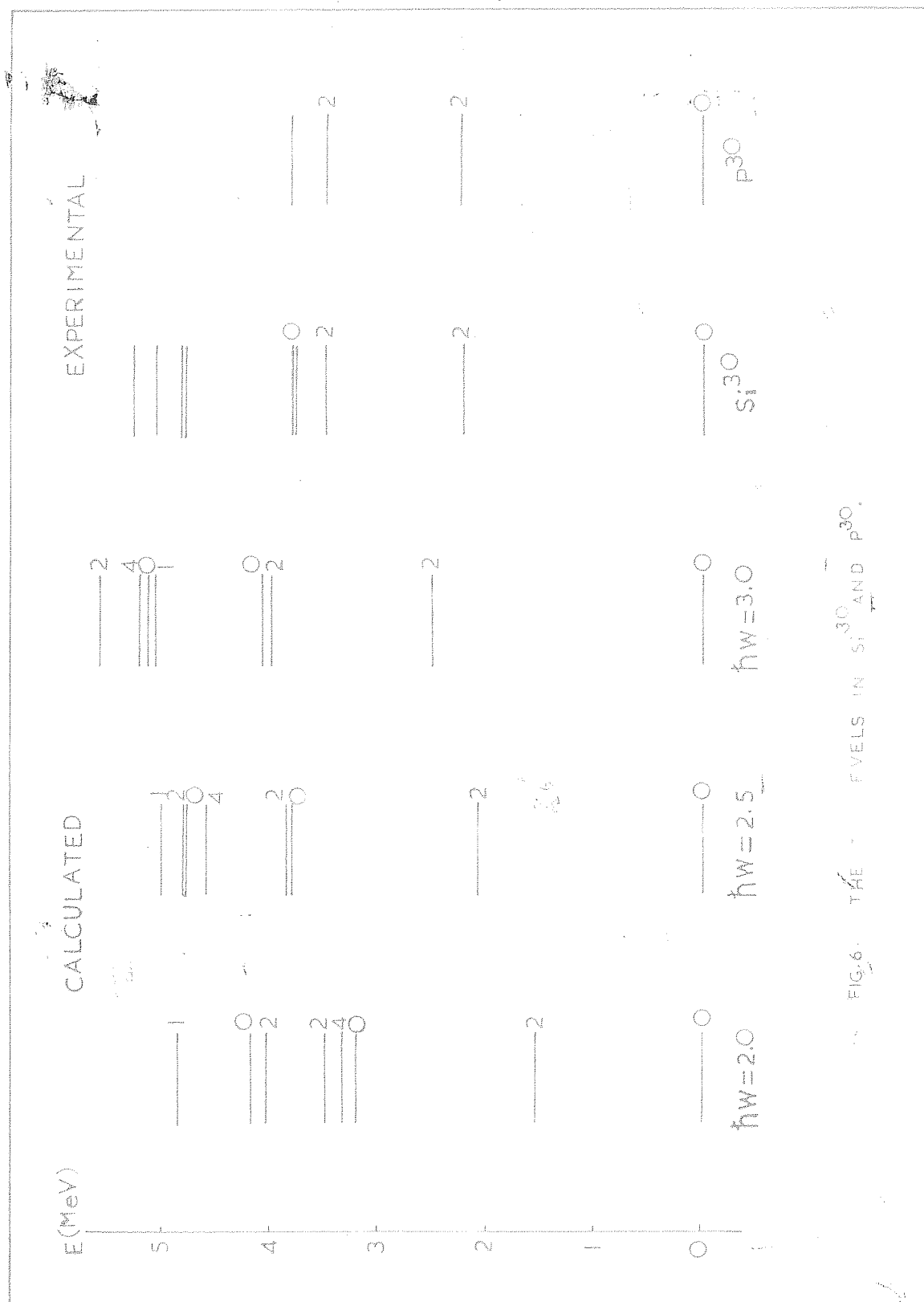


FIG. 6. THE ENERGY LEVELS IN Si^{30} AND P^{30} .

be desirable. The energies of the lowest four $I = 1$ states in p^{30} (Bat60) agree very well with the corresponding energies in Si^{30} . This agreement suggests that the spin of the 4.50 MeV level in p^{30} should also be 0^+ . It is also desirable to check carefully if this level is also a close doublet.

We may make some general remarks on the systematics of the energy levels emerging from our study. The occurrence of a low-lying 0^+ level is of particular interest. For parameters in the reasonable range of our choice, the energy levels are: ground state 0^+ , first excited state 2^+ , next a close doublet 0^+ , 2^+ , and a group of higher levels which includes a 4^+ as the lowest member. The observed spectrum (Goe60) of Mg^{26} shows the level order to be 0^+ , 2^+ , 0^+ , 2^+ , and that of S^{32} shows the level order to be 0^+ , 2^+ , 0^+ upto excitations of 4 MeV. It is thus possible that the properties of these nuclei could also be very well explained on the basis of an intermediate-coupling collective model. Of course, this needs further extensive calculations. We note that the structure of the Ca^{42} level spectrum also shows a low 0^+ state just above the first excited state 2^+ .

The work reported in this section supplements the calculations of Raz (Raz59) on collective and interparticle forces in even-even nuclei. He has considered the intrinsic states of two nucleons to be those of the $(f_{7/2})^2$ configuration, $J = 0, 2, 4, 6$. Already this leads to large

Hamiltonian matrices, and practically precludes study of mixed configurations for the particle states. For our study we have chosen a simpler configuration which enables us to include the effect of configuration mixing in our calculations. It may be noticed that the results of Raa do not predict a low-lying 0^+ state as is observed in Ca^{42} and to be of practical interest, his calculations would have to include mixed configurations. We do not compare our results with those of Raa, since they are addressed to complementary problems, but note that the two calculations taken together now form a complete study of the systematics of even-even nuclei in terms of an intermediate-coupling collective model.

5.2. Electromagnetic Transitions

We have calculated the electromagnetic transition probabilities for the transitions $2 \rightarrow 0$, $2^+ \rightarrow 0$ and $2^+ \rightarrow 2$ for $\hbar\omega = 2.5$ MeV, $\chi = -0.2$, $q = 0.4, 0.6, 0.8$ and 1.0 as well as for $q = 0.6$, $\chi = 0.0$ and $+0.2$. The results are shown in tables XI to XIV and figures 7 and 8.

Unfortunately, we do not have any quantitative data for the transition probabilities in these nuclei (Si^{30} and P^{30}) with which we can compare the calculated results. Qualitatively, Brunde and Dove (Bre60) have reported transitions from the second excited state 2^+ and from a level at 3.73 MeV to the first excited state of

TABLE XI

Reduced E2 transition probabilities for the
transitions $2 \rightarrow 0$, $2^* \rightarrow 0$ and $2^* \rightarrow 2$ in Si^{30} .

Quantity	$\chi = -0.2$				$q = 0.6$	
	$q=0.4$	$q=0.6$	$q=0.8$	$q=1.0$	$\chi = 0.0$	$\chi = +0.2$
$k^2 B(E2; 2 \rightarrow 0)$	5230	9505	13044	12339	6411	413
$k^2 B(E2; 2^* \rightarrow 0)$	552	2068	5050	7539	4412	5123
$k^2 B(E2; 2^* \rightarrow 2)$	81	714	2333	5356	473	9
$\frac{B(E2; 2^* \rightarrow 0)}{B(E2; 2 \rightarrow 0)}$	0.106	0.218	0.388	0.611	0.688	12.401
$\frac{B(E2; 2^* \rightarrow 2)}{B(E2; 2 \rightarrow 0)}$	0.016	0.076	0.198	0.431	0.074	0.023
$\frac{B(E2; 2^* \rightarrow 0)}{B(E2; 2^* \rightarrow 2)}$	6.813	2.895	1.955	1.357	9.323	549.72

TABLE XII

E2 transition probabilities for the
transition $2 \rightarrow 0$ in Si^{30} .

x	q (MeV)	ΔE (MeV)	$T(E2) \quad (10^{11} \text{ sec}^{-1})$			
			$k = 10$	$k = 20$	$k = 30$	$k = 40$
-0.2	0.4	2.30	152.74	45.69	20.31	10.92
	0.6	2.06	200.83	60.22	22.32	12.56
	0.8	1.81	137.56	34.39	15.28	8.60
	1.0	1.54	58.02	14.51	6.45	3.23
0.0	0.6	1.84	73.39	12.35	8.16	4.59
+0.2		0.63	0.01	0.003	0.001	0.000

TABLE VII

E2 transition probabilities for the
transition $2^+ \rightarrow 0$ in Si^{30} .

χ	q (MeV)	ΔE (MeV)	$B(E2) (10^{11} \text{ sec}^{-1})$			
			k = 10	k = 20	k = 30	k = 40
-0.2	0.4	3.22	253.31	65.83	29.25	15.46
	0.6	3.25	949.73	237.43	105.53	59.36
	0.8	3.76	2064.27	513.67	229.36	123.02
	1.0	3.66	2687.97	671.99	299.56	167.99
0.0	0.6	3.14	731.08	192.77	81.23	45.69
+0.2		2.22	149.97	37.49	16.66	9.37

TABLE XV

Transition probabilities for the transition $2^+ \rightarrow 2$ in ^{30}Si .

χ	q (MeV)	ΔE (MeV)	$\Gamma(E2) \text{ (} 10^{11} \text{ sec}^{-1} \text{)}$				$\Gamma(E1)$ (10^{11} sec^{-1})
			$k = 10$	$k = 20$	$k = 30$	$k = 40$	
-0.2	0.4	1.58	0.432	0.108	0.048	0.027	38.713
	0.6	1.77	6.737	1.884	0.749	0.421	70.901
	0.8	1.95	39.610	9.903	4.401	2.473	94.182
	1.0	2.12	129.205	32.301	14.356	8.075	81.733
0.0	0.6	1.30	0.953	0.236	0.106	0.050	55.833
+0.2		1.67	0.066	0.016	0.007	0.004	4.034

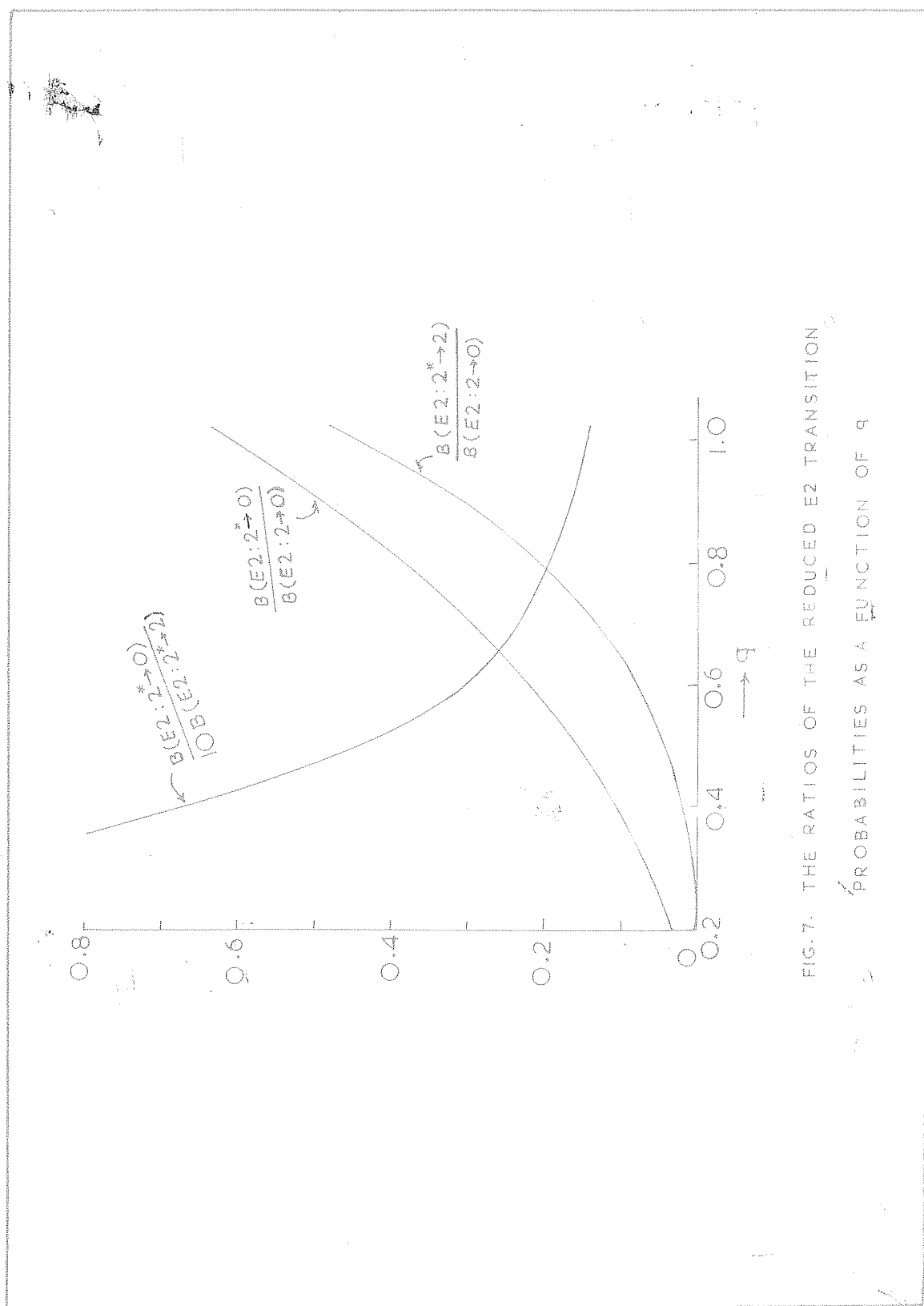


FIG. 7. THE RATIOS OF THE REDUCED E2 TRANSITION PROBABILITIES AS A FUNCTION OF q

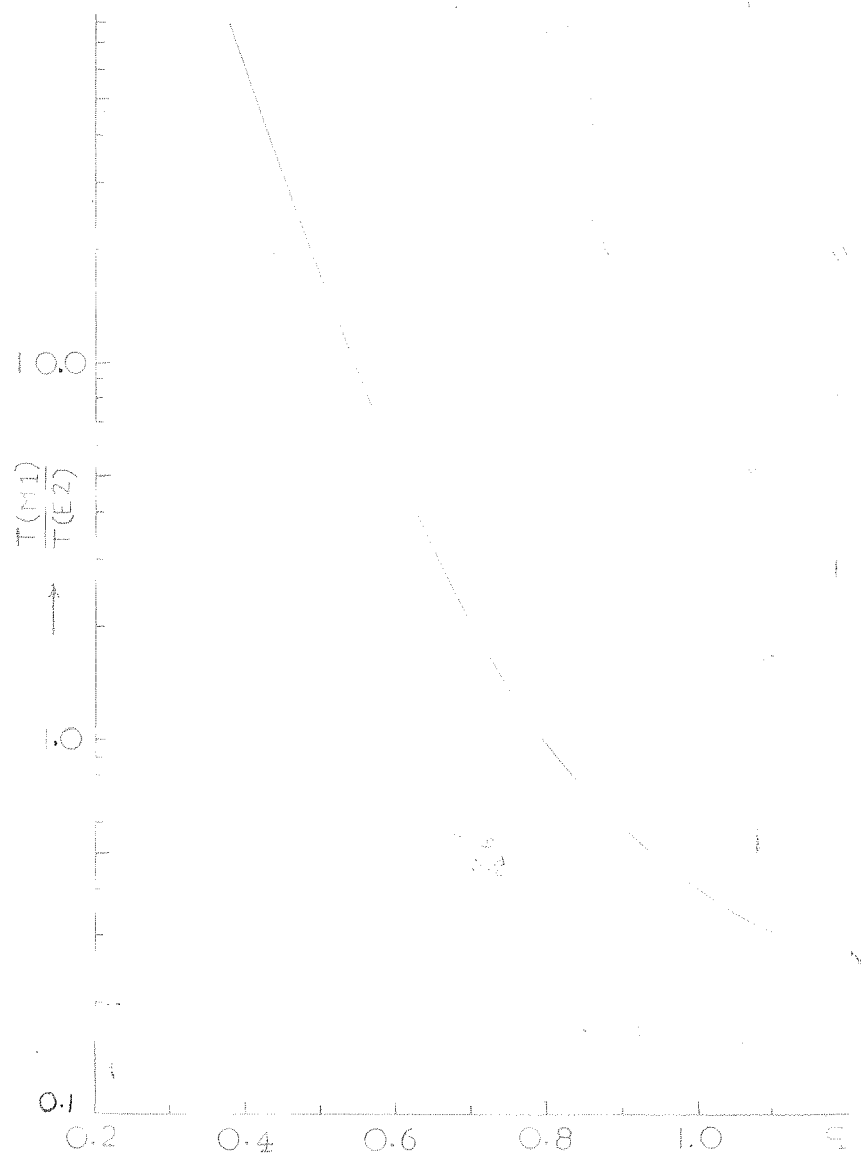


FIG.8. THE MULTIPOLE RATIO OF THE TRANSITION PROBABILITIES FOR THE TRANSITION $2^+ \rightarrow 2$, AS A FUNCTION OF ϵ (k=20 MeV).

spin 2, as well as a cross-over transition to the ground state from the 2^+ state. No direct transition is seen from the 3.79 MeV level (or levels if this is really a doublet) to the ground state. Most of these features are predicted by our model, as can be seen from the tables. The calculations further predict that the decay of the 2^+ state to the state 2 in Si^{30} is mainly through an M1 transition. Although no data is available for Si^{30} , it has been found that for O^{16} the $2^+ \rightarrow 2$ decay takes place through a purely M1 radiation (Goe60). Further accumulation of quantitative data on electromagnetic transition probabilities or lifetimes and M1 - E2 mixtures would greatly increase our understanding of the collective effects.

If the levels of Si^{30} were to be interpreted as a purely vibrational spectrum, one would expect no cross-over transition from the 2^+ state to the ground state and the ratio of the reduced transition probabilities for the transitions $2^+ \rightarrow 2$ and $2 \rightarrow 0$ would be $B(E2; 2^+ \rightarrow 2)/B(E2; 2 \rightarrow 0) = 2$. The wavefunctions of these states shown in tables VIII, IX and X show that this ideal situation is not exactly realized; in particular, the 2^+ state is predominantly a particle state $|1/2 \ 3/2 \ 3; 00\rangle$, and not a two-phonon state. Thus the results for electromagnetic transitions in the framework of the intermediate-coupling collective model are very different from those expected on the basis of a simple vibrational model.

Certain interesting features emerge from the results shown in table XI, where the reduced transition probabilities as well as their ratios are listed for different transitions; and tables XII - XIV:

- (1) For $q \leq 0.8$, the energy of the first excited state, 2^+ , decreases and at the same time $B(E2; 2 \rightarrow 0)$ increases with increasing value of q . This behaviour is also reported by *nas* and is in agreement with the data for a large number of even-even nuclei.
- (2) The values of $B(E2; 2 \rightarrow 0)$ show considerable increase over the shell model values for the transition $d_{3/2} \rightarrow s_{1/2}$.
- (3) The ratio $B(E2; 2^+ \rightarrow 0)/B(E2; 2^+ \rightarrow 2)$ decreases with increasing values of q .
- (4) The ratio $B(E2; 2^+ \rightarrow 2)/B(E2; 2 \rightarrow 0)$ increases rapidly with q , from 0.015 for $q = 0.4$ to 0.450 for $q = 1.0$.
- (5) For the transition $3^+ \rightarrow 2$, the ratio $I(E1)/I(E2)$ decreases very rapidly and is < 1 for $q \geq 0.9$. An experimental determination of this ratio should be very helpful in determining the degree of deformation of the nucleus.
- (6) The cross-over transition from the 2^+ state to the ground state predominates over the direct

transition $2^+ \rightarrow 2$ for $q \geq 0.8$ MeV, for $k \leq 25$ MeV, the cross over transition is always favoured over the direct transition.

Most of these results agree with the calculations of Raa (Raa59). To compare the two sets of results, we must note that with our values of the parameters ($q = 0.8$ MeV, $\hbar\omega = 3.5$ MeV), we get for $j = 7/2$, $\alpha = 0.20 - 0.25$.

Finally, we conclude that the results of the intermediate-coupling collective model for Si^{30} as reported above show a considerable departure from the results to be expected on the basis of a simple vibrational model, and give a much better agreement with the observed level spectrum of Si^{30} and the general trend of electromagnetic transition probabilities.

6. Discussion of the Parameters

In this section we shall examine the validity of the model, primarily by discussing the values of the parameters of the model obtained in the previous sections, and comparing them with similar parameters obtained by other authors.

The parameters pertaining to the independent particle motion are Δ , the separation of the single particle levels $2s_{1/2}$ and $1d_{3/2}$, and the interparticle interaction. The value of Δ obtained by us, viz., 2 MeV, appears to be quite

reasonable. If the splitting of the sub-levels of a given oscillator shell (in this case the $d_{5/2}$, $d_{3/2}$ and $d_{1/2}$ levels of the $n = 2$ shell) is determined by the simple spin-orbit interaction $a\vec{l}\cdot\vec{s}$, we get for $\Delta = 2$ MeV, $a = 1.33$ MeV. We would like to emphasize that Δ is primarily a phenomenological constant.

The strengths of the interparticle forces in spin-singlet and spin-triplet states ($I = 1$) are found to be $v_s = -41.6$ MeV and $v_t = -20.9$ MeV respectively corresponding to our value of $\kappa = -0.2$. As we pointed out in a previous section, a better treatment of the $I = 2$ states of Si^{30} may result in an increase in the magnitude of κ , and if $\kappa = -0.3$, we would have for the singlet and triplet strengths, -43.7 MeV and -18.1 MeV. Thus the forces in both the spin states are found to be attractive, the singlet forces being stronger than the triplet forces. In a recent analysis Peaslee (Pea61) suggests the values $v_s = -30 \pm 3$ MeV and $v_t = 0 \pm 6$ MeV. Our potential appears to be somewhat stronger. It should, however, be noted that there is considerable disagreement regarding the nature of the effective nucleon-nucleon forces in nuclei amongst various authors, and in particular the strength of the odd-state force v_t is not at all well-known. The range of the potential (for the choice of a Gaussian shape) is 2.0×10^{-13} cm. This agrees with the choice of most of the authors as may be seen from table XV. We conclude that the parameters of the interparticle forces in Si^{30} appear to be quite reasonable.

TABLE XV

Comparison of the parameters obtained by various authors for the intermediate-coupling collective vibrational model.

Nucleus	Core	$\hbar\omega$ (MeV)	k^2/c	k (MeV)	C (MeV)	Q (MeV)	V_0 (MeV)	R_0 (fm)	γ	$\bar{\rho}$	Ref.
$^{15}\text{P}^{31}$	$^{14}\text{Si}^{30}$	2.5	10.05	20	40	1.00	-	-	-	0.40	present
$^{80}\text{Zr}^{17}$	$^{80}\text{Zr}^{18}$	2.0	30.19	40	53	1.55	-	-	-	0.31	1)
$^{90}\text{Zr}^{19}$	$^{10}\text{Ne}^{20}$	1.63	48.48	40	33	1.79	-	-	-	0.33	1)
$^{82}\text{Pb}^{206}$	$^{82}\text{Pb}^{208}$	3.6	1.40	40	1140	0.45	- 8	1.85	-1.00	0.09	2)
"	"	3.0	1.60	40	1000	0.44	-	2.0	-	0.09	3)
$^{82}\text{Pb}^{210}$	"	3.0	0.80	40	3000	0.31	-	1.95	-	0.06	3)
$^{81}\text{Y}^{206}$	"	3.0	1.60	40	1000	0.44	-23	2.0	-0.05	0.09	4)
$^{83}\text{Y}^{210}$	"	3.0	1.60	40	1000	0.44	-24	2.0	-0.16	0.09	4)
$^{20}\text{Ca}^{42}$	$^{20}\text{Ca}^{40}$	1.0	20.86	13	10	0.53	- 9	2.7	-0.33	0.18	5)
$^{146}\text{Sm}^{30}$	$^{146}\text{Sm}^{28}$	2.5	3.62	30	110	0.6	-25	2.0	-0.2	0.34	present

References for Table XV:

- 1) C.S.Warke and G.Abraham: Nuclear Physics, 10, 306 (1959).

The coupling between the collective and the independent particle motions is denoted by the parameter $P = (3/4) (q/\hbar\omega)^2$. $P = 0.75$ for O^{17} and 1.5 for P^{19} .

- 2) W.W.True and E.W.Ford: Phys. Rev. 102, 1075 (1958).

The value of $\hbar\omega$ is as given in an earlier paper by True (Phys. Rev. 101, 1342 (1956)). A purely singlet potential, $V = V_0 \exp(-r^2/\beta^2)$, with $V_0 = V_s = -32.5$ MeV is used. In our notation,

$$V_0 = \frac{1}{4} (3V_t + V_s) \quad ; \quad \alpha = \frac{V_t - V_s}{4 V_0}$$

where, V_t and V_s denote the triplet part and the singlet part of the potential respectively.

- 3) V.N.Guzan, Yu.I.Kharitonov, L.A.Sliv and G.A.Sogomonova: Nuclear Physics, 23, 192 (1961).

Their parameters describing the internucleon forces are $-V_s$, $-V_t$ and $\rho = \rho_0$. The values of $-V_s$ and $-V_t$ are not separately determined, but the effective sum of $-V_s$ and $-V_t$ is determined to be 25 MeV for Pb^{208} and 35 MeV for Pb^{210} .

- 4) L.A.Sliv, G.A.Sogomonova and Yu.I.Kharitonov: Sov. Phys.JETP, 12, 661 (1961).

The parameters are the same as in 3). They obtain $-v_t = 22$ MeV, $-v_s = 27$ MeV for ^{206}Pb and $-v_t = 20$ MeV, and $-v_s = 35$ MeV for ^{210}Pb .

5) H.J.Hart: Phys.Rev. 114, 1118 (1959).

The coupling constant is $\alpha = (5/24)^{1/2} (g/\hbar\omega)$. Best value of $\alpha \approx 0.7$ and $C = 10 \hbar\omega$; $\hbar\omega \approx 1$ MeV for Ca^{48} .

The collective motion is described by the parameter $\hbar\omega$, and the coupling of the extra-core nucleons to the core oscillations by the parameters q and k . We have determined $\hbar\omega = 2.5$ MeV. Paenbergh and Goldhammer considered the hydrodynamical value of $\hbar\omega \approx 3$ MeV. However, it is now known that a hydrodynamical description is quite inadequate. Aranjó (Aro59) has used a semi-classical model to calculate theoretically the parameters for collective quadrupole oscillations of Si^{28} . He obtains $\hbar\omega = 1.31$ MeV and $C = 29.5$ MeV. In his calculations he has chosen $\Delta = 4.1$ MeV, which is rather large compared to our value of 2.0 MeV. The strength of the coupling constant q , we find to be 0.6 MeV for Si^{30} and 1.0 MeV for P^{31} . It is not surprising to find a larger coupling constant for the odd-even nucleus P^{31} than for the even-even nucleus Si^{30} . However, we also found $q = 0.6$ MeV for Si^{29} and P^{29} . This is somewhat surprising, since one would have expected a larger coupling constant in this case analogous to P^{31} . We should keep in mind that this determination of q follows from the separation of the $3/2$ and $3/2^+$ states, and the structure of the level spectrum for Si^{29} (and P^{29}) is different from that of P^{31} for states above 2 MeV. In view of the limited application of our model to Si^{29} and P^{29} , we shall not discuss their parameters in this section.

With the above mentioned values of q and $\hbar\omega$, we get

$$\begin{aligned} (k^2/C) &= \pi (q^2/\hbar\omega) = 10.05 \text{ for } \text{P}^{31} \\ &= 3.62 \text{ for } \text{Si}^{30} \end{aligned} \quad (52)$$

It was pointed out that the strength of the electromagnetic transitions in nuclei depend upon the parameter $(RC)^{-1}$ which can be expressed in terms of (q/k) since $\hbar\omega = \hbar \sqrt{C/S}$. Thus a study of the electromagnetic transitions would enable us to determine k . Unfortunately, the available information is not sufficient to do this. However, we found that a qualitative understanding of the experimental results can be obtained (particularly for P^{31}) by taking $k \leq 10$ MeV. This remark needs to be qualified. We had observed that the magnetic moment of the ground state of P^{31} predicted by the theory is rather high by a factor of 2 to 3, and to bring it down to the observed value, the matrix element of the magnetic dipole operator has to be reduced by such a factor. If this phenomenological adjustment be made, the calculated transition probability for the magnetic dipole transition, $T(M1)$, which involves square of the matrix element concerned, would also be reduced. Then table V shows that in this case it may be possible to obtain agreement with experimental data even for a larger k , say $k = 30$ MeV. Therefore, pending a more exact determination of k , we may choose $k = 20$ MeV. This may be compared to the usual value $k = 40$ MeV adopted by many authors. Brink (Br56) has however mentioned that $k = 10$ MeV seems to be a more reasonable value rather than $k = 40$ MeV.

Now, it is useful to introduce a root-mean-square deformation in the vibrational model, which can be compared to the equilibrium deformation in the rotational model.

This is defined as (Brk60)

$$(\bar{\beta})^2 = \frac{5}{2} \hbar (BC)^{-1/2} = \frac{5}{2} \cdot \frac{\hbar \omega}{C} = 20\pi (g^2/k^2) \quad (53)$$

$$\text{or } \bar{\beta} \approx 8 (g/k)$$

With the value of $k = 20$ MeV, we find $\bar{\beta} = 0.40$ for P^{31} and 0.24 for Si^{30} . Brink has listed this mean deformation $\bar{\beta}$ for several even-even nuclei with vibrational spectra, and the values range from 0.17 to 0.23 in the region $A = 94 - 116$. Thus the value for Si^{30} is satisfactory and as previously mentioned one would expect a larger value for P^{31} . It should now be noted that for smaller values of k , one would obtain unreasonably large mean deformation and this seems to be a strong argument for adopting $k = 20$ MeV rather than a smaller value.

With $k = 20$ MeV, we may obtain from equation (52), $C = 40$ MeV for P^{31} and $C = 110$ MeV for Si^{30} . Comparing these with Araujo's value of 30 MeV (and the hydrodynamical value of 45 MeV) for Si^{28} core without any extra-core nucleons, we note that the Si^{30} core in P^{31} appears to be a little more stable to collective vibrations than the pure Si^{28} core, whereas the Si^{28} core in Si^{30} is made considerably more stable to oscillations by the addition of a pair of neutrons.

7. Conclusion

The results of the calculations presented in chapter II and this chapter show that whereas the simple shell model description is not adequate for describing the properties of the nuclei Si^{28} , P^{29} , Si^{30} , P^{31} etc., a unified model with weak-coupling collective vibrations gives a very reasonable description of the observed properties of these nuclei. This model is at least as good as, if not better than, the collective rotational model, also applied to these nuclei. A further test of these two models and in particular, the quantitative estimates of the weak-coupling collective vibrational model for electromagnetic transitions, can only be made when more exact measurements of the decay properties of the various levels are available. This would also enable us to determine more satisfactorily parameters like k and C .

REFERENCES

1. Alm58 G.Abraham and C.S.Warke: Nuclear Physics, 8, 69 (1958)
2. Aro59 J.M.Araujo: Nuclear Physics, 12, 360 (1959).
3. Bat60 E.E.Baart, L.L.Green and J.C.Willmott: Proc. Int.Conf.Nuclear Structure, Kingston (1960), p.668.
4. Bat62 E.E.Baart, L.L.Green and J.C.Willmott: Proc. Phys.Soc. (London), 72, 237 (1962).
5. Bor52 A.Bohr: Dan.Nat.Fys.Medl. 24, no.14 (1962).
6. Bor53 A.Bohr and B.Mottelson: Dan.Nat.Fys.Medl. 27, no.15 (1963).
7. Bre58a C.Broude, L.L.Green and J.C.Willmott: Proc. Phys.Soc.(London), 72, 1097, 1115 (1958).
8. Bre58b C.Broude, L.L.Green and J.C.Willmott: Proc. Phys.Soc.(London), 72, 1122 (1958).
9. Bre60 C.Broude and H.E.Gove: Bull.Am.Phys.Soc. ser.II, 5, 348 (1960).
10. Brk60 D.M.Brink: Prog.Nucl.Phys. 8, 97 (1960).
11. Bry57a D.A.Bromley, H.E.Gove, E.B.Paul, A.E.Litherland and E.Almqvist: Can.J.Phys. 35, 1042 (1957).

12. Bry57b D.A.Bronley, H.E.Gove and A.E.Litherland: Can.J.Phys. 35, 1057 (1957).
13. Can54 B.C.Carlson and I.Talmi: Phys.Rev. 95, 436 (1954).
14. Chy54 D.C.Choudhury: Can.Mat.Pys.Natl. 22, no. 4 (1954).
15. Peg51 E.Peenberg and E.C.Hammett: Phys.Rev. 81, 225 (1951).
16. Peg53 E.Peenberg: "Shell Theory of the Nucleus", Princeton University Press (1953).
17. Ford58 E.W.Ford and C.Levinson: Phys.Rev. 100, 1 (1958).
18. Fey50 L.L.Foley and F.F.Helford: Phys.Rev. 82, 751 (1950).
19. Goe50 H.E.Gove: Proc.Int.Conf.Nuclear Structure, Kingston (1950), p.458.
20. Gol56 P.Gollhammer: Phys.Rev. 101, 1375 (1956).
21. Gun51 V.N.Guman, L.A.Sliv and G.A.Segomonova: Sov. Phys. JETP, 12, 232 (1961).
22. Jan51 H.A.Jahn: Proc.Roy.Soc. A205, 192 (1951).
23. Ker53 A.E.Kerman: Phys.Rev. 92, 1175 (1953).
24. L1458 A.E.Litherland, H.McManis, N.B.Paul, D.A.Bronley and H.E.Gove: Can.J.Phys. 36, 378 (1958).

25. Mil44 F.J.Milford: Phys.Rev. 52, 1337 (1944).
26. Win53 S.C.Wilson: Dan.Mat.Fys.Medd. 21,
no. 15 (1953).
27. Pen51 D.C.Penslee: Phys.Rev. 121, 839 (1961).
28. Rah42 C.Racah: Phys.Rev. 52, 438 (1942).
29. Raf30 J.Raimwater: Phys.Rev. 72, 432 (1950).
30. Raz37 B.J.Raz: Phys.Rev. 107, 1201 (1957).
31. Raz59 B.J.Raz: Phys.Rev. 114, 1115 (1959).
32. Raz60 B.J.Raz: Phys.Rev. 120, 169 (1960).
33. Rov61 A.N.Romanov: Sov.Phys.JETP, 12, 1072 (1961).
34. Ser55 G.Scharff-Goldhaber and J.Wemmer: Phys.Rev. 92, 212 (1953).
35. Sliv61 L.A.Sliv, G.A.Segomonova and Yu.I.Kharitonov: Sov.Phys.JETP, 12, 661 (1961).
36. Tre53 W.W.Truo: Phys.Rev. 101, 1342 (1953).
37. Tre58 W.W.Truo and K.W.Ford: Phys.Rev. 102,
1975 (1952).
38. Tre61 W.W.Truo: Nuclear Physics, 25, 155 (1961).
39. Wei49 O.Wentzel: "Quantum Theory of Fields", ch.II,
Interscience Publishers, New York (1949).
40. Who60 R.E.White: Phys.Rev. 112, 767 (1960).

APPENDIX I

We give below the Hamiltonian Matrices for nuclei with one or two nucleons outside the core Si^{28} or Si^{30} .

The following abbreviations are used:

- C = Core
- $(C + n)$ = n nucleons outside the core C .
- Δ = $\epsilon(113/2) - \epsilon(2s_{1/2})$
- \hbar = $\hbar(kw/8 \pi C)^{1/2}$
- a = $\langle (s_{1/2})^2 | H_{10} | (s_{1/2})^2 \rangle_{J=0}$
- b = $\langle (s_{1/2}^{\uparrow} d_{3/2}^{\uparrow}) | H_{10} | (s_{1/2}^{\uparrow} d_{3/2}^{\uparrow}) \rangle_{J=2} + \Delta$
- c = $\langle (d_{3/2})^2 | H_{12} | (d_{3/2})^2 \rangle_{J=0} + 2\Delta$
- d = $\langle (d_{3/2})^2 | H_{12} | (d_{3/2})^2 \rangle_{J=2} + 2\Delta$
- e = $\langle (s_{1/2}^{\uparrow} d_{3/2}^{\uparrow}) | H_{12} | (s_{1/2}^{\uparrow} d_{3/2}^{\uparrow}) \rangle_{J=1} + \Delta$
- (aa) = $\langle (s_{1/2})^2 | H_{12} | (d_{3/2})^2 \rangle_{J=0}$
- (dd) = $\langle (s_{1/2}^{\uparrow} d_{3/2}^{\uparrow}) | H_{12} | (d_{3/2})^2 \rangle_{J=2}$

0

-1.4142q $\Delta + hw$

(C + 1) : I = 1/2

0 -0.8944q 2hw

0 1.1833q 0 $\Delta + 2hw$

0 0 0 -1.0954q 3hw

0 0 -1.6733q -0.6325q 0 $\Delta + 3hw$

$$(C + I) = I = 3/2$$
[illegible]

hw

0 $\Delta + hw$

0 -0.6325q 2hw

-0.6325q -0.5452q 0 $\Delta + 2hw$

-1.5492q 0.8281q 0 0 $\Delta + 2hw$

0 0 0 -0.3381q -0.8281q 3hw

0 0 0 -1.3093q 0.5345q 0 3hw

0 0 -0.3381q -0.4518q 0.4426q 0 0 $\Delta + 3hw$

0 0 -1.0054q -0.5355q -0.5376q 0 0 0 $\Delta + 3hw$

0 0 -1.3732q 0.7340q 0.7491q 0 0 0 $\Delta + 3hw$

$$(0 + 1) : L = 5/2$$

Δ + Δ

b919c.1

0.33314

1.13324

0

0

0

0

0

Δ

0

0

0

0

0.71714

-0.70714

0.32244

Δ + Δ

0

0.46324

1.13324

0.13074

0.20184

1.00514

Δ + Δ

-0.62114

0.22244

0.60614

-0.23304

-0.22244

Δ

0

0

0

0

Δ

Δ + Δ

Δ + Δ

Δ + Δ

(C + 1) : 1 = 7/2

$(C + 2) + 1 = 2$

a

(ac) c

0 0 a + 2hr

2q -1.4142q -1.2550q b + hr

0 0 0 0 a + 3hr

0 0 0 1.1532q -1.5102q b + 2hr

0 0 (ac) -0.2044q 0 0 c + 2hr

0 2q 0 0 (bd) 0 -1.6733q 1.2550q d + hr

0 0 0 -1.6733q 0 (bd) 0 0 d + 2hr

0 0 -2.3554q 0 0 0.6325q -1.6733q 0 -0.2044q b+3hr

0 0 0 0 (ac) 0 -1.0354q 0 0 1.5344q 0 c+3hr

0 0 0 0 0 -0.2044q 2.3554q 0 0 (bd) 0 d+3hr

0.70719 5 12

0.7071g 0 0 + 1m

100-2 : 1-1

$$0 \quad 0.5916q \quad -0.5916q \quad b + 2hr$$

g. (b1) 0 -0.8367g d + bar

0 0.4472q 0.4472q 0 0.6325q • + 2hr

0 -0.5916q 0.5916q 0 -0.8367q 0 • + 2hr

$$0 \quad -0.8367q \quad -0.8367q \quad (nd) \quad 0 \quad 0 \quad 0 \quad d + 2hw$$
$$0 \quad 0 \quad 0 \quad 0.3162q \quad 0 \quad 0.8967q \quad -0.3162q \quad -0.4472q \quad b + 3hw$$
$$0 \quad 0 \quad 0 \quad -0.7746q \quad 0 \quad 0 \quad -0.7746q \quad 1.0954q \quad 0 \quad b + 3m$$

0 0 0 0.5477q 0 0 0.5477q 0.7746q 0 0 • + 3hw

0 0 0 -0.3162g 0 0.0967g 0.3162g -0.4472g 0 0 0 • + 3hr

$$0 \quad 0 \quad 0 \quad -0.4472q \quad 0 \quad 1.1832q \quad -0.4472q \quad 0 \quad (ba) \quad 0 \quad 0 \quad 0 \quad d + 3hr$$
$$0 \quad 0 \quad 0 \quad 1.0954q \quad 0 \quad 0 \quad -1.0954q \quad 0 \quad 0 \quad (bd) \quad 0 \quad 0 \quad 0 \quad d + 3hw$$

$a + hw$ $-0.8944q \quad b$ $0 \quad 0 \quad a + 2hw$ $0 \quad 0.8367q \quad -1.2650q \quad b + hw$ $(c + 2) : \underline{1 = 2}$ $(ac) \quad -0.6325q \quad 0 \quad 0 \quad c + hw$ $0 \quad (bd) \quad 0 \quad -1.1832q \quad 0.8944q \quad d$ $-0.3657q \quad 0 \quad 0 \quad 0.5292q \quad -0.4000q \quad 0 \quad b + 2hw$ $-1.2650q \quad 0 \quad 0 \quad -0.2535q \quad -0.8944q \quad 0 \quad 0 \quad b + 2hw$ $-1.6971q \quad 0 \quad 0 \quad 0.4535q \quad -1.2000q \quad 0 \quad 0 \quad 0 \quad b + 2hw$ $0 \quad 0 \quad (ac) \quad -0.8944q \quad 0 \quad 0 \quad 0 \quad 0 \quad 0 \quad c + 2hw$ $0 \quad -0.5477q \quad 0 \quad 0 \quad 0 \quad -0.7746q \quad -0.3464q \quad -0.3873q \quad 0.6928q \quad 0 \quad e + hw$ $0 \quad -1.1832q \quad 0 \quad (bd) \quad 0 \quad 0 \quad -0.7483q \quad 0.3586q \quad -0.6414q \quad 1.2650q \quad 0 \quad d + hw$ $0 \quad 0 \quad 0 \quad -0.3873q \quad 0 \quad 0 \quad 0 \quad 0 \quad 0 \quad 0 \quad -0.5916q \quad -0.5477q \quad e + 2hw$ $0 \quad 0 \quad 0 \quad -0.7483q \quad 0.3657q \quad 0 \quad (bd) \quad 0 \quad 0 \quad 0 \quad -0.4899q \quad 0 \quad 0 \quad d + 2hw$ $0 \quad 0 \quad 0 \quad 0.3586q \quad 1.2650q \quad 0 \quad 0 \quad (bd) \quad 0 \quad 0 \quad -0.5477q \quad 0 \quad 0 \quad 0 \quad d + 2hw$ $0 \quad 0 \quad 0 \quad -0.6414q \quad 1.6970q \quad 0 \quad 0 \quad 0 \quad (bd) \quad 0 \quad 0.9798q \quad 0 \quad 0 \quad 0 \quad 0 \quad d + 2hw$

$a+2hw$

1.26509 $b+hw$

0 0.33819 $b+2hw$

0 0.88649 0 $b+2hw$

(ac) -0.89449 0 0 $c+2hw$

0 (bd) -0.47819 -1.25359 1.26509 $d+hw$

0 0.70719 0 0 0 -1.00009 $c+2hw$

0 -0.47819 (bd) 0 0 0 0 $d+2hw$

0 -1.25359 0 (bd) 0 0 0 0 $d+2hw$

0 0 -1.12129 -1.06909 0 0 0 0 $a+3hw$

-0.67619 0 0.18079 0.47389 -0.47819 0 -0.31909 -0.25569 -0.67019 0 $b+3hw$

0.73039 0 0.73199 -0.05129 0.51649 0 0.28589 -1.03579 0.07249 0 0 $b+3hw$

1.06909 0 0.78579 -0.44279 -0.75599 0 -0.17939 -1.01129 0.62619 0 0 $b+3hw$

-1.86149 0 0 0.64429 -1.31669 0 0.83279 0 -0.93949 0 0 $b+3hw$

0 0 -0.79289 -0.53459 0 0 0 0.12129 1.06909 0 0 $c+3hw$

0 0 -0.32739 0.34239 0 0 0.27399 -0.46299 0.48559 (ac) 0 0 $c+3hw$

0 0 -0.62689 -0.17939 0 0 -0.52449 -0.88649 -0.25569 0 0 $c+3hw$

0 0 -1.51149 -0.47019 -0.1819 0 -0.53459 0 0 0 (bd) 0 0 $d+3hw$

0 0 -1.03519 0.07249 -0.72039 0 0.40419 0 0 0 0 (bd) 0 0 $d+3hw$

0 0 -1.11129 0.23619 1.06909 0 -0.25569 0 0 0 0 (bd) 0 0 $d+3hw$

0 0 0 -0.17939 1.86149 0 1.12129 0 0 0 0 0 (bd) 0 0 $d+3hw$

(C+2): $I=4$

APPENDIX II

Given below are some of the relations in the algebra of tensor operators that are employed in the derivation of certain expressions in this chapter:

The tensor product of two tensor operators of rank r , s is defined as

$$[T^r \times U^s]_m^t = \sum_q C_{q, m-q}^{r s t} T_q^r U_{m-q}^s \quad (1)$$

and the scalar product as

$$(T^r \cdot U^s) = \delta_{rs} \sum_q (-1)^q T_q^r U_{-q}^s \quad (2)$$

The reduced or double-barred matrix element of a tensor operator is given by the Wigner-Eckart Theorem,

$$\langle \alpha j m | T_q^k | \alpha' j' m' \rangle = (-1)^m \frac{C_{m' q m}^{j' k j}}{\sqrt{2j+1}} \langle \alpha j || T^k || \alpha' j' \rangle \quad (3)$$

The matrix elements of a tensor operator in an angular momentum representation are given by the relations

$$\begin{aligned} \langle j_1 j_2 J || T^k || j_1' j_2' J' \rangle \\ = \delta_{j_2 j_2'} \left[(2J+1) (2J'+1) \right]^{\frac{1}{2}} (-1)^{k+j_2-j_1'-J} \\ W(j_1 J j_1' J'; j_2 k) \langle j_1 || T^k || j_1' \rangle \end{aligned} \quad (4)$$

and

$$\begin{aligned}
 & \langle j_1 j_2 J \| U_2^{(k)} \| j_1' j_2' J' \rangle \\
 &= \delta_{j_1 j_1'} (-1)^{k+j_1-j_2-J'} \left\{ \frac{(2J+1)(2J'+1)}{(2j_1+1)(2j_2+1)} \right\}^{1/2} \times \\
 & \quad \cdot W(j_2 J j_2' J' : j_1 k) \langle j_2 \| U^{(k)} \| j_2' \rangle
 \end{aligned} \tag{5}$$

and the matrix elements of the product (scalar or tensor) of two tensor operators by

$$\begin{aligned}
 & \langle j_1 j_2 JM | (T_1^{(k)} U_2^{(k)}) | j_1' j_2' J' M \rangle \\
 &= (-1)^{j_1+j_2'-J} W(j_1 j_2 j_1' j_2' : J k) \langle j_1 \| T^{(k)} \| j_1' \rangle \times \\
 & \quad \cdot \langle j_2 \| U^{(k)} \| j_2' \rangle.
 \end{aligned} \tag{6}$$

and

$$\begin{aligned}
 & \langle j_1 j_2 J \| [T_1^r \times U_2^s]^t \| j_1' j_2' J' \rangle \\
 &= \left[(2J+1)(2J'+1)(2t+1) \right]^{1/2} \left\{ \begin{matrix} j_1 & j_2 & J \\ j_1' & j_2' & J' \\ r & s & t \end{matrix} \right\} \times \\
 & \quad \cdot \langle j_1 \| T^r \| j_1' \rangle \langle j_2 \| U^s \| j_2' \rangle.
 \end{aligned} \tag{7}$$

where, T operates only on particle 1 in the angular momentum states j_1 and j_1' and U operates only on particle 2 in the states j_2 and j_2' .

Also, for the angular momentum operator,

$$\langle j \| J^{-1} \| j' \rangle = \delta_{jj'} \sqrt{j(j+1)(2j+1)} \quad (8)$$

ooo o ooo

CHAPTER IV

NUCLEAR INTERACTIONS IN THE $D_{3/2} - G_{9/2}$ CONFIGURATIONS

1. Introduction

In this chapter, we propose to investigate the nature of the two-body nuclear interaction in nuclei with $A \approx 90$. The early qualitative predictions of Ford (For55) regarding the theoretically expected level scheme in Zr^{90} were soon confirmed experimentally by Johnson et al (Jon55). Later a quantitative calculation by Lane for this nucleus, based on the simple jj -coupling shell model with a short-range (δ -type) interaction between the nucleons, is reported (Lan55) to be in poor agreement with the levels of the $(G_{9/2})^2$ configuration as observed in Zr^{90} . Since the observed splitting of the levels $0^+ - 2^+$ of this configuration is of the same order of magnitude as that of the $2^+ - 4^+$ or $4^+ - 6^+$ levels, and since the short-range interaction would give a much larger depression of the 0^+ level relative to the other levels of the configuration, the necessity of taking into account the finite range of the interaction is obvious. This was done by Dayman et al (Day55) and independently by Thanappan, Waghmare and Pandya (Tho59, 61). Further, Talmi and Umm (Tni60) have attempted to determine the matrix elements of the nuclear interaction from the observed spacing of the energy levels

in a number of nuclei in this region. We shall give below an account of the method and results of our calculations together with a comparison of our results with those of the other authors.

2. Calculations and Results

Following Ford (Ford55), we assume that the low-lying levels of Zr^{90} are given by the last two protons in the configurations $(f_{7/2})^2$, $J = 0^+$; $(f_{7/2}g_{7/2})$, $J = 4^+$, 5^+ and $(g_{7/2})^2$, $J = 0^+$, 2^+ , 4^+ , 6^+ , 8^+ . The interaction between the protons is assumed to be of the form

$$H_{12} = (a + b \vec{\sigma}_1 \cdot \vec{\sigma}_2) \exp [-(r/r_0)^2] \quad (1)$$

and the Hamiltonian for the system will be given by eq. (2) of chapter II. The single-particle wavefunctions are taken to be of the harmonic oscillator type (eq.(1) of chapter II), the radial parts being given by

$$R_{2p}(r) = \left(\frac{2}{\pi}\right)^{1/4} \frac{4\sqrt{5}}{\sqrt{3} r_p^{3/2}} \left(\frac{r}{r_p}\right) \left(1 - \frac{4}{5} \frac{r^2}{r_p^2}\right) e^{-r^2/r_p^2}$$

and

$$R_{1g}(r) = \left(\frac{2}{\pi}\right)^{1/4} \frac{32\sqrt{2}}{3\sqrt{105} \cdot r_g^{3/2}} \left(\frac{r}{r_g}\right)^4 e^{-r^2/r_g^2} \quad (2)$$

The matrix elements of H_{12} are calculated using eq.(4) of chapter II. Calculations are made for the range parameter $\lambda = r_0/r_p = r_0/r_g = 0.7, 0.8, 0.9$ and 1.0. The relevant Slater

TABLE I

Slater integrals for the $2p - 4g$ subshells

$F^k(l_1 l_2' : l_1 l_2)$	$\lambda = 0.7$	$\lambda = 0.8$	$\lambda = 0.9$	$\lambda = 1.0$
$F^0(44;44)$	0.03648	0.03063	0.05726	0.08511
$F^2(44;44)$	0.12761	0.15841	0.13530	0.20626
$F^4(44;44)$	0.10794	0.10939	0.10313	0.09207
$F^6(44;44)$	0.05440	0.04300	0.03138	0.02197
$F^8(44;44)$	0.02001	0.01191	0.00722	0.00310
$F^0(11;11)$	0.05343	0.07313	0.09599	0.12148
$F^2(11;11)$	0.09237	0.11083	0.12893	0.13978
$F^0(41;41)$	0.03364	0.04933	0.06331	0.08041
$F^2(41;41)$	0.09148	0.11633	0.13969	0.15911
$F^3(41;14)$	0.07171	0.08207	0.08844	0.09073
$F^3(44;11)$	0.07171	0.08207	0.08844	0.09073
$F^5(41;14)$	0.05234	0.04875	0.04184	0.03412
$F^5(44;11)$	0.05234	0.04875	0.04184	0.03412

TABLE II

Matrix elements of the two-body interaction in

the $p_{1/2} - g_{9/2}$ configurations

Matrix element	J^π	coefficient of a					coefficient of b				
		$\lambda = 0.7$	$\lambda = 0.8$	$\lambda = 0.9$	$\lambda = 1.0$	$\lambda = 1.0$	$\lambda = 0.7$	$\lambda = 0.8$	$\lambda = 0.9$	$\lambda = 1.0$	$\lambda = 1.0$
$\langle (p_{1/2})^2 (p_{1/2})^2 \rangle$	0^+	0.0534	0.0732	0.0950	0.1215	0.1215	-0.0671	-0.0835	-0.0997	-0.1150	-0.1150
$\langle p_{1/2} g_{9/2} p_{1/2} g_{9/2} \rangle$	4^+	0.0289	0.0443	0.0615	0.0873	0.0873	0.0200	0.0303	0.0423	0.0545	0.0545
"	5^+	0.0332	0.0488	0.0630	0.0861	0.0861	-0.0389	-0.0491	-0.0593	-0.0696	-0.0696
$\langle (g_{9/2})^2 (g_{9/2})^2 \rangle$	0^+	0.0855	0.1033	0.1275	0.1494	0.1494	-0.1297	-0.1532	-0.1773	-0.2021	-0.2021
"	2^+	0.0518	0.0743	0.0935	0.1181	0.1181	-0.0490	-0.0691	-0.0921	-0.1170	-0.1170
"	4^+	0.0323	0.0467	0.0634	0.0837	0.0837	-0.0207	-0.0279	-0.0374	-0.0491	-0.0491
"	6^+	0.0249	0.0369	0.0494	0.0655	0.0655	-0.0075	-0.0082	-0.0093	-0.0111	-0.0111
"	8^+	0.0216	0.0374	0.0533	0.0712	0.0712	0.0001	0.0048	0.0117	0.0208	0.0208
$\langle (g_{9/2})^2 (p_{1/2})^2 \rangle$	0^+	-0.0106	-0.0039	-0.0053	-0.0069	-0.0069	0.0537	0.0537	0.0306	0.0500	0.0500

integrals $r(k)$ are given in table I and the matrix elements are tabulated in table II in terms of a and b .

The parameters to be determined are $\Delta = \epsilon(1g_{9/2}) - \epsilon(2p_{1/2})$, a , b and λ . From the data on ^{80}Zr (Way53), we take $\Delta = 1.0$ MeV. The parameters a , b and λ are determined from the experimental data by the following procedure: The energy levels are calculated for the pure configuration $(g_{9/2})^2$ for different values of λ . For each value of λ , a and b are determined by fitting the experimental separation of the levels 2^+ , 4^+ and 6^+ of ^{80}Zr . The other matrix elements are evaluated then for this choice of the parameters. The results are shown in figure 1. The levels 2^+ , 4^+ and 6^+ are normalised to the observed values and the positions of the other levels of the pure configurations are shown relative to these. The configuration mixing of the two 0^+ levels and the consequent repulsion of these is shown by dotted lines. The experimental values of the energy levels as reported by Bjornholm et al (Bj50) are also shown.

Firstly, we note that the position of the 6^+ level is not very sensitive to the variation of λ ; as λ changes from 0.7 to 1.0, the shift in the position of this level is only about 0.1 MeV. If the position of the 0^+ level of the $(g_{9/2})^2$ configuration were known, it would at once enable us to determine the value of λ (and hence of a and b). Since this is not known, we may apply another test to

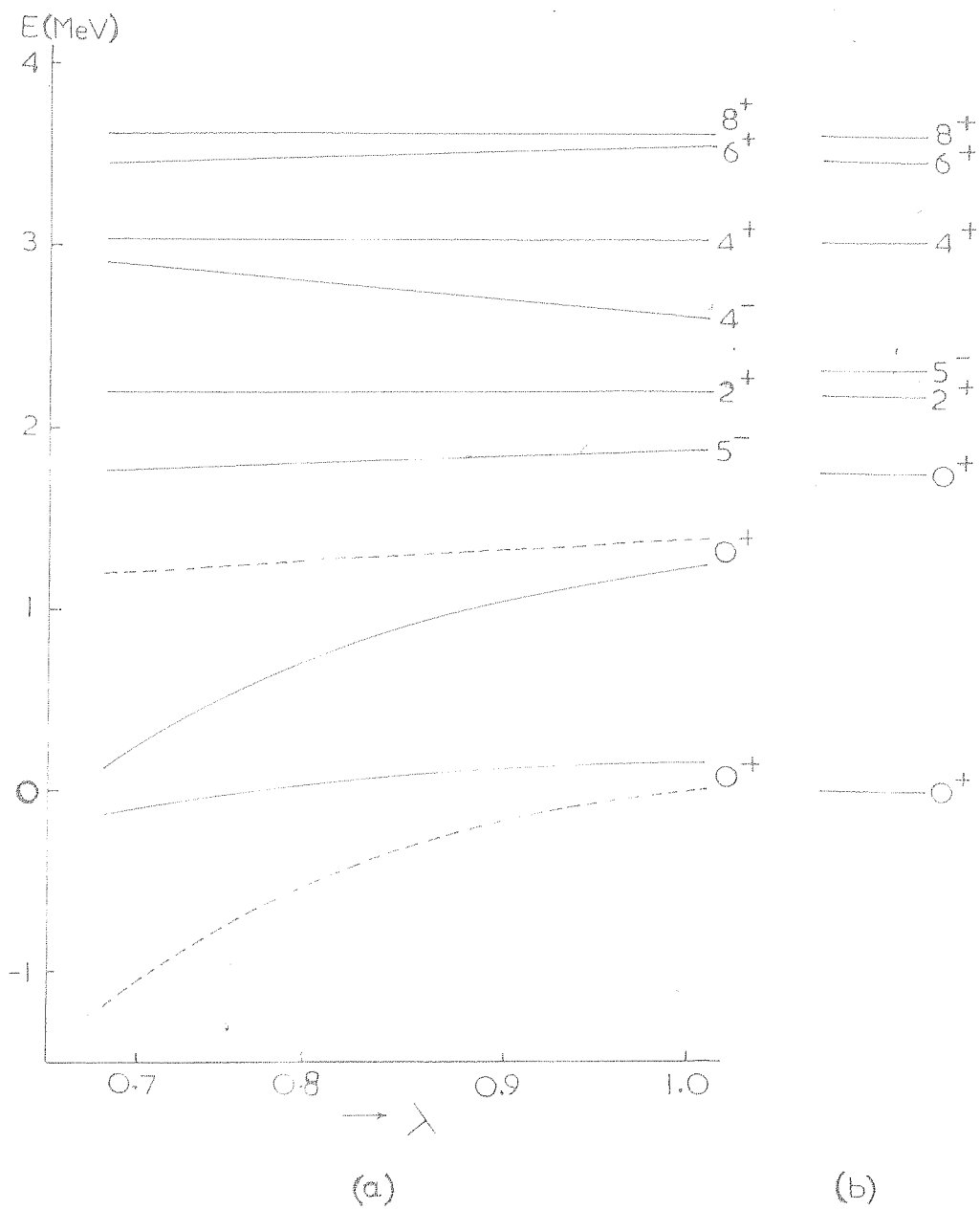


FIG. 1. ENERGY LEVELS OF Zr^{90} .
(a) CALCULATED, (b) OBSERVED

Determine a value of λ which will describe the energy levels of the $(g_{9/2})^2$ configuration. It is well known that the $7/2^+$ state of the $(g_{9/2})^{\pm 3}$ configuration occurs very close to (and sometimes even below) the $9/2^+$ state of the configuration. For example, in Sr^{85} , the $7/2^+$ state occurs 0.825 MeV above the $9/2^+$ state (May58) while in Ag^{107} it is 0.033 MeV below the $9/2^+$ state (Lak62). We calculate the energy levels of the $(g_{9/2})^3$ configuration for various values of λ from the corresponding calculated levels of the $(g_{9/2})^2$ configuration using the relation,

$$E_J [(g_{9/2})^3] = 3 \sum_{J_1} X_{J_1} E_{J_1} [(g_{9/2})^2] \quad (3)$$

where,

$$X_{J_1} = \langle (g_{9/2})^2_{J_1} | (g_{9/2})^3_J \rangle$$

denotes the coefficients of fractional parentage. They are tabulated by Flowers (Fla55) and are reproduced in table III. In fig. 2 we show the calculated levels together with the experimental levels of Sr^{85} and Ag^{107} . The depression of the $9/2^+$ state due to configuration interaction with the $(p_{1/2})^2 (g_{9/2})^{-1}$ state is not included, but this will be only of the order of 0.1 to 0.2 MeV. It is seen that a fairly good agreement between the calculated and the observed levels is obtained for $\lambda = 1.0$. The corresponding values of a and b are -15.9 MeV and +4.8 MeV respectively.

TABLE III

The values of $x_{J_1}^2 = |\langle (g_{g/2})^2_{J_1} | (g_{g/2})^3_J \rangle|^2$

's' denotes seniority.

$J \backslash J_1$	0	2	4	6	8
$9/2(s = 1)$	0.2967	0.6833	0.1500	0.3167	0.2833
$7/2(s = 3)$	-	0.5253	0.1399	0.0020	0.3329
$5/2(s = 3)$	-	0.2778	0.1969	0.5253	-
$3/2(s = 3)$	-	-	0.7273	0.2727	-
$9/2(s = 3)$	-	0.0328	0.4283	0.4854	0.0535

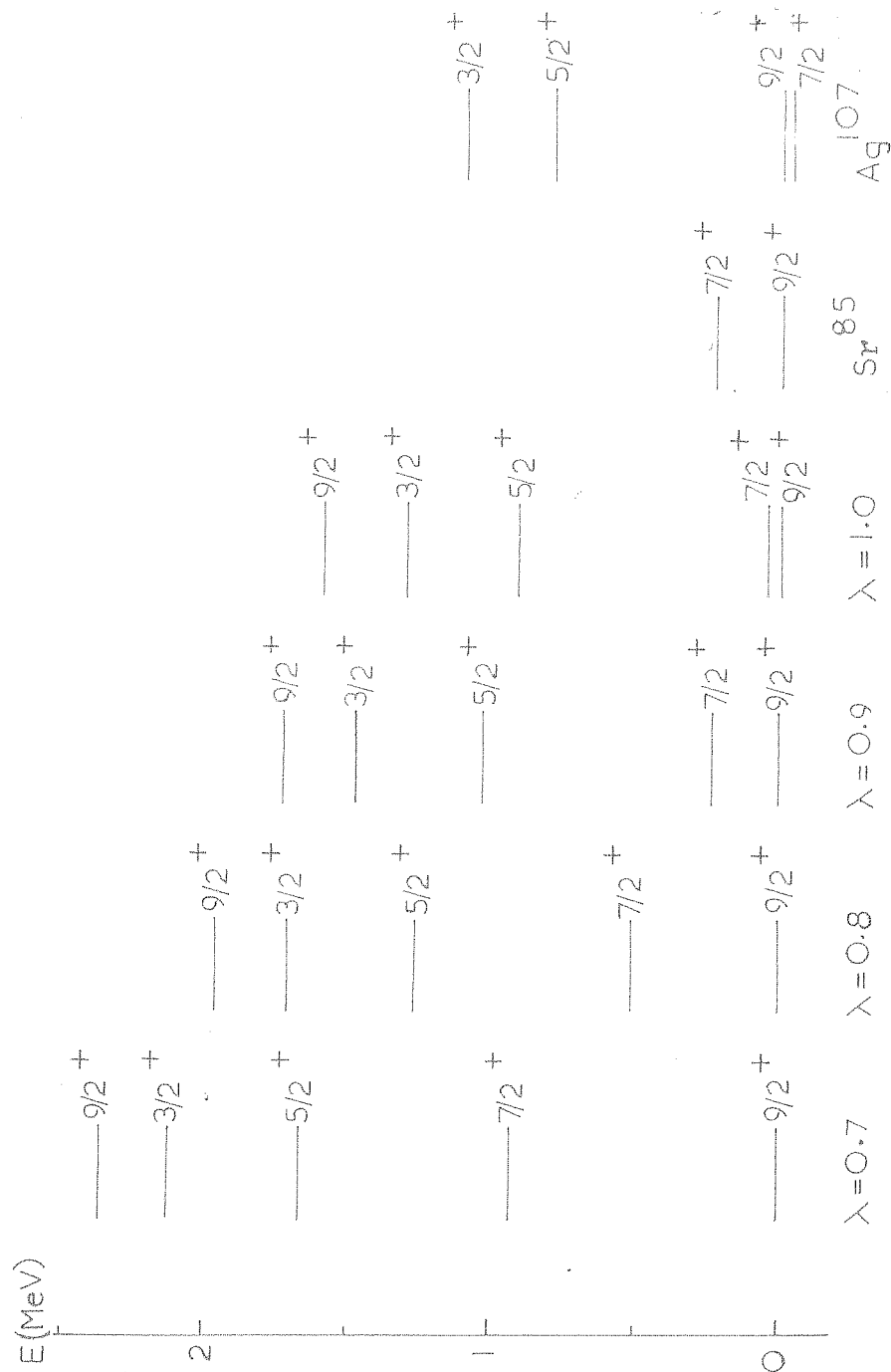


FIG. 2. LEVELS OF THE $(9_{9/2})$ CONFIGURATION

Let us now consider the relative positions of the two 0^+ levels. It is clear from the figure that for $\lambda < 0.7$, the two 0^+ levels cross over and hence the ground state would be predominantly $(g_{9/2})_0^2$; therefore in what follows we consider only values of $\lambda \geq 0.7$. The analysis of the data on β -decay of Y^{89} and the γ -decay of the 2^+ state of Zr^{90} by Bayman et al (1963) gives for the wavefunction of the two 0^+ states

$$\begin{aligned}\psi(0^+) &= 0.8 \psi[(p_{1/2})_0^2] - 0.6 \psi[(g_{9/2})_0^2] \\ \psi(0^-) &= 0.6 \psi[(p_{1/2})_0^2] + 0.8 \psi[(g_{9/2})_0^2]\end{aligned}\quad (4)$$

Now, the calculations show that the separation of the pure 0^+ states as well as the magnitude of the interconfiguration matrix element vary rapidly with the value of λ . The separation of the pure 0^+ levels decreases from 1.14 MeV at $\lambda = 1.0$ to 0.33 MeV at $\lambda = 0.7$, while the shift of each due to the interconfiguration matrix element,

$V = \langle (g_{9/2})_0^2 | H_{12} | (p_{1/2})_0^2 \rangle$, changes from 0.13 MeV at $\lambda = 1.0$ to 0.97 MeV at $\lambda = 0.7$. The observed splitting of the two levels (1.75 MeV) and the composition of the wavefunctions mentioned above can be reasonably well obtained for $\lambda = 0.8$, the calculated value of the separation being 1.73 MeV and the wavefunction of the ground state

$$\psi(0^+) = 0.84 \psi[(p_{1/2})_0^2] - 0.55 \psi[(g_{9/2})_0^2] \quad (5)$$

However, it will be noticed that relative to the 2^+ , 4^+ , 6^+ levels, the 0^+ levels are now predicted too low by about 0.5 MeV. For $\lambda = 1.0$, the ground state energy is predicted correctly, but the excited 0^+ level is too low by 0.35 MeV and the configuration mixing is quite small. We shall later remark on the implications of these results.

Of the negative parity states, only 3^- is observed, and for the range of λ of interest to us it is predicted below the 2^+ level. However, the excitation energy of this level above the ground state is correctly obtained for $\lambda = 0.8$. The 4^- state is predicted above the 3^- , the separation of the two decreasing rapidly with increasing λ , being 0.95 MeV for $\lambda = 0.8$ and 0.64 MeV for $\lambda = 1.0$. One would thus expect it to be observed at ~ 3.0 MeV excitation provided the nature of the nuclear interaction in this $(p_{1/2}^2 g_{7/2})$ configuration is not very different from that in the other configurations.

We would like to emphasize that since the $6^+ - 8^+$ separation is not very sensitive to λ , we have to rely on the $3/2^+ - 7/2^+$ separation of the $(g_{7/2})^2$ configuration to obtain a unique value of λ . It turns out that this quantity is a very sensitive test for the choice of the interaction parameters (as pointed out also by Talmi and Umm (Talmi60)), and even a small change in the parameters (particularly b) in going from $\lambda = 1.0$ to 0.9

produces a considerable shift of the $7/2^+$ level.

We may now look at the fitting of the levels of Zr^{90} (especially the ground state 0^+) from a somewhat different point of view. The two 0^+ states, their energies and eigenfunctions are described by the matrix

$$\begin{pmatrix} 1.75 - \kappa & V \\ V & \kappa \end{pmatrix}$$

Since the value of $(1.75 - \kappa)$ (the energy of the $(g_{9/2})^2$, $J = 0$ state) is effectively known from the analysis of the $(g_{9/2})^2$ configuration, we may ask ourselves the question: Where should be the unperturbed $(p_{1/2})^2_0$ level and what should be the strength of the configuration mixing matrix element V to produce the experimental level spectrum and the eigenfunctions given by eq. (4) for these states? It is then easily found that for $\lambda = 1.0$ and 0.9 the separation of the unperturbed 0^+ states, $\delta = (1.75 - 2\kappa)$, should be roughly 0.76 and 0.36 MeV and for the matrix element, $V = 0.80$ and 0.86 MeV respectively. These may be compared with the calculated values $\delta = 1.15$ MeV and 0.95 MeV and $V = 0.35$ and 0.50 MeV. Thus the nuclear interaction which gives correct matrix elements for the configuration $(g_{9/2})^2$ gives for other configurations results that are in error by ~ 0.5 MeV. In nuclear spectroscopy calculations where one is satisfied with approximate agreements within $\sim 0.2 - 0.3$ MeV, such configuration dependence of the interaction would be masked. It is only when one attempts

to make a refined analysis and look for precise predictions such as the $9/2^+ - 7/2^+$ separation in Sr^{85} that the information on the detailed nature of the nuclear interaction becomes available.

If the nuclear interaction H_{12} is written in a conventional way as

$$H_{12} = \sum_k f_k(r_1, r_2; \vec{\sigma}_1, \vec{\sigma}_2) P_k(\cos \theta_{12}) \quad (6)$$

it is easily seen that the matrix element of the interaction for the $(p_{1/2})_0^2$ state, as well as for the $(p_{1/2}g_{9/2})$ states, will depend only upon $k = 0, 2$ terms, whereas the matrix elements for the $(g_{9/2})^2$ states will depend upon $k = 0, 2, 4, 6, 8$ terms. On the other hand, the matrix element V will depend upon only $k = 3, 5$. We can push our analysis further to derive from the empirical matrix elements the nature of the interaction in these various substates of relative angular momentum. In the attempt to obtain a consistent interpretation of these matrix elements, one may be led to an empirical non-local potential.

3. Comparison With other Results

Our results are similar to those of Bayman et al (Ban50). We have not taken into account the coulomb interaction of the two protons and our method of choosing the 'best fit' parameters of the two-body interaction is also different from theirs, so that we get somewhat different

results for the parameters. However, the separation of the odd parity states predicted by them agrees well with our estimate. The best fit obtained by Bayman et al shows the 5^+ and the excited 0^+ levels lower and the 2^+ , 4^+ , 6^+ levels a little higher than the observed positions.

TABLE IV

The values of the parameters of the two-body nuclear interaction. The values obtained by Bayman et al are shown in the last column.

λ	0.7	0.8	0.9	1.0	0.75
a	-18.0	-15.7	-15.5	-15.9	$-31.8 < a < -11.7$
b	17.4	11.1	7.3	4.8	$5.6 < b < 11.7$

In table IV we show the variation of the parameters a and b with λ together with the 'best fit' values of Bayman et al. It is clear that the effective nuclear interaction obtained for Zr^{90} has an exchange nature similar to that obtained by French and Ham (Fra55) from an analysis of the data on Calcium isotopes, but the well-depth for Zr^{90} is about twice as much. However, this interaction is quite different in its exchange nature from the other effective interactions used in light nuclei (Rod48, Elt57) or in heavy nuclei in the Pb region (Car60). Thus the simple central two-body interaction

conventionally used in the nuclear shell model appears to be not only configuration-dependent in the same nucleus, but also dependent on the mass of the nucleus.

Talmi and Ussu (Tn60) have carried out an analysis of the level spectra of Er^{90} and other neighbouring nuclei. The analysis is based on an attempt to rewrite the experimental data in terms of the numerical values of the matrix elements of the effective nuclear interaction in various states. Such an approach is valuable in correlating a large number of experimental data and in predicting new levels. The advantage of this technique is its independence of the detailed assumptions regarding the explicit nature of the two-body interaction and the independent particle wavefunctions. Hence, such an analysis cannot yield any information on the properties (parameters) of the phenomenological two-body interaction which is the aim of our study. It may be seen that the results of Talmi and Ussu interpreted in terms of a two-body central interaction do confirm our results that such an interaction seems to be configuration-dependent or non-local. The matrix elements relevant to our calculations are

$$\begin{aligned} \gamma &= E \left[(g_{9/2})^2_{J=2} \right] - E \left[(g_{9/2})^2_{J=0} \right] = 0.866 \text{ MeV} \\ \delta &= E \left[(g_{9/2})^2_{J=0} \right] - E \left[(p_{1/2})^2_{J=0} \right] = 0.836 \text{ MeV} \quad (7) \\ |V| &= \left| \langle (g_{9/2})^2_{J=0} | H_{12} | (p_{1/2})^2_{J=0} \rangle \right| = 0.708 \text{ MeV}. \end{aligned}$$

where the numerical values are as required by Talmi and Umana to explain the experimental level schemes, and we have included in δ the single-particle energy difference 2β . It may be seen from fig. 1 that the value of γ is obtained for $\lambda = 1.0$. It is thus clear that the energy levels of the pure configuration $(g_{9/2})^2$ can be correctly predicted by the interaction H_{12} with parameters corresponding to $\lambda = 1.0$. A three-parameter model is then sufficient to predict all the energy levels of $(g_{9/2})^n$ configurations of identical particles. This interaction would also predict a low-lying $7/2^+$ state of the $(g_{9/2})^3$ configuration and the failure of the earlier attempts at obtaining a simple phenomenological potential which would give such a state is not at all surprising in view of our earlier remarks. The empirical and the calculated values of δ and V have already been discussed. The splitting of the odd parity states is predicted by Talmi and Umana to be 0.04 MeV, whereas our calculations as well as those of Bayman et al based on explicit interactions predict it to be at least ten times larger.

4. Conclusion

We have seen that a unique choice of the parameters of the central two-body interaction (eq.(1)) cannot explain all the low-lying levels of Kr^{90} with complete accuracy. The choice $\lambda = 1.0$ adequately explains the

energy levels of the $(s_{3/2})^2$ configurations, but the same choice would not satisfactorily give the levels of the $(p_{1/2})^2$ and $(p_{1/2}s_{3/2})$ configurations. On the other hand, for $\lambda = 0.8$, the 0^+ levels and the 5^- level can be obtained in agreement with experiment, but the remaining levels would be pushed up so that they would be predicted above the observed positions. It is difficult to avoid the conclusion that the simple two-body interaction assumed here is configuration-dependent. For further elucidation of the situation, the experimental identification of the as yet unobserved 4^- level would be of great help. This is also of importance in view of the conflicting predictions mentioned in the previous section for the $4^- - 5^-$ separation. It would also be of interest to determine the low-lying odd-parity states of nuclei such as Nb^{91} and Sr^{85} , for, these would belong to the configurations $(p_{1/2})(s_{3/2})^2$ and would give rise to doublets $J \pm 1/2$. The splitting of such doublets can be calculated in terms of the splitting of the $J = 4^-, 5^-$ states of the $(p_{1/2}s_{3/2})$ configuration and would therefore indirectly give a measure of it.

REFERENCES

1. Ban59 B.F.Bayman, A.C.Reiner and R.K.Sheline:
Phys.Rev. 115, 1627 (1959).
2. Bja59 B.Bjornholm, O.B.Nielsen and R.K.Sheline:
Phys.Rev. 115, 1613 (1959).
3. Car60 J.C.Carter, W.T.Pinkston and W.W.True:
Phys.Rev. 120, 804 (1960).
4. Eli57 J.P.Elliott and D.H.Flowers: Proc.Roy.Soc.
A242, 57 (1957).
5. Fla52 D.H.Flowers: Proc.Roy.Soc. A215, 398 (1952).
6. For55 K.W.Ford: Phys.Rev. 92, 1516 (1953).
7. Fra56 J.S.French and B.J.Rae: Phys.Rev. 104,
1411 (1956).
8. Jon55 O.E.Johnson, R.C.Johnson and L.N.Langer:
Phys.Rev. 98, 1517 (1955).
9. Lak62 H.L.Lark, P.F.A.Goudsmit, J.P.W.Jansen,
J.E.J.Oberski and A.H.Vapstra: To appear
in Nuclear Physics.
10. Lar58 H.H.Lazar, G.D.O'Kelley, J.H.Hamilton,
L.N.Langer and W.O.Smith: Phys.Rev. 110,
513 (1958).

11. Rod48 I. Rosenfeld: "Nuclear Forces", North-Holland Publishing Company (1948).
12. Tai60 I. Talmi and I. Ussis: Nuclear Physics, 12, 225 (1960).
13. Tha59 V.K. Shankarappa and Y.R. Waghmare: Prog.Theo. Phys. 22, 459 (1959).
14. Tha61 V.K. Shankarappa, Y.R. Waghmare and S.P. Pandya: Prog.Theo. Phys. 24, 22 (1961).
15. Way58 K. Way et al: "Nuclear Level Schemes", U.S.A.E.C. Report TID-5300 (1958).

ooo o ooo

CHAPTER V

SUMMARY

We have described in chapter I the experimental regularities observed in nuclei in the $2s - 1d$ shell and have pointed out that there is a marked change in the energy level systematics in the region $A = 28 - 32$. The theoretical consequences of various nuclear models have been reviewed in terms of these observed systematics and arguments have been presented favouring consideration of collective vibrations in these nuclei.

In chapter II, we have applied the jj -coupling shell model to the nuclei Si^{29} , P^{29} , Si^{30} , P^{30} , P^{31} and Si^{31} . It was found that this simple model is not adequate to explain all the observed properties such as the energy levels, ground state magnetic moments and electromagnetic transition probabilities in these nuclei.

In chapter III, the vibrational collective model has been applied to nuclei with mass number 29, 30 and 31. The results have been compared with the observed properties of Si^{29} , P^{29} , P^{31} , Si^{30} and P^{30} . The agreement was found to be satisfactory for the low-lying energy levels and the gamma ray transition probabilities but the predicted values of the ground state magnetic moments of Si^{29} , P^{29} and P^{31} are two to three times larger than the observed values.

The need for the determination of the absolute transition probabilities in these nuclei have been stressed.

Finally, in chapter IV, we have investigated the nature of the two-body nuclear interactions in the $2p_{1/2} - 1g_{9/2}$ configurations with particular reference to the nuclei Zr^{90} and Sr^{88} . It was found that the parameters which give a good agreement with the levels of the $(g_{9/2})^1$ configurations, do not give equally well the levels of the $(p_{1/2})^2$ and $(p_{1/2}g_{9/2})$ configurations. It is concluded that the central two-body interaction conventionally assumed in shell model calculations is configuration-dependent or non-local. Further experimental measurements have been suggested for the elucidation of this point.

APPENDIX

Reprints of papers published during the work for the thesis:

1. V.K.Thankappan and Y.R.Waghmare: Energy levels of Zr^{90} , Prog.Theo.Phys. 22 (1959), 459.
2. V.K.Thankappan and S.P.Paniya: Collective vibrations in p^{31} , Nuclear Physics, 19 (1960), 303.
3. V.K.Thankappan, Y.R.Waghmare and S.P.Paniya: Nuclear interactions in the $p_{1/2} - s_{9/2}$ configurations, Prog.Theo.Phys. 25 (1961), 22.
4. V.K.Thankappan and S.P.Paniya: Collective vibrations in even-even nuclei, Proc. of the Rutherford Jubilee International Conference, Manchester (1961), p.253.

Energy Levels of Zr^{90}

V. K. Thankappan
and Y. R. Waghmare

*Physical Research Laboratory,
Ahmedabad 9, India*

July 11, 1959

Ford's prediction,¹⁾ based on simple shell model considerations, of a 0^+ level as the first excited state of Zr^{90} was soon experimentally confirmed.²⁾ Recently Lazar et al.³⁾ have measured the low-lying energy levels of Zr^{90} and found them to be in agreement with the qualitative conjectures of Ford. However, they report that a quantitative calculation by Lane³⁾ based on a short-range interaction between the nucleons, gives poor agreement with the experimentally observed splitting of the $(g_{9/2})^2$ configuration. We have calculated the level-scheme for a more realistic shell model, by taking a finite range for the nuclear interaction, and obtained considerably better agreement with the experimental results.

Following the two-nucleon model as suggested by Ford,¹⁾ we consider the low levels of Zr^{90} to arise from the interactions of the last two protons in the configurations $(p_{1/2})^2$, $J=0$; $(g_{9/2})^2$, $J=0, 2, 4, 6, 8$; and $(p_{1/2} g_{9/2})$, $J=4, 5$. From the data on Y^{89} we take the separation energy of the single particle levels to be 1.0 Mev.⁴⁾ We assume harmonic oscillator wave functions for the nucleons, and a central two-body internucleon potential of the gaussian shape viz., $(a+b\sigma_1 \cdot \sigma_2) \exp(-r^2/r_0^2)$

where a and b are parameters giving the exchange character of the potential, and are determined by comparison with the experimental data; r_0 denotes the range of the interaction and only enters the calculations in the combination, $\lambda = r_0/r_1$, where r_1 determines the range for the nucleon wave-function.⁵⁾

The energy levels are calculated for $\lambda=0, 0.5$, and 1.0 , and a and b are determined by fitting the experimental energy separations of the 2^+ , 4^+ and

Table I. Calculated and experimental energy levels

Configuration	J	Calculated energy in Mev.			Experimental energy (Mev.)
		$\lambda=0$	$\lambda=0.5$	$\lambda=1.0$	
$(p_{1/2})^2$	0^+	0	0	0	0
$(p_{1/2} g_{9/2})$	4^-	2.50	3.39	2.24	?
	5^-	1.14	2.30	1.72	2.32
$(g_{9/2})^2$	0^+	-4.00	-0.92	1.18	1.76
	2^+	1.68	2.80	2.04	2.19
	4^+	2.53	3.60	2.93	3.08
	6^+	2.94	4.00	3.32	3.45
	8^+	3.20	4.51	3.38	3.59

6^+ levels except for $\lambda=0$. In this last case only one parameter is needed, and this is fixed by fitting the experimental separation of 2^+ and 6^+ levels. Table I lists the excitation energies of the levels relative to the ground state 0^+ .

We note that the separation of the two 0^+ levels and the splitting of the levels of $(g_{9/2})^2$ configuration are quite sensitive to the range parameter λ . It is clear that a satisfactory agreement with the experimental results can be obtained only for a rather large value

of λ viz. $\lambda \approx 1.0$. The energy values reported in Table I do not include the effect of the repulsion of the 0^+ levels. A rough estimate shows this to be small, giving a shift of ≈ 0.1 Mev. in each of the two 0^+ levels, for $\lambda = 1.0$. This, however, further improves the agreement between the predicted and the observed values; in particular, the discrepancy between the predicted and the observed separation of the 0^+ levels is now reduced to 0.38 Mev. We believe that in view of the simplicity of the model, the agreement between theory and experiment is quite satisfactory.

The values of the parameters a and b for $\lambda = 1.0$ are found to be -17.5 Mev and 3.8 Mev respectively. It may be noted that the large value of the range and the relative strengths of the spin-independent and spin-dependent interactions are in qualitative agreement with the results obtained for nuclei near $A = 40$.⁽⁶⁾

We finally remark that while this model provides reasonably good agreement for a splitting of the energy levels within a given configuration, the rela-

tive separations of the levels of different configurations is not so well given. However, the calculation predicts the separation of the levels of the configuration $(p_{1/2}, n_{9/2})$ to be ≈ 0.5 Mev., and this would place the as yet unobserved 4^- level at about 2.8 Mev., i.e. very close to the 4^+ level.

Acknowledgement :

We are greatly indebted to Dr. S. P. Pandya for suggesting the problem and for discussions during the course of the work. This work was supported by a research grant from the University Grants Commission, India, and Ministry of Education, Government of India.

- 1) K. W. Ford, Phys. Rev. **98** (1955), 1516.
- 2) Johnson, Johnson and Langer, Phys. Rev. **98** (1955), 1517.
- 3) N. H. Lazar et al., Phys. Rev. **110** (1958), 513.
- 4) The exact value is 0.913 Mev. as reported in Nuclear Level Schemes, compiled by K. Way et al., U.S.A.E.C. Report TID-5300 (1955).
- 5) I. Talmi, Helv. Phys. Acta, **25** (1952), 185.
- 6) J. B. French and B. J. Raz, Phys. Rev. **104** (1956), 1411.

Reprinted from :

NUCLEAR PHYSICS VOLUME 19 No. 3 (1960)

V. K. THANKAPPAN and S. P. PANDYA

COLLECTIVE VIBRATIONS IN P^{31}



NORTH-HOLLAND PUBLISHING COMPANY - AMSTERDAM

COLLECTIVE VIBRATIONS IN P^{31}

V. K. THANKAPPAN and S. P. PANDYA

Physical Research Laboratory, Ahmedabad-9, India†

Received 20 April 1960

Abstract: An attempt is made to explain the energy levels and the electromagnetic transitions in P^{31} in terms of the collective vibrational model. The results are found to be fairly satisfactory.

1. Introduction

The role of collective motion in explaining the properties of nuclei of mass $A \approx 30$ is recently being investigated with much interest, in view of the successful demonstration of the existence of the collective rotational motion of nuclei of mass $A \approx 25$, and the experimental observation of enhanced E2 transitions in some $A = 29$ and $A = 31$ nuclei¹⁾. In particular, it is found in these nuclei that the E2 cross-over transition from the second excited state of spin $J = \frac{5}{2}$ to the ground state of spin $J = \frac{1}{2}$ is about hundred times more intense than the possible M1 transition to the first excited state of spin $J = \frac{3}{2}$. This and other properties of these nuclei are explained with a fair amount of success by a model which describes them in terms of a single odd particle interacting with a deformed rotating nuclear core.

Analysis of nuclear stripping reaction data for these nuclei by French and Mcfarlane²⁾ shows evidence of considerable mixing of shell model configurations in the ground state of P^{31} . However, detailed calculations on the basis of nuclear shell model including mixed configurations, predicting the energy levels, magnetic moments, etc., are not yet available.

It should be of interest to examine the predictions of the collective vibrational model for nuclei of $A \approx 30$, for several reasons. One of us has earlier described a preliminary calculation for the properties of Si^{29} in terms of this model³⁾. In view of the considerably more detailed information now available for the energy levels of P^{31} , we present here results for this nucleus. Earlier calculations of Goldhammer⁴⁾ on similar lines were based on assumptions quite different from those we adopt here; our emphasis is at present on detailed comparison of the predicted and observed energy level spectra.

† Supported by the Department of Atomic Energy, India and the University Grants Commission, India.

2. Energy Levels

We consider the P^{31} nucleus as a spherical core of 14 protons and 16 neutrons, filling up the nuclear subshells upto $1d_{\frac{3}{2}}$ and $2s_{\frac{1}{2}}$ respectively, and the last odd proton in the $2s_{\frac{1}{2}}$ or $1d_{\frac{3}{2}}$ subshell. The collective properties of the core are described in terms of quadrupole surface oscillations which are quantised. The single particle states of the odd proton are then coupled to the 0, 1 and 2 quanta states of the core. The mathematical formalism for such a model is well-known, and detailed calculations are exactly similar to those described in ref. 3). We follow the notation described there.

It is implicit in the model that the collective properties of the core should be approximately the same as those observed in the Si^{30} nucleus. We interpret the first excited state of Si^{30} at 2.24 MeV⁵⁾ as the one-quantum vibrational state of the core, which gives $\hbar\omega = 2.24$ MeV. Of course, on the basis of such a simple model we should expect to see in Si^{30} a degenerate triplet of states of spins 0, 2 and 4 arising from two-quanta excitation at 4.5 MeV. However, the experiments show only a close doublet at 3.51 and 3.79 MeV, and further excited states are not clearly known. This result should not be surprising as for excitation energies ≥ 4 MeV, this simple model may not be adequate; in particular, effects of inter-nucleon forces and particle excitations from the core may have to be taken into account more explicitly. It is for this reason that we confine our attention to (even parity) states of P^{31} below 4 MeV.

The other two parameters of the model, viz. the separation Δ of the single particle states $2s_{\frac{1}{2}}$ and $1d_{\frac{3}{2}}$, and the constant q indicating the strength of coupling of the odd particle to the collective oscillations of the core, are considered as free parameters, and are adjusted to obtain the best agreement of the calculated and the observed energy levels. The Hamiltonian matrices for $J = \frac{1}{2}, \frac{3}{2}, \frac{5}{2}$ and $\frac{7}{2}$ are constructed, and are explicitly diagonalised for various values of Δ and q . The results for the lowest few states of each J are shown in fig. 1. The experimental results are shown in fig. 2.

We note that qualitatively the order of the energy levels is correctly given by the theory. To find the best choice of the parameters Δ and q , we remark[†] that the separation of the states $\frac{3}{2}$ and $\frac{3}{2}^*$, and the splitting of the triplet $\frac{5}{2}^*$, $\frac{1}{2}^*$ and $\frac{3}{2}^{**}$ is quite sensitive to variation in the value of q and is relatively unaffected by variation of Δ ; this enables us to choose the best value of q as ≈ 1.0 . With this choice for q , the variation of the excitation energy of the $\frac{3}{2}$ state with Δ determines the best value for Δ viz., $\Delta \approx 2.0$ MeV. Fig. 2 also shows the predicted energy levels for $q = 1.0$, $\Delta = 2.0$ MeV. It may be noted that experimentally the spin of the 3.41 MeV state is not determined. Moreover, Simons⁶⁾ assigns spin $\frac{1}{2}$ to the 3.51 MeV level, whereas Broude *et al.*¹⁾ find spin

[†] The notation here is that the unstarred, starred and double starred values refer to the lowest, the first and the second excited states of a given J .

$\frac{3}{2}$ for the same level. Though we have shown in fig. 2 the spin sequence of the triplet as $\frac{5}{2}$, $\frac{1}{2}$, $\frac{3}{2}$, the possibility that the 3.41 MeV state is $\frac{3}{2}$ and the 3.51 MeV state is $\frac{1}{2}$ cannot be ruled out from our calculations, as these levels cross in the

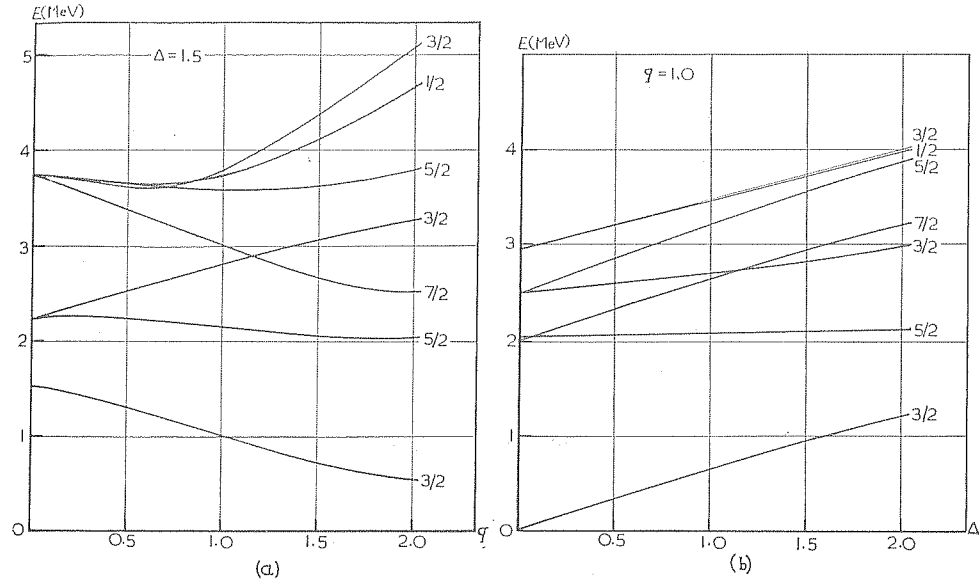


Fig. 1. Variation of the energy level scheme of P^{31} with q (fig. 1(a)) and with Δ (fig. 1(b)). The levels are normalised to $E = 0$ for the ground state.

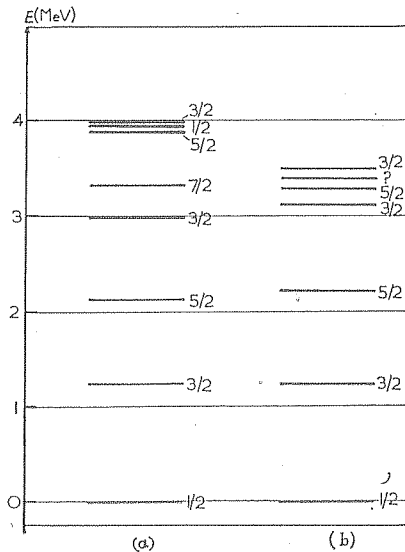


Fig. 2. Comparison of the calculated energy levels ($\Delta = 2.0$ MeV, $q = 1.0$ MeV) with the observed energy levels below 4 MeV. (a) Calculated levels. (b) Experimental levels.

neighbourhood of $q \approx 1.0$, as may be seen from fig. 1a. The close triplet of levels $\frac{5}{2}^*$, $\frac{1}{2}^*$ and $\frac{3}{2}^{**}$ is predicted about 0.5 MeV higher than the observed triplet. This discrepancy is not regarded as serious in view of the remark earlier made regarding the higher energy levels, and the availability of only two parameters in the calculation.

The really serious difficulty in the predictions of this model is the presence of the $J = \frac{7}{2}$ level between the $\frac{3}{2}^*$ level and the higher triplet. This level is not seen experimentally. We stress this feature as important, since no reasonable variation of the parameters can avoid placing this level below ≈ 4 MeV. The only comment we make is that since the observed levels in this region are very close, the probability that the $\frac{7}{2}$ level is degenerate with $\frac{3}{2}^*$ or $\frac{5}{2}^*$ should be considered. Small changes in the parameters A and q may easily cause this to happen. It may be noted that for $q > 1$, this $\frac{7}{2}$ level would occur below 3 MeV, and would almost certainly have been detected. This is perhaps an additional argument against choosing $q > 1.0$.

3. Electromagnetic Transitions

It is characteristic of the collective vibrational model that although E2 transitions can be considerably enhanced by introducing even a small amount of collective vibrations, the static values of the electromagnetic moments are not changed very much from the simple shell model values. P^{31} belongs to that group of $s_{\frac{1}{2}}$ nuclei which show a very large deviation of the observed magnetic moment from the Schmidt value. It is thus not surprising that as in the case of Si^{29} , the vibrational model fails to predict the observed value of the magnetic moment of P^{31} . The calculated value for the magnetic moment is (for $q = 1.0$, $A = 2.0$ MeV) $\mu = 2.56$ n.m., which may be compared to the observed value $\mu = 1.13$ n.m., and the Schmidt value $\mu = 2.79$ n.m.

The wavefunctions of the ground state and the first two excited states are listed in table 1. These show features very similar to those calculated for Si^{29} . The two important characteristics of the electromagnetic transitions in P^{31} are as follows:

- a) large E2 component in the decay of the first excited state,
- b) the possible M1 transition from the second excited state $\frac{5}{2}$ to the first excited state $\frac{3}{2}$ is less than 5 % of the crossover E2 transition to the ground state $\frac{1}{2}$.

Qualitatively these features are easily explained by the structure of the wavefunctions found for these states. We note that the ground state is $\approx 80\%$ pure single particle $s_{\frac{1}{2}}$ state, whereas the first excited state $\frac{3}{2}$ has a large admixture of the single particle state $d_{\frac{3}{2}}$, and the $s_{\frac{1}{2}}$ state coupled to one vibrational quantum. The presence of the latter large component would give rise to an enhanced E2 transition to the ground state. On the other hand the second

excited state arises almost entirely from the coupling of the $s_{\frac{1}{2}}$ state to one vibration quantum state of the core. Hence we should expect a strong E2 transition to the ground state, whereas the M1 transition to the first excited state is almost forbidden. We hope to report on detailed calculations of the

TABLE I

Eigenfunctions of the states $J = \frac{1}{2}, \frac{3}{2}, \frac{5}{2}$ of P^{31} for $q = 1.0, A = 2.0$ MeV

n	k	j	$J = \frac{1}{2}$	$J = \frac{3}{2}$	$J = \frac{5}{2}$
0	0	$\frac{1}{2}$	0.948	—	—
0	0	$\frac{3}{2}$	—	0.709	—
1	2	$\frac{1}{2}$	—	— 0.625	0.924
1	2	$\frac{3}{2}$	0.308	— 0.247	— 0.175
2	0	$\frac{1}{2}$	0.056	—	—
2	2	$\frac{1}{2}$	—	0.079	— 0.039
2	4	$\frac{1}{2}$	—	—	—
2	0	$\frac{3}{2}$	—	0.153	—
2	2	$\frac{3}{2}$	— 0.053	0.129	0.090
2	4	$\frac{3}{2}$	—	—	0.325

The tabulated quantity is the amplitude of the single particle state of spin j coupled to the state of the nuclear core with n quanta coupled to the resultant spin k .

electromagnetic transitions in such odd-proton nuclei later in another context. It may be emphasised in the meanwhile that absolute measurements of the various transition probabilities in these nuclei would be very useful.

We should like to add a remark on the interpretation of these electromagnetic transitions within the framework of simple shell model ideas, as we fear that this aspect has perhaps been misrepresented elsewhere. On the basis of the simple shell model, one would interpret the ground and the first excited states as pure single particle states $s_{\frac{1}{2}}$ and $d_{\frac{3}{2}}$, whereas the second excited state would be due to the excitation of a $d_{\frac{3}{2}}$ particle from the underlying closed shell to perhaps the $s_{\frac{1}{2}}$ shell, resulting in the configuration $(d_{\frac{3}{2}})^{-1}(s_{\frac{1}{2}})^2$ for this state. Even on the basis of such a simple model, it is clear that the $\frac{5}{2} \rightarrow \frac{3}{2}$ transition would be absolutely forbidden (as it involves two-particle transitions), whereas $\frac{5}{2} \rightarrow \frac{1}{2}$ transition can take place as $d \rightarrow s$ transition. The introduction of collective effects would serve to enhance the E2 transitions. It is therefore unfair to infer from the large crossover transition that the shell model fails, and deformation of the core must be invoked. Perhaps a proper shell model calculation taking into account the mixing of configurations would also give quite good results.

4. Conclusions

We conclude that the collective vibrational model explains satisfactorily the seven energy levels of P^{31} observed below 4 MeV, but predicts an unobserved

level $J = \frac{7}{2}$. We hope that further experimental observations may elucidate this point. One may compare the predictions of this simple two-parameter model to those of the collective rotational model of Broude *et al.*¹⁾ for the low lying energy levels. It appears that both models are about equally successful. It is important to remark that though the rotational model predicts the $\frac{7}{2}$ level above 4 MeV, the position of this level is displaced to a large extent by the rotation-particle coupling between the bands 8 and 11.

The values of the parameters A and q obtained here are also quite reasonable. In particular the small value of q and the calculated wavefunctions for all the states considered here show that the amplitudes of the two-quanta excitation states of the core are small, and the neglect of more than two-quanta excitations of the core is justified.

Finally, the observed features of the electromagnetic transitions in P^{31} are also quite easily understood, at least qualitatively, on the basis of this unified model.

References

- 1) D. A. Bromley, H. E. Gove, E. B. Paul, A. E. Litherland and E. Almquist, Can. J. Phys. **35** (1957) 1042;
D. A. Bromley, H. E. Gove and A. E. Litherland, Can. J. Phys. **35** (1957) 1057;
C. Broude, L. L. Green and J. C. Willmott, Proc. Phys. Soc. **72** (1958) 1097, 1115, 1122
- 2) M. H. Mcfarlane and J. B. French, NYO-2846, The University of Rochester, Rochester N.Y.
- 3) S. P. Pandya, Prog. Theor. Phys. **21** (1959) 431
- 4) P. Goldhammer, Phys. Rev. **101** (1956) 1375
- 5) P. M. Endt and C. M. Braams, Revs. Mod. Phys. **29** (1957) 683
- 6) L. Simons, Nuclear Physics **10** (1959) 215

DIY.

With Contributions of the Author

Nuclear Interactions in the $p_{1/2}$ - $g_{9/2}$ Configurations

V. K. THANKAPPAN, Y. R. WAGHMARE
and S. P. PANDYA

Reprinted from Progress of Theoretical Physics, Volume 26, Number 1
July 1961

Nuclear Interactions in the $p_{1/2}-g_{9/2}$ ConfigurationsV. K. THANKAPPAN, Y. R. WAGHMARE
and S. P. PANDYA*Physical Research Laboratory, Ahmedabad-9, India*

(Received February 9, 1961)

Zr^{90} offers a very good case for the study of $T=1$ levels in the $p_{1/2}-g_{9/2}$ subshells and has recently been explored by several authors. Here earlier calculations of Thankappan and Waghmare are extended and analysed in detail. It is found that a simple central two-body interaction can be constructed which will give correctly the energy levels of the $(g_{9/2})^2$ configuration, and hence also the levels of a $(g_{9/2})^n$ configuration. However, the same interaction fails to give correctly the levels of the other configurations $(p_{1/2})(g_{9/2})$ and $(p_{1/2})^2$. This simple two-body nuclear interaction is thus shown to be configuration dependent. It is pointed out that experimental identification of the as yet unobserved 4^- level would be very helpful for further elucidation of this phenomenon. The results are compared with those of the other authors.

§ 1. Introduction

It is of considerable interest for elucidation of the phenomenology of the nuclear spherical shell model to be able to determine the region of validity of the model, the nature of the coupling scheme for the nucleons and the nature of the two-body effective interaction which will adequately explain and predict the low-lying energy levels of nuclei in this region. Some work in this direction has been done recently in the region $A \cong 90$, $p_{1/2}-g_{9/2}$ subshell. The early qualitative predictions of Ford¹⁾ regarding the theoretically expected energy level scheme in Zr^{90} were easily confirmed experimentally.²⁾ Later a quantitative calculation by Lane³⁾ for this nucleus, based on the assumptions of a simple jj coupling scheme for wave functions and a short-range (δ -type) interaction between the nucleons, gave results which were in poor agreement with the experimentally observed splitting of the levels of the $(g_{9/2})^2$ configuration. Since the observed splitting of the levels $0^+ - 2^+$ of this configuration is of the same order of magnitude as the splitting of the $2^+ - 4^+$ or $4^+ - 6^+$ levels, whereas the short-range interaction would give a much larger depression of the ground state 0^+ relative to the other levels of the configuration, the necessity of taking into account the finite range of the nuclear interaction is quite obvious. This was done by Bayman et al.,⁴⁾ and independently by Thankappan and Waghmare⁵⁾ at the same time. Finally, Talmi and Unna⁶⁾ have recently attempted to determine the matrix elements (diagonal as well as off-diagonal) of the nuclear interaction from the observed spacing of the energy levels in a

number of nuclei in this region. In this paper we would like to present a somewhat improved version of the calculations of Thankappan and Waghmare, compare the various results in some detail and offer some additional comments on the nature of the two-body interaction.

§ 2. Analysis of calculations for Zr^{90}

The theoretical calculation for Zr^{90} is straightforward, and was described by Thankappan and Waghmare and also in more detail by Bayman et al. We sketch a brief outline here for completeness. The levels of the configurations $(p_{1/2})^2$, $J=0^+$; $(g_{9/2})^2$, $J=0^+$, 2^+ , 4^+ , 6^+ , 8^+ ; and $(p_{1/2})(g_{9/2})$, $J=4^-$, 5^- for the last two protons in Zr^{90} are considered. We assume the equality of the radial oscillator parameters $r_p=r_g$. We take the separation energy for the single particle states $p_{1/2}$ and $g_{9/2}$ to be $E[g_{9/2}]-E[p_{1/2}]=1.0$ Mev from the data⁷ on Y^{89} . A central two-body interaction between the two-protons of the type $(a+b\sigma_1\cdot\sigma_2)V(r)$ is assumed where a and b are constants and for convenience in calculations $V(r)$ is taken to be of the Gaussian shape $V(r)=\exp[-(r/r_0)^2]$. The range parameter r_0 only enters the calculations in the combination $\lambda=r_0/r_p=r_0/r_g$. The matrix elements of the two-body interaction for the various states of the two nucleons are calculated by the well-known techniques, which we need not describe here.

We consider a , b and λ as variable parameters and attempt to fit them from the available experimental data by using the following procedure. The energy levels are calculated for the pure configuration $(g_{9/2})^2$, and for different values of λ . For each value of λ , the exchange character of the two-body interaction given by a and b is determined by fitting the experimental energy separations of the levels 2^+ , 4^+ and 8^+ . The rest of the matrix elements are then evaluated for this choice of the parameters. The results are shown in Fig. 1. The levels 2^+ , 4^+ and 8^+ are normalized to the observed values and the positions of the other levels of the pure configura-

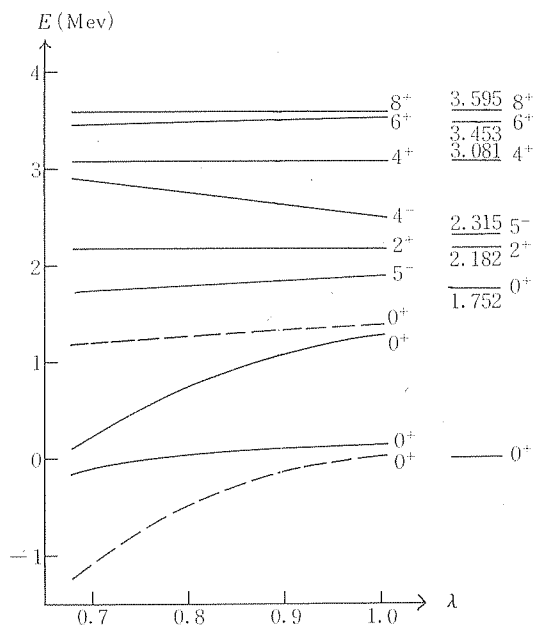


Fig. 1. The calculated and the observed energy levels of Zr^{90} . The observed levels are shown on the right. The full lines show the energies of the pure configuration states and the dotted lines show the energies including the effect of configuration mixing.

tions are shown relative to these. The configuration mixing of the two 0^+ levels, and the consequent repulsion of these is shown by dotted lines. The experimental values of the energy levels as reported by Björnholm et al.⁸⁾ are also shown.

Firstly, we remark that the position of the 6^+ level is not very sensitive to variations of λ (we remind the reader that for each λ there is a different set of values of parameters a and b). As λ changes from 0.5 to 1.0, the shift in the position of the 6^+ level is only about 0.1 Mev. If the position of the pure 0^+ level of this configuration were known, it would at once enable us to determine a suitable value of λ (and a , b). Since this is not known, we may apply another test to determine a value of λ which will describe the energy levels of the $(g_{9/2})^2$ configuration. It is well known that in the $(g_{9/2})^3$ configuration the $J=7/2^+$ state occurs very close to the ground state $J=9/2^+$ and sometimes even becomes the ground state. For example,⁷⁾ in Sr^{86} the $7/2^+$ level occurs at 0.225 Mev above the ground state $9/2^+$. For various values of λ , and the corresponding calculated energy levels of the pure $(g_{9/2})^2$ configuration, we calculate the separation of the $9/2^+ - 7/2^+$ states of $(g_{9/2})^3$, and the results are shown in Table I. It is obvious that for $\lambda=0.9-1.0$, one obtains a low-lying $7/2^+$. We therefore conclude that the levels of the pure $(g_{9/2})^2$ configuration are correctly given at the value $\lambda=1.0$. The corresponding values of the constants a and b are -15.9 Mev and $+4.8$ Mev respectively.

Table I. Levels of $(g_{9/2})^3$ configuration normalized to $E=0$ for the ground state $9/2^+$.

Spin	$\lambda=0.7$	$\lambda=0.8$	$\lambda=0.9$	$\lambda=1.0$
$7/2^+$	0.93	0.51	0.23	0.04
$5/2^+$	1.67	1.27	1.03	0.91
$3/2^+$	2.13	1.71	1.47	1.30
$9/2^+$	2.36	1.96	1.72	1.59

Next, we discuss the relative positions of the two 0^+ levels. It is clear from the Figure that for $\lambda < 0.7$, the two 0^+ levels cross over, and hence the ground state would be predominantly $(g_{9/2})_0^2$; thus in what follows we consider only values of $\lambda > 0.7$. The analysis of the data on the β -decay of Y^{90} and the γ -decay of the 2^+ state of Zr^{90} by Bayman et al.⁴⁾ gives for the wave functions of the two 0^+ states:

$$\begin{aligned} \Psi(0^+) &= 0.8\Psi[(p_{1/2})_0^2] - 0.6\Psi[(g_{9/2})_0^2], \\ \Psi'(0^+) &= 0.6\Psi[(p_{1/2})_0^2] + 0.8\Psi[(g_{9/2})_0^2]. \end{aligned} \quad (1)$$

Now the calculations show that the separation of the two pure states as well as the magnitude of the inter-configuration matrix element varies rapidly with the value of λ . The separation of the pure 0^+ levels decreases from 1.14 Mev at $\lambda=1.0$ to 0.33 Mev at $\lambda=0.7$, while the shift of each due to the inter-configuration matrix element

$$\langle (g_{9/2})_0^2 | V_{12} | (p_{1/2})_0^2 \rangle = V.$$

changes from 0.12 Mev at $\lambda=1.0$ to 0.97 Mev at $\lambda=0.7$. The observed splitting of the two levels (1.76 Mev) and the composition of the wave functions mentioned above can be reasonably well obtained for $\lambda=0.8$, the calculated value for the separation being 1.76 Mev, and the wave function of the ground state

$$0.84 \psi[(p_{1/2})_0^2] - 0.55 \psi[(g_{9/2})_0^2].$$

However, it will be noticed that relative to the 2^+ , 4^+ , 8^+ levels, the 0^+ levels are now predicted too low by about 0.5 Mev. For $\lambda=1.0$, the ground state energy is predicted correctly, but the excited 0^+ state is too low by 0.35 Mev and the configuration mixing is quite small. We later remark on the implications of these results.

Finally, we discuss the odd parity states. Only 5^- is observed, and it is predicted below the 2^+ state for the range of λ of interest in our calculation. However, the excitation energy above the ground state is correctly obtained for $\lambda=0.8$ Mev. The 4^- state is predicted above 5^- , the separation of the two decreases rapidly with increasing λ , and is 0.95 Mev for $\lambda=0.8$ and 0.64 Mev for $\lambda=1.0$. One would thus expect to observe it at ~ 3.0 Mev excitation, provided the nature of the nuclear interaction in this $(p_{1/2})(g_{9/2})$ configuration is not violently different from that in the other configurations.

To summarize briefly, then, it appears that with a unique choice of the parameters of the central two-body interaction assumed here, one cannot explain all the low-energy levels of the Zr^{90} nucleus with complete accuracy. The choice $\lambda=1.0$ adequately explains the energy levels of the $(g_{9/2})^n$ configurations, but the same choice would not satisfactorily give the lower levels in agreement with the observed values. On the other hand, for $\lambda=0.8$, the lower levels 0^+ , 0^+ and 5^- can be satisfactorily explained, but the remaining levels would be pushed up, so that they would be predicted above the observed positions. It is difficult to avoid the conclusion that such a simple two-body interaction appears to be configuration-dependent. For further elucidation of the situation it would be of considerable interest to locate the as yet unobserved 4^- level experimentally.

We would like to emphasize that since the $6^+ - 8^+$ separation is not very sensitive to the choice of λ , we have to rely on the $9/2^+ - 7/2^+$ separation of the $(g_{9/2})^3$ configuration to obtain a unique value of λ . It turns out that this parameter is a very sensitive test of the choice of the interaction parameters (as pointed out also by Talmi and Unna⁶⁾), and even a small change in the parameters (particularly b) in going from $\lambda=1.0$ to 0.9 produces a considerable shift of the $7/2^+$ level. We can now look at the fitting of the other levels (in particular the ground state 0^+) from a somewhat different point of view. The two 0^+ states, their energies and eigenfunctions, are described by the matrix

$$\begin{pmatrix} 1.76-x & V \\ V & x \end{pmatrix}.$$

Since the value of $(1.76-x)$ (the energy of the $(g_{9/2})_0^2$ state) is effectively known from the analysis of the $(g_{9/2})^2$ configuration, we may ask ourselves the question: where should the unperturbed $(p_{1/2})_0^2$ level be, and what should be the strength of the configuration mixing matrix element V to produce the experimental level spectrum and the eigenfunctions given by Eq. (1) for these states? It is then easily found that for $\lambda=1.0$ and 0.9 the separation of the unperturbed 0^+ states, $\delta=-(2x-1.76)$, should be roughly 0.76 and 0.36 Mev, and for the matrix element $V=0.8$ and 0.86 Mev respectively. These may be compared with the calculated values $\delta=1.15$ and 0.95 Mev and $V=0.35$ and 0.50 Mev. Thus the nuclear interaction which gives correct matrix elements for the $(g_{9/2})^2$ configuration gives for other configurations the results that are in error by ~ 0.5 Mev. In nuclear spectroscopy calculations where one is satisfied with approximate agreements within $\sim 0.2-0.3$ Mev, such configuration dependence of the interaction would be masked. It is only when one attempts to make a refined analysis and look for precise predictions such as $9/2^+-7/2^+$ separation that the information on detailed nature of the nuclear interaction becomes available.

If the nuclear interaction V_{12} is written in a conventional way as

$$V_{12} = \sum_k f_k(r_1, r_2; \sigma_1, \sigma_2) P_k(\cos \theta_{12}),$$

it is easily seen that the matrix element of the interaction for the $(p_{1/2})_0^2$ state, as well as for the $(p_{1/2})(g_{9/2})$ configuration states, will depend only upon $k=0, 2$ terms, whereas the matrix elements in the $(g_{9/2})^2$ states will depend upon $k=0, 2, 4, 6, 8$ terms. On the other hand, the matrix element V will depend only upon $k=3, 5$. We can push our analysis further to derive from the empirical matrix elements the nature of the interaction in these various substates of relative angular momentum. An analysis along these lines for this nucleus as well as in the s - d shell is now in progress. To obtain a consistent interpretation of these matrix elements one may be led to an empirical non-local potential.

§ 3. Comparison with other results

Our results are, in a broad sense, similar to those of Bayman et al.⁴⁾ We have not taken into account the Coulomb interaction of the two protons. Our method of choosing the 'best fit' parameters of the two-body interaction is different from theirs, and gives somewhat different results for the parameters. However, the separation of the odd-parity levels predicted by them agrees well with our estimate. The best fit obtained by Bayman et al. shows the 5^- and the excited 0^+ levels lower and the $2^+, 4^+$, and 6^+ levels a little higher than

the observed positions. Table II shows the variation of our parameters a , b with λ , and also the 'best fit' values of Bayman et al. It is clear that the effective nuclear interaction obtained for Zr^{90} has an exchange nature similar to that obtained by French and Raz⁹⁾ from an analysis of the data on Calcium isotopes, but the well-depth for Zr^{90} is about twice as much. We should like to emphasize, however, that this interaction is quite different in its exchange nature from the other effective interactions used in light nuclei (Rosenfeld¹⁰⁾ or Elliott and Flowers¹¹⁾) or in heavy nuclei in the Pb region (Carter et al.¹²⁾). The simple central two-body interaction conventionally used in the nuclear shell model appears to be not only configuration-dependent in the same nucleus, but also varies with the mass of the nucleus. We hope to deal with this extremely interesting phenomenon in a separate paper.

Table II. Nuclear interaction parameters obtained in our calculations. The values obtained by Bayman et al. are shown in the last column.

λ	0.7	0.8	0.9	1.0	0.75
a	-18.0	-15.7	-15.5	-15.9	$-31.2 < a < -11.7$
b	17.4	11.1	7.2	4.8	$5.5 < b < 11.7$

Talmi and Unna⁶⁾ have recently carried out an analysis of the level spectra of Zr^{90} and other neighbouring nuclei. The analysis is based on an attempt to rewrite the experimental data in terms of the numerical values of the matrix elements of the effective nuclear interaction in various states, rather than the parameters of the interaction itself. Such an approach is very valuable in correlating a large number of experimental data and in predicting new levels. The advantage of this technique is obviously its independence of the detailed assumptions regarding the explicit nature of the two-body interaction and the independent-particle wave functions. Hence, such an analysis cannot, by its very nature, yield any information on the properties of the phenomenological two-body interaction which it is the aim of our study. It may be seen that the results of Talmi and Unna interpreted in terms of a two-body central interaction do confirm our conclusion that such an interaction should be regarded as non-local or configuration-dependent. The matrix elements relevant to our calculations are

$$\begin{aligned}\gamma &= E[(g_{9/2})^2_{J=2}] - E[(g_{9/2})^2_{J=0}] = 0.866 \text{ Mev}, \\ \partial_2 &= E[(g_{9/2})^2_{J=0}] - E[(p_{1/2})^2_{J=0}] = 0.836 \text{ Mev}, \\ |V| &= |\langle (g_{9/2})^2_{J=0} | H_{12} | (p_{1/2})^2_{J=0} \rangle| = 0.708 \text{ Mev},\end{aligned}$$

where the numerical values are as required by Talmi and Unna to explain the experimental level schemes, and we have included in ∂_2 the single-particle energy

difference 2β . From Fig. 1 it may be seen that the value of γ is obtained for $\lambda=1.0$. It is thus clear, as we previously remarked, that the energy levels of the pure $(g_{9/2})^2$ configuration can be correctly predicted by the interaction H_{12} with parameters corresponding to $\lambda=1.0$. A three-parameter model is then sufficient to predict all the energy levels of $(g_{9/2})^n$ configurations of identical particles. This interaction would also predict a low-lying $7/2^+$ state of the $(g_{9/2})^3$ configuration, and the failure of the earlier attempts in the search of a simple phenomenological potential that will give such a state is not at all surprising in view of our earlier remarks. The empirical and calculated values of δ and V have already been discussed earlier.

The splitting of the odd-parity states 4^- and 5^- is predicted by Talmi and Unna to be 0.04 Mev, whereas our calculations (as also those of Bayman et al.) based on explicit interactions predict it to be at least ten times larger. We feel that an experimental identification of the 4^- states assumes added importance in view of these conflicting predictions. In this connection, it would also be very helpful to determine low-lying odd-parity states of nuclei such as Nb⁹¹ or Sr⁸⁶, for these would belong to the configurations $(p_{1/2})(g_{9/2})^2_J$ and would give rise to doublets $J \pm 1/2$. The splitting of such doublets can immediately be calculated in terms of the splitting of $J=4^-, 5^-$ states of $(p_{1/2})(g_{9/2})$ configuration, and would therefore indirectly give a measure of it.

Acknowledgements

We are grateful to the University Grants Commission, Ministry of Education and the Department of Atomic Energy, Government of India, for research grants during the course of this work.

References

- 1) K. W. Ford, Phys. Rev. **98** (1955), 1516.
- 2) O. E. Johnson, R. G. Johnson and L. M. Langer, Phys. Rev. **98** (1955), 1517.
- 3) Reported in a paper by N. H. Lazar et al., Phys. Rev. **110** (1958), 513.
- 4) B. F. Bayman, A. S. Reiner and R. K. Sheline, Phys. Rev. **115** (1959), 1627.
- 5) V. K. Thankappan and Y. R. Waghmare, Prog. Theor. Phys. **22** (1959), 459.
- 6) I. Talmi and I. Unna, Nuclear Phys. **19** (1960), 225.
- 7) Nuclear Level Schemes, compiled by K. Way et al., U. S. A. E. C. Report TID-5300 (1955).
- 8) S. Bjørnholm, O. B. Nielsen and R. K. Sheline, Phys. Rev. **115** (1959), 1613.
- 9) J. B. French and B. J. Raz, Phys. Rev. **104** (1956), 1411.
- 10) L. Rosenfeld, "Nuclear Forces" (North-Holland Publishing Company), pp. 543.
- ✓ 11) J. P. Elliott and B. H. Flowers, Proc. Roy. Soc. A **242** (1957), 57. ~~115 (1957), 57.~~
- 12) J. C. Carter, W. T. Pinkston and W. True, Phys. Rev. **120** (1960), 504.

COLLECTIVE VIBRATIONS IN EVEN-EVEN NUCLEI

V. K. THANKAPPAN and S. P. PANDYA

The energy level spectra of even-even nuclei have been studied in terms of many different models. One of these is the collective vibrational model. Most of the investigations till now have considered the collective vibrations of the even-even nucleus as a whole, neglecting the effect of the inter-nucleon forces. Raz¹ has recently considered the two-nucleon model of the even-even nucleus, with the addition of the collective oscillations of the core interacting with the states of the two external nucleons. We had independently started a calculation of the level spectrum of an even-even nucleus including vibrations of the core, forces between the two external nucleons as well as configuration mixing effects (not taken into account by Raz). Owing to the computational difficulties Si³⁰ was chosen as a simple test case, but the results are expected to have a wider validity. The formalism is very similar to that of Raz.

We consider two nucleons outside the Si²⁸ core, in $s_{1/2}$ and $d_{3/2}$ subshells, the particle states being $(s_{1/2})^2_{0, 2}$, $(d_{3/2})^2_{0, 2}$, and $(s_{1/2} d_{3/2})_{1, 2}$. The interaction between these particles is chosen as

$$H_{12} = V_0[1 + x \sigma_1 \cdot \sigma_2] \exp[-(r/r_0)^2]$$

with $\lambda = r_0/r_s = r_0/r_d = 0.8$ and V_0 for a given value of x is chosen to give correctly the separation of the $J = 0, 2$ states of $(d_{3/2})^2$ configuration observed in Si³⁴. The collective vibrations of the Si²⁸ core are quantized and up to three-phonon excitations are included in the calculations. The free parameters in the calculations are x , Δ the separation of the single particle $s_{1/2}$, $d_{3/2}$ states, ω the one-phonon excitation energy and $q = k(\hbar\omega/8\pi C)^{1/2}$ the parameter describing the strength of the particle-phonon interactions. The values of Δ and $\hbar\omega$ chosen here are found to be reasonable for this region earlier.² The hamiltonian matrices for $J = 0, 2, 4, 1$ are constructed and explicitly diagonalized. The results are summarized in the figures. In Figure 1, the energy levels are plotted against the strength of the two-body interaction. Figure 2 shows the variation of the energy levels with the strength of the coupling parameter q . The results are easy to understand qualitatively and we cannot discuss the details here. The following points may, however, be noted:

1. For values of $x > 0$, the odd-spin level 1^+ appears too low, in disagreement with the experimental data.
2. The first excited state is almost always 2^+ , and changes its character from a mainly vibrational one-phonon state for small V_0 to a largely particle state $(s_{1/2} d_{3/2})_2$ for large value of V_0 . Correspondingly the quadrupole-transition probability to the ground state must change drastically.
3. The second excited state may be 0^+ or 2^+ , the other one being generally close by. The lowest 4^+ state is not shown in Figure 1, but as shown in Figure 2, generally lies above the 0^+-2^+ doublet.

4. The possibility of having a low 0^+ level is striking, and such a state is seen in Mg^{26} , Si^{30} , S^{32} , and should be the third excited state in S^{34} ; perhaps this may also explain the 1.84 MeV 0^+ state in Ca^{42} .
5. The energy of the lowest 2^+ state increases as it changes its structure from a shell model state to a collective vibrational state and decreases as the strength of q is increased.

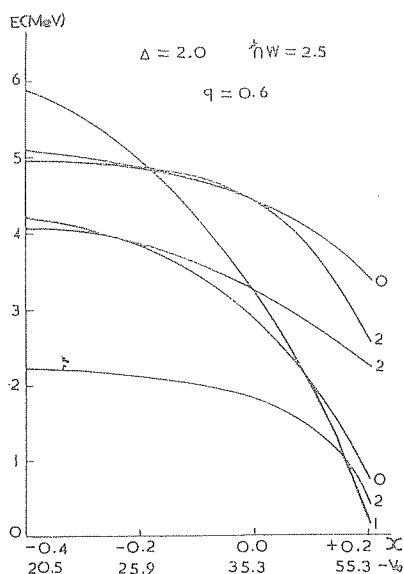


Figure 1.

Variation of the energy levels normalized to 0^+ -ground state with the strength of the two-body interaction

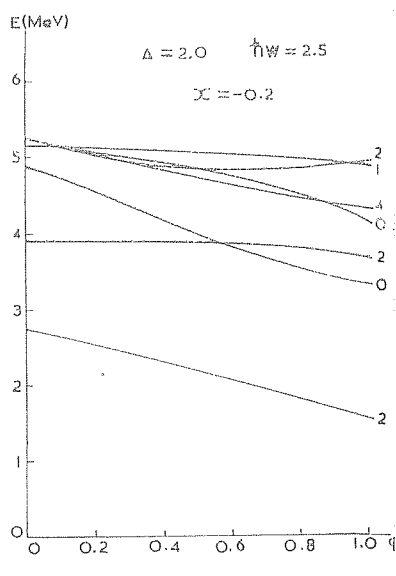


Figure 2.

Variation of the energy levels normalized to 0^+ -ground state with the coupling parameter $q = k[\hbar\omega/8\pi C]^{1/2}$

A detailed study of the quadrupole transitions in these nuclei will provide interesting information on the structure of the low-lying states, and will also check the validity of the unified model for their description.

References

1. RAZ, B. J. *Phys. Rev.* **114**, 1116 (1959)
2. THANKAPPAN, V. K. and PANDYA, S. P. *Nuclear Physics*, **19**, 303 (1960)